DTU

22485 lectures

X-ray tomography

X-Ray computed tomography (CT)

Medical CT

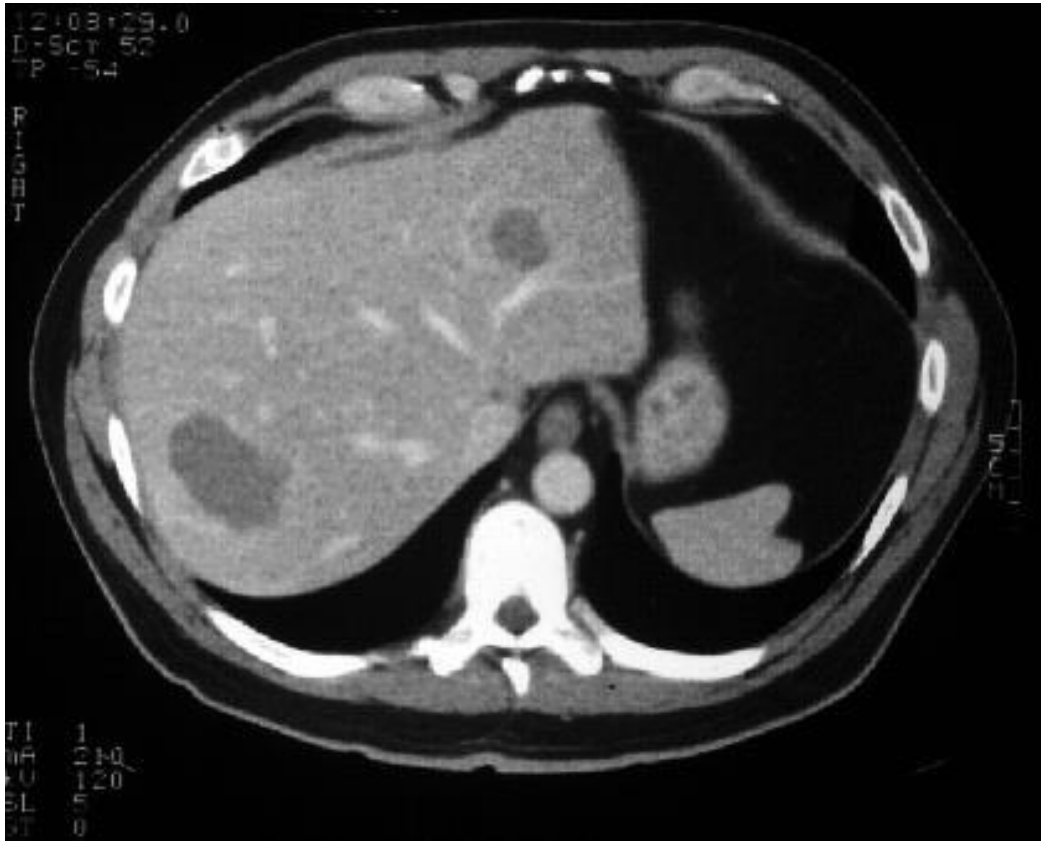

X-ray tomography (CT)

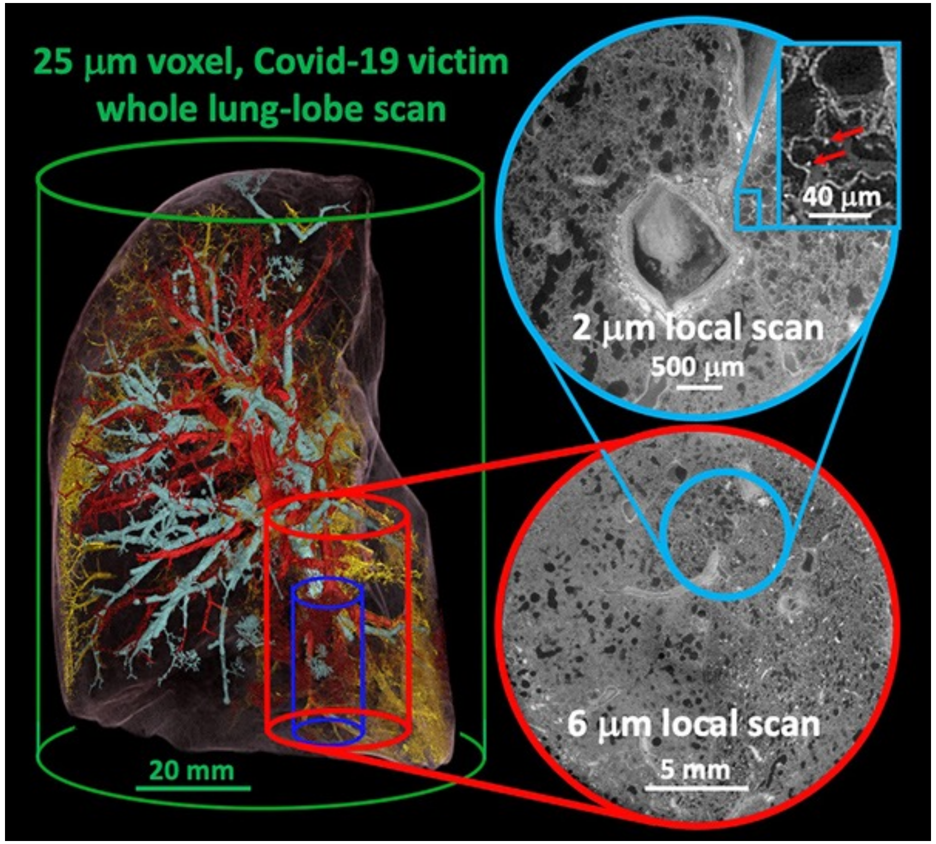

Credit: P.Tafforeau/ESRF

Plan for lecture

- Recap from X-ray physics
- Principles of X-ray tomography
- Basics of reconstructions
- Examples

Recap of X-ray physics

X-ray properties

Electro magnetic waves (light)

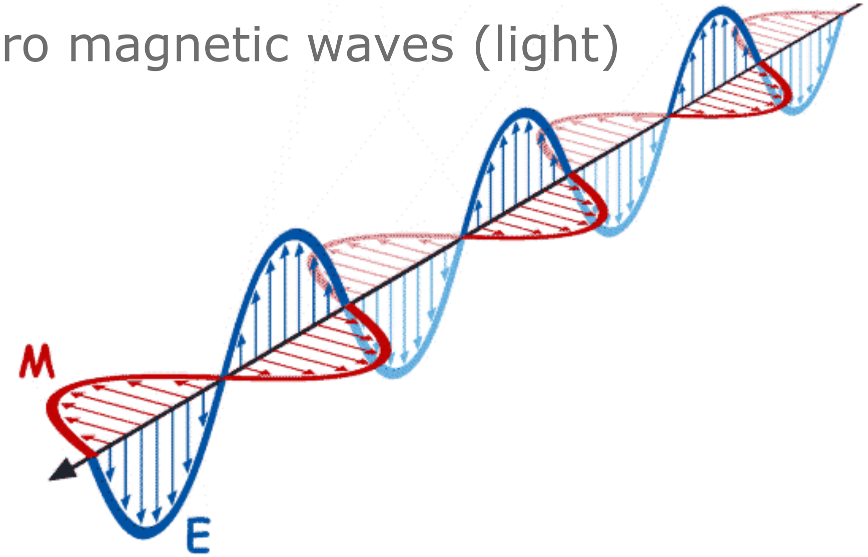

Interference with matter:

- **Scattering**
- **Photoabsorption**

Wavelength ~ 1^{-10} m (1 Å)

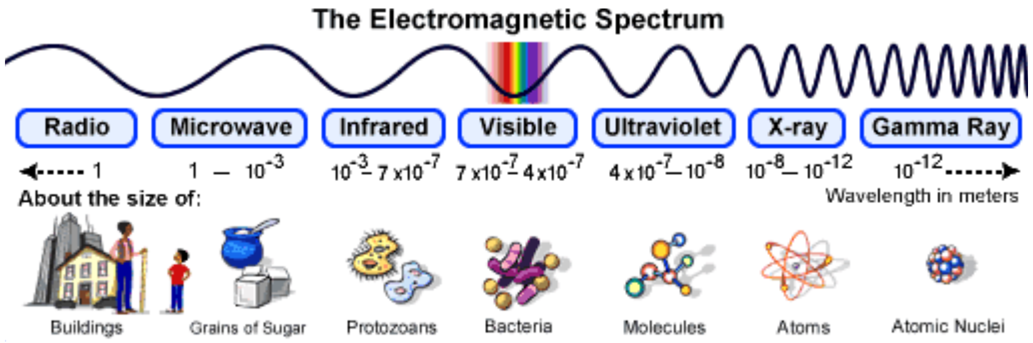

X-ray Generation

- Electrons are emitted by a cathode, strike an anode containing a target material.
- Electrons excite the atoms in the target material, which release energy in the X-ray spectrum

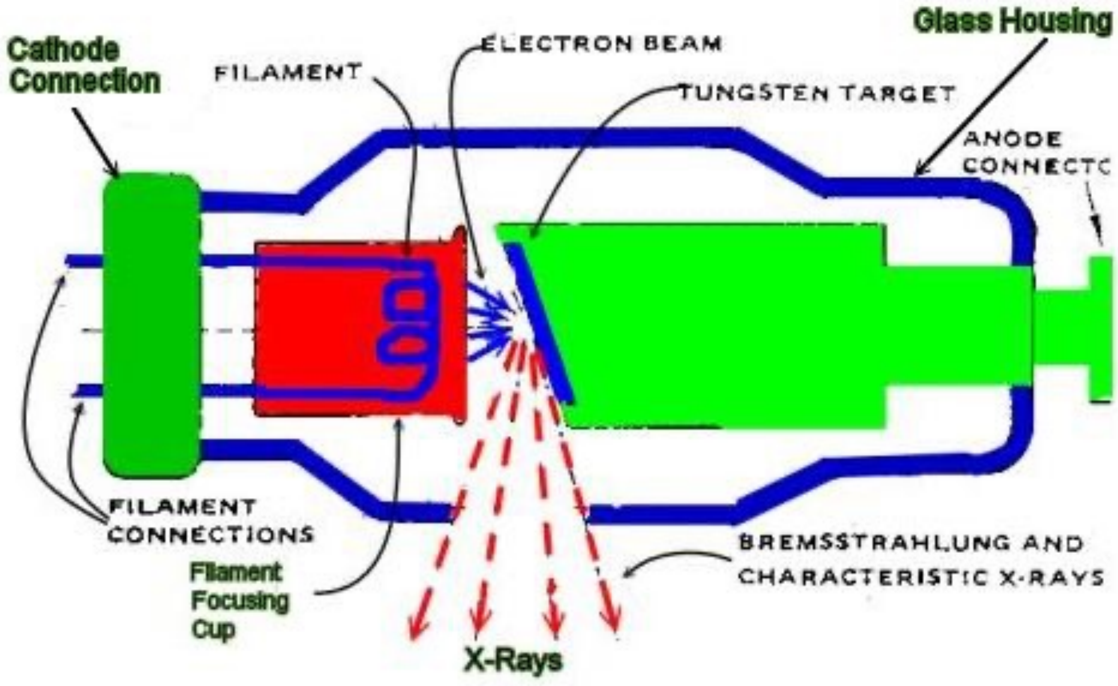

Target Materials & X-ray Spectra

- Different target materials produce different characteristic emission lines, as well as different broad-band emission spectra all the way up to the accelerating voltage (*bremsstrahlung*)
- Common target materials:
  - **Tungsten (W)**, Copper (Cu), Vanadium (V), Chromium (Cr), Molybdenum(Mo)

Element	$K\alpha_1$	$K\alpha_2$	$K\beta_1$	$L\alpha_1$	$L\alpha_2$	$L\beta_1$	$L\beta_2$	$L\gamma_1$	$M\alpha_1$
63 Eu	41,542.2	40,901.9	47,037.9	5,845.7	5,816.6	6,456.4	6,843.2	7,480.3	1,131
64 Gd	42,996.2	42,308.9	48,697	6,057.2	6,025.0	6,713.2	7,102.8	7,785.8	1,185
65 Tb	44,481.6	43,744.1	50,382	6,272.8	6,238.0	6,978	7,366.7	8,102	1,240
66 Dy	45,998.4	45,207.8	52,119	6,495.2	6,457.7	7,247.7	7,635.7	8,418.8	1,293
67 Ho	47,546.7	46,699.7	53,877	6,719.8	6,679.5	7,525.3	7,911	8,747	1,348
68 Er	49,127.7	48,221.1	55,681	6,948.7	6,905.0	7,810.9	8,189.0	9,089	1,406
69 Tm	50,741.6	49,772.6	57,517	7,179.9	7,133.1	8,101	8,468	9,426	1,462
70 Yb	52,388.9	51,354.0	59,370	7,415.6	7,367.3	8,401.8	8,758.8	9,780.1	1,521.4
71 Lu	54,069.8	52,965.0	61,283	7,655.5	7,604.9	8,709.0	9,048.9	10,143.4	1,581.3
72 Hf	55,790.2	54,611.4	63,234	7,899.0	7,844.6	9,022.7	9,347.3	10,515.8	1,644.6
73 Ta	57,532	56,277	65,223	8,146.1	8,087.9	9,343.1	9,651.8	10,895.2	1,710
74 W	59,318.24	57,981.7	67,244.3	8,397.6	8,335.2	9,672.35	9,961.5	11,285.9	1,775.4
75 Re	61,140.3	59,717.9	69,310	8,652.5	8,586.2	10,010.0	10,275.2	11,685.4	1,842.5
76 Os	63,000.5	61,486.7	71,413	8,911.7	8,841.0	10,355.3	10,598.5	12,095.3	1,910.2
77 Ir	64,895.6	63,286.7	73,560.8	9,175.1	9,099.5	10,708.3	10,920.3	12,512.6	1,979.9
78 Pt	66,832	65,112	75,748	9,442.3	9,361.8	11,070.7	11,250.5	12,942.0	2,050.5
79 Au	68,803.7	66,989.5	77,984	9,713.3	9,628.0	11,442.3	11,584.7	13,381.7	2,122.9
80 Hg	70,819	68,895	80,253	9,988.8	9,897.6	11,822.6	11,924.1	13,830.1	2,195.3
81 Tl	72,871.5	70,831.9	82,576	10,268.5	10,172.8	12,213.3	12,271.5	14,291.5	2,270.6

X-ray emission lines for various elements

Source: X-ray Data Booklet (xdb.lbl.gov)

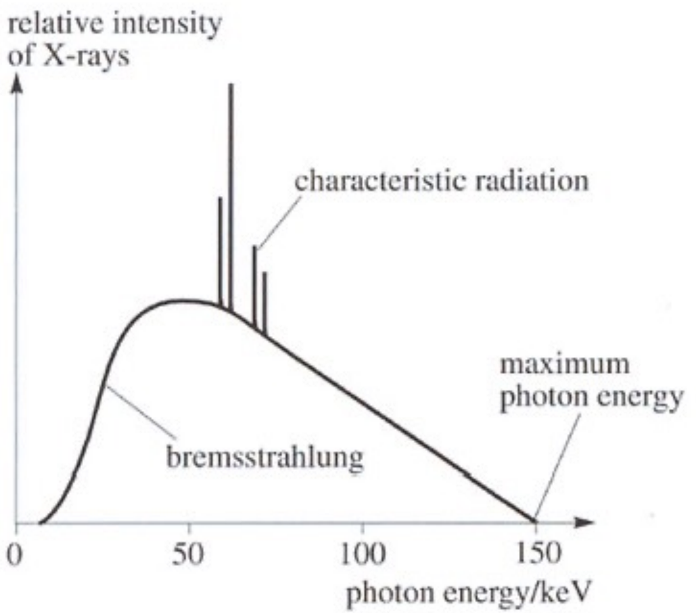

X-ray emission from a W laboratory X-ray source

Source: labspace.open.ac.uk

Radiation path

- How can you describe the radiation path with increasing distance from source?

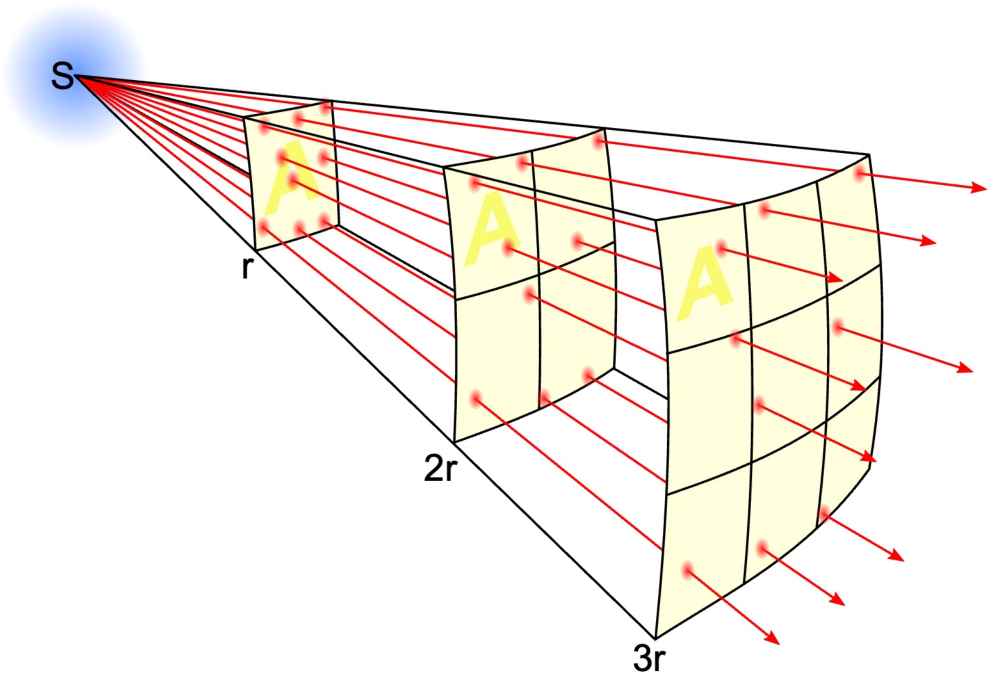

Inverse square law:

$$A \propto \frac{1}{r^2}$$

Figure from https://en.wikipedia.org/wiki/Inverse-square_law

Geometry and magnification

D = detector size
d = sample size
FOD = distance from source to object
SDD = distance from source to detector
M = magnification
dis = pixel to pixel distance/pixel pitch
vs = efficient pixel size

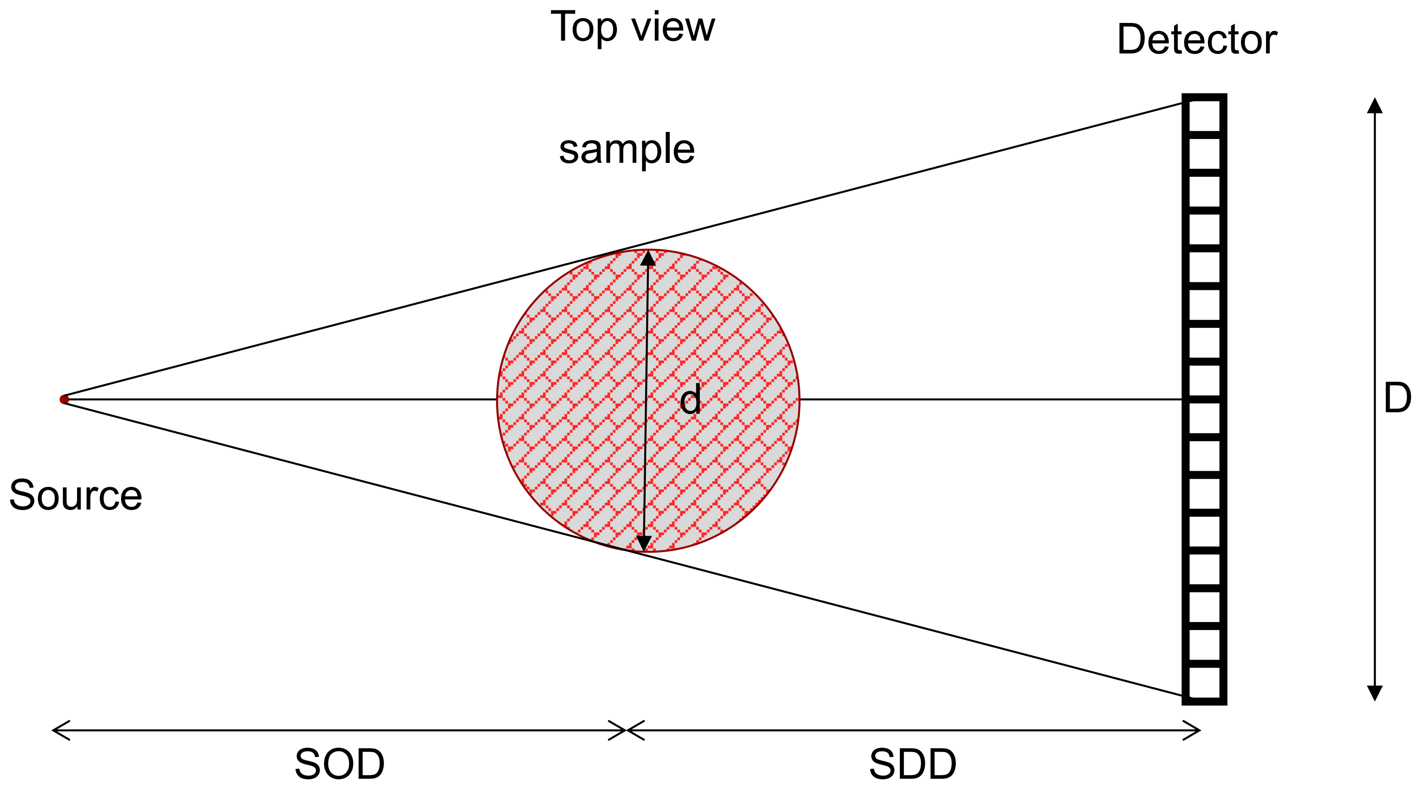

$$M = \frac{SDD + SOD}{SOD} \quad M_{Max} = \frac{D}{d} \quad vs = \frac{dis}{M}$$

Geometric spot blurring effect

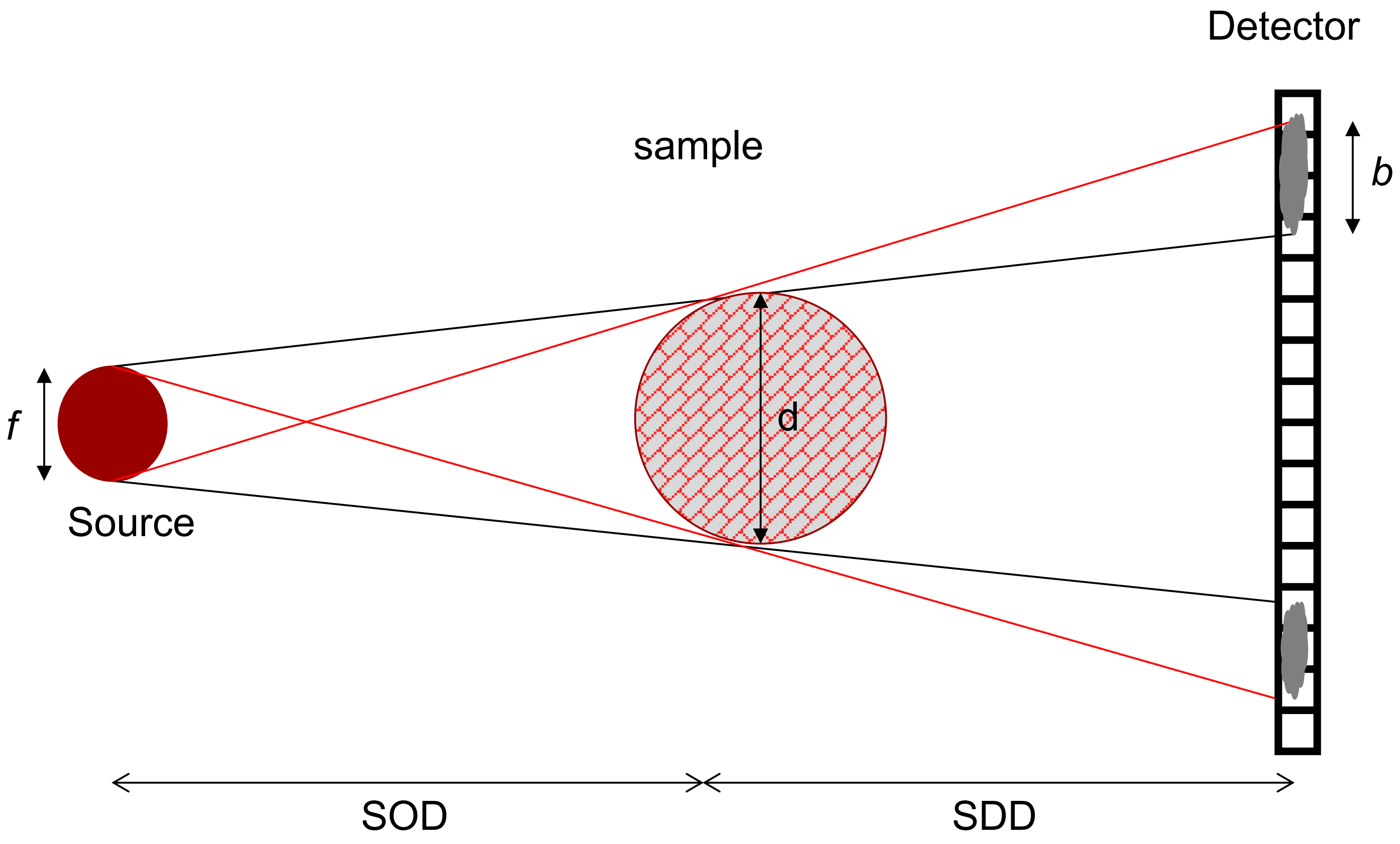

$$\frac{f}{SOD} = \frac{b}{SDD}$$

Magnification, *M:*

$$M = \frac{SDD + SOD}{SOD}$$

⇕

$$b = f(M-1)$$

The image resolution is limited by the blurring effect

Beer-Lamberts law

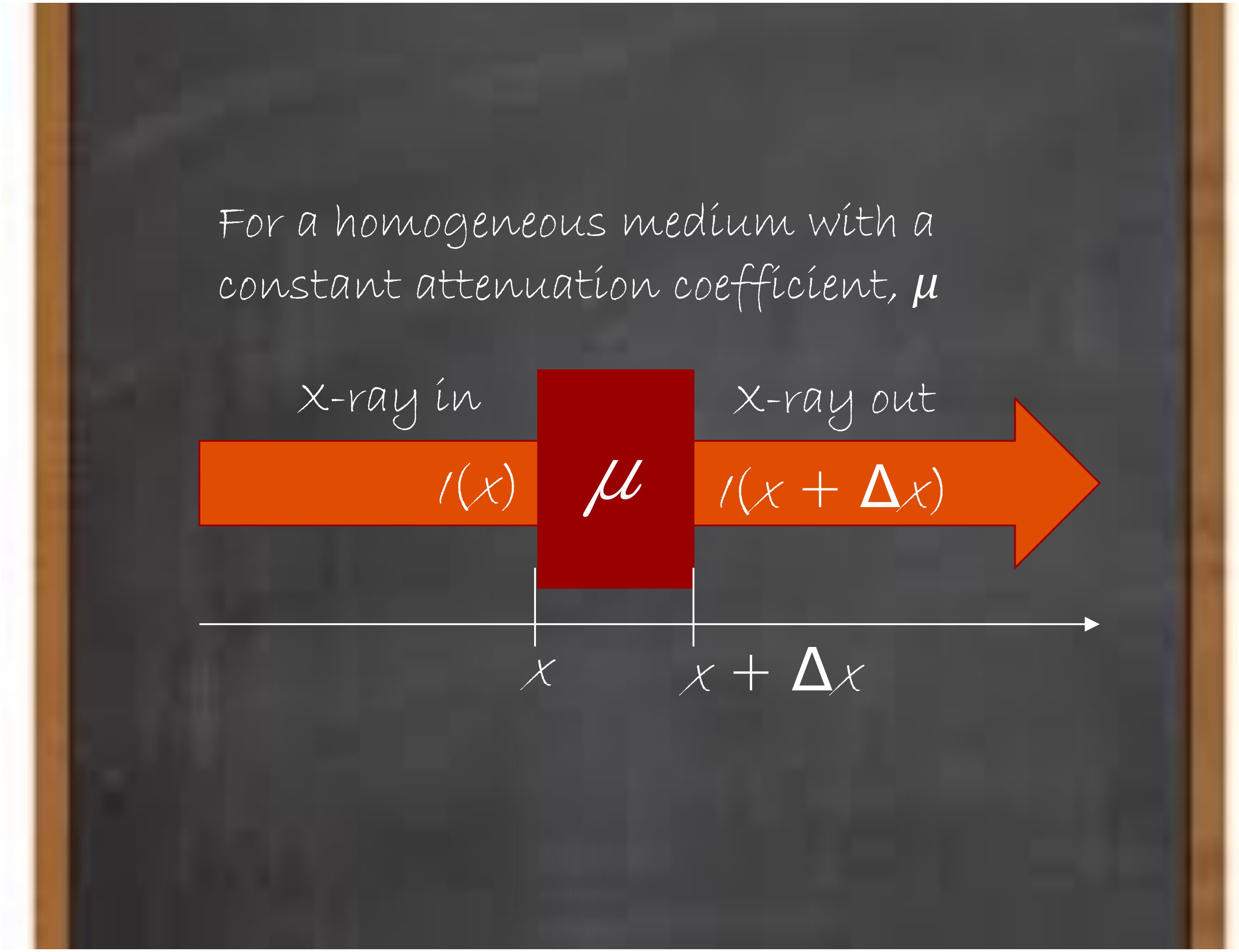

$$I(x) = I_0 e^{-\mu x}$$

I_0 = initial intensity

$$absorption \propto \frac{Z^4}{\mathcal{E}^3}$$

Beer-lambert law for non homogenous materials

As seen the X-ray spectrum from most X-ray sources are not a monochromatic spectrum and as a result, we need to calculate the attenuation for each energies in the spectrum

We then include an integral over the energy range $$I(x) = \int I_0 e^{-\int \mu(x)dx}\, dE$$

$$photoelectric\ absoption:\ \alpha = k\frac{\rho}{A}\frac{Z^4}{(h\omega)^3}$$

How much does each mechanism contribute?

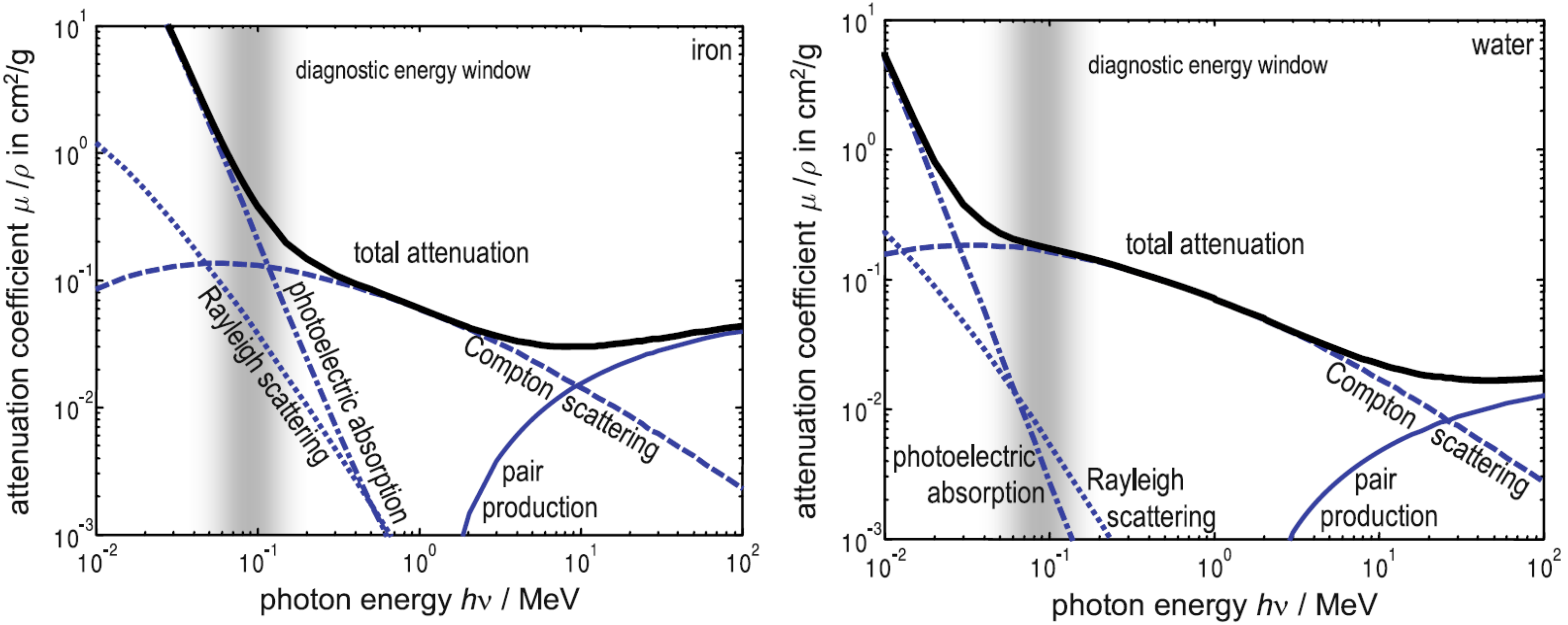

Reference: Thorsten M. Buzug Computed Tomography

X-rays

19 Nobel Prizes Based on X-ray Work

CHEMISTRY:

1936 – Peter Debye

1962 – Max Perutz & Sir John Kendrew

1964 – Dorothy Hodgkin

1976 – William Lipscomb

1985 – Herbert Hauptman & Jerome Karle

1988 – Johann Deisenhofer, Robert Huber & Hartmut Michel*

1997 – Paul D. Boyer & John E. Walker*

2003 – Peter Agre & Roderick Mackinnon*

2006 – Roger Kornberg*

* Used SYNCHROTRON RADIATION

PHYSICS:

1901 – Wilhelm Röntgen

1914 – Max Von Laue

1915 – Sir William Henry Bragg & Sir William Lawrence Bragg

1917 – Charles Barkla

1924 – Karl Manne Siegbahn

1927 – Arthur Compton

1981 – Kai Siegbahn

MEDICINE:

1946 – Hermann Joseph Muller

1962 – Francis Crick, James Watson & Maurice Wilkins

1979 – Alan M. Cormack & Sir Godfrey N. Hounsfield

Principles of X-ray tomography

What is X-ray CT?

- CT: Computed Tomography
- The word *tomography* is derived from the Greek *tomē* ("cut") or *tomos* ("part" or "section") and *graphein* ("to write").
- It refers to imaging by sections or sectioning, through the use of waves of energy, first proposed in the early 1900s
- 1970’s introduced the use of computers to do tackle the extensive math required
- In the medical field, it is also called CAT or Computerize Axial Tomography.

History of tomography

Mathematics behind CT been developed in the early 19th century by Bockwinkel, Radon, Ehrenfest, Cramer, Wold and more.
Development of the Radon transform by Johann Radon in 1917[1]

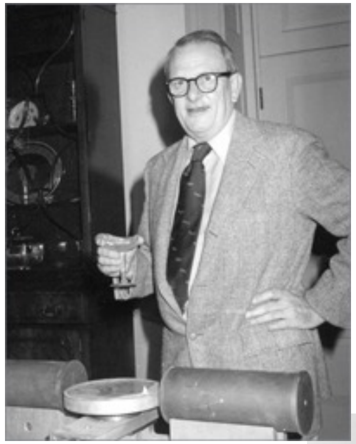

Theoretic framework for medical CT by Allan Cormack in 1963[2]

First full body scanner build by Godfrey Hounsfield in 1975, at EMI

[1] "Über die Bestimmung von Funktionen durch ihre Integralwerte längs gewisser Mannigfaltigkeiten",
Reports on the Proceedings of the Royal Saxonian Academy of Sciences at Leipzig, Mathematical and Physical Section], Leipzig: Teubner (69): 262–277
[2] "Representation of a function by its line integrals, with some radiological applications." J Appl Physics. 1963; 34: 2722-2727

Standard Architecture of CT

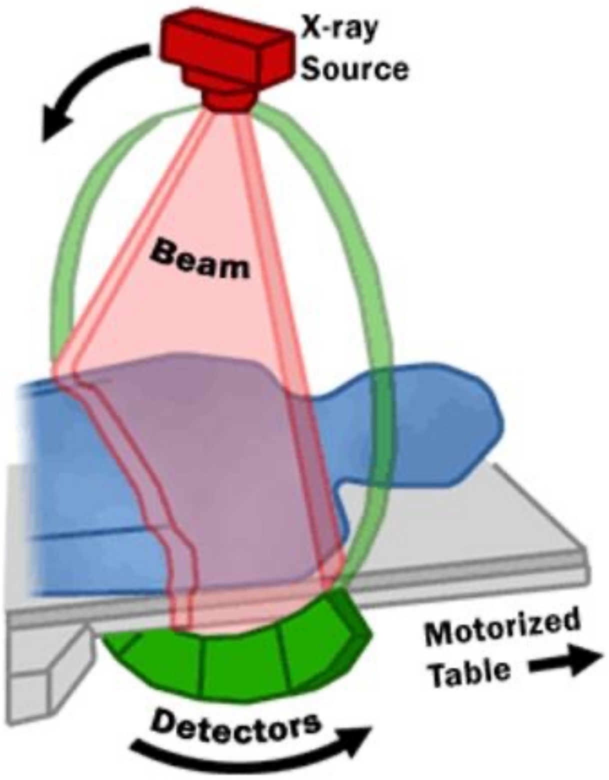

Medical Scanners

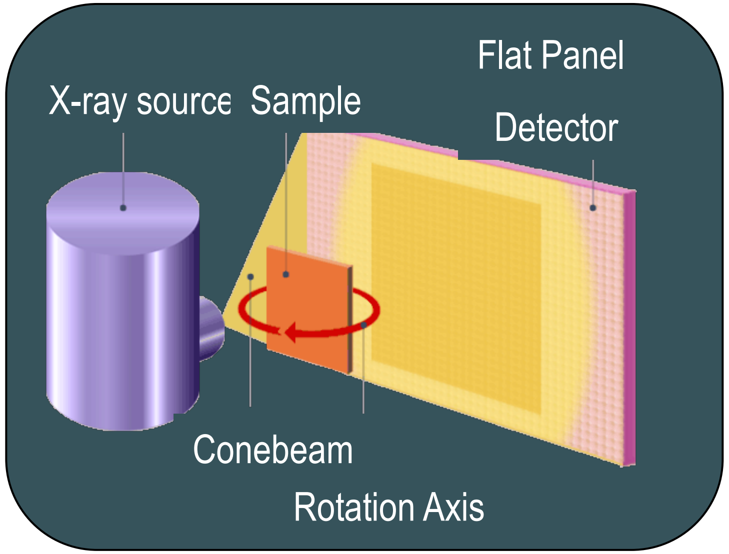

Traditional Micro CT Scanners

Medical CT development

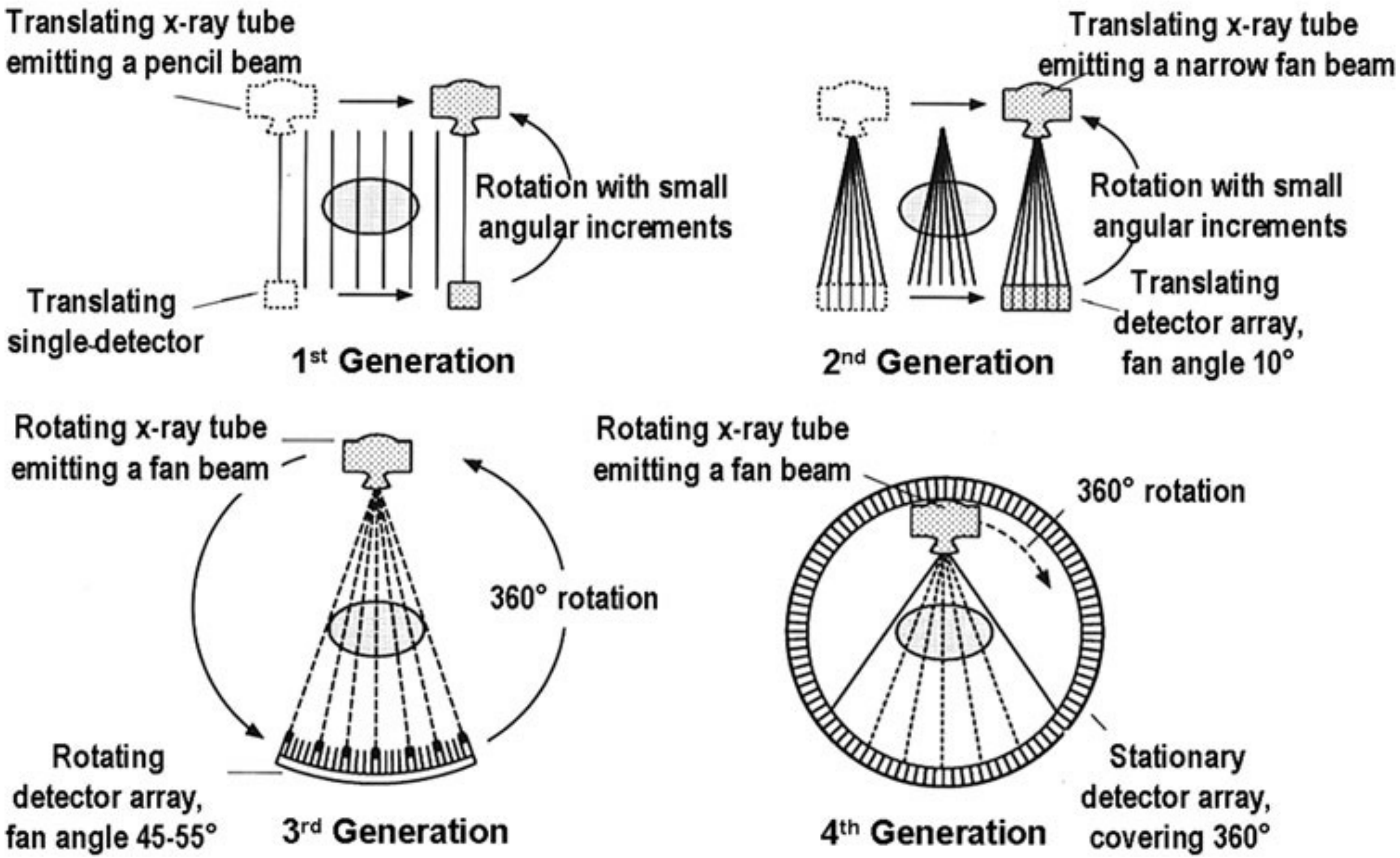

Figure 1 from Curr Radiol Rep (2013) 1:52–63, DOI 10.1007/s40134-012-0005-5

Industrial and micro CT

Inside the box

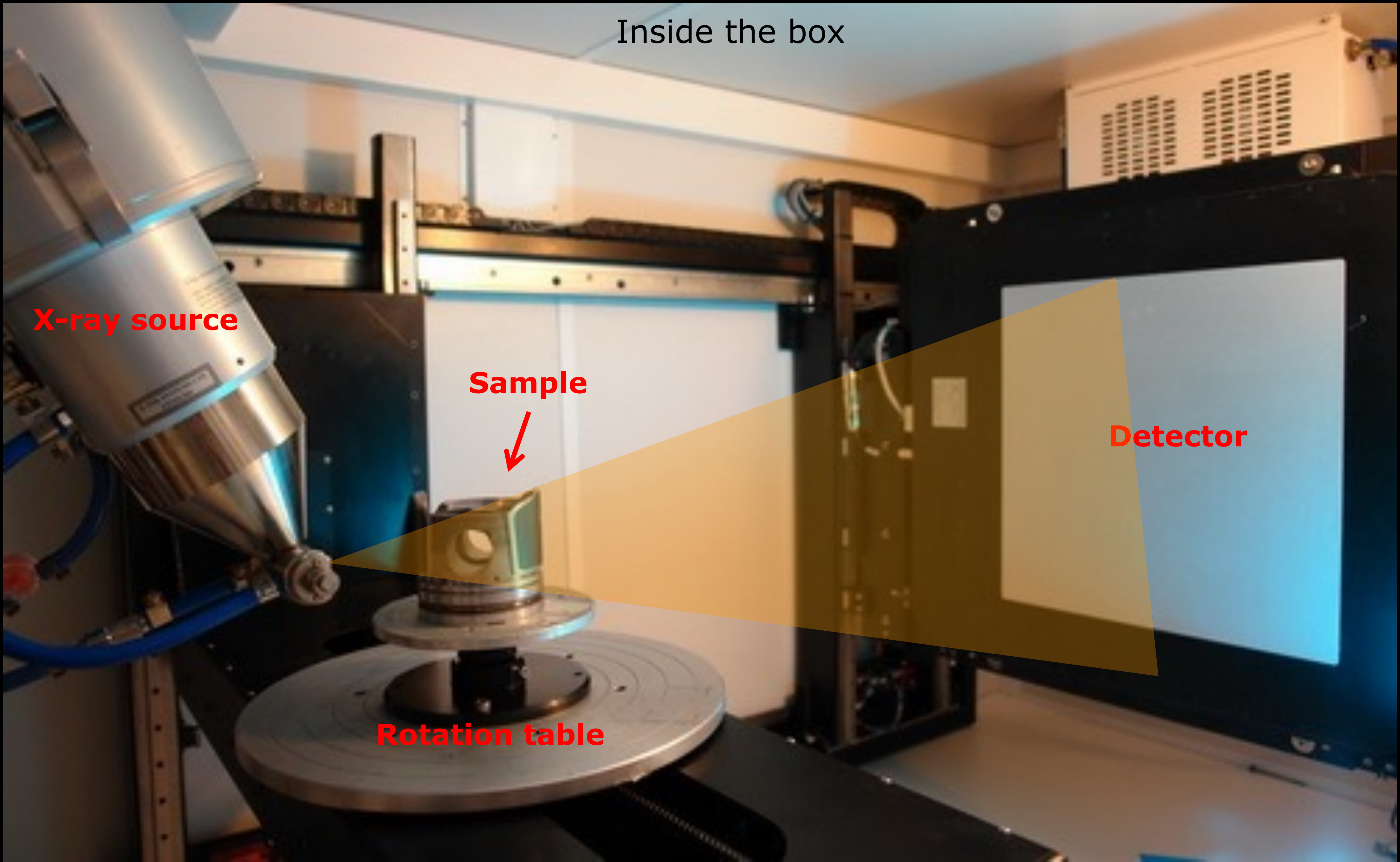

X-ray divergence

Lab sources

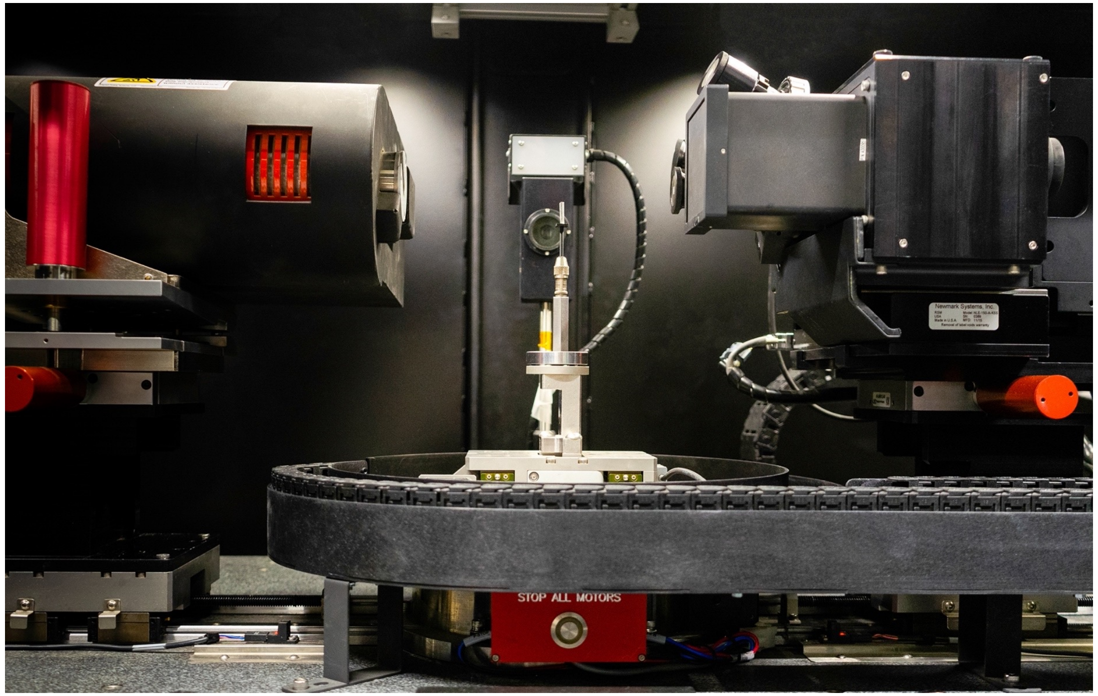

One of our scanners at DTU 3D imaging center

Divergence up to 10s of degrees

Large scale facilities

The synchrotron MAX IV in Lund, Sweden

Divergence measured in mrad

Add optical magnification to the system

- Image resolution given by is mainly defined by geometric magnification **AND** objectives

$$\text{Total Magnification} = \text{Optical magnification} * \text{Geometric magnification}$$

$$\text{Geometric magnification} = \frac{\text{Source to detector distance}}{\text{Source to sample distance}} = \frac{a+b}{a}$$

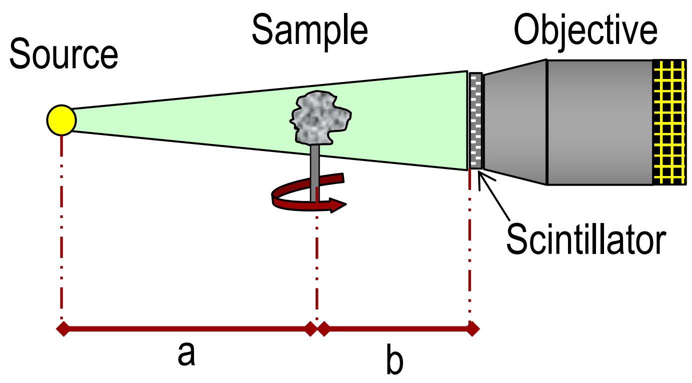

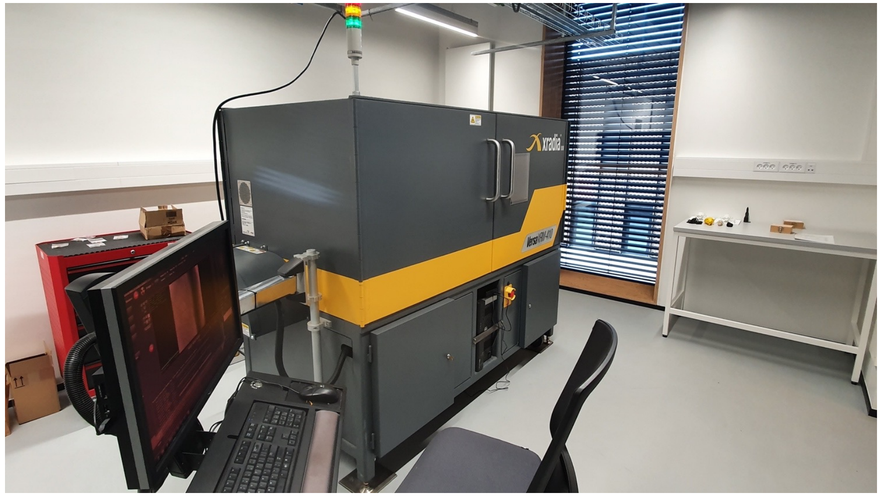

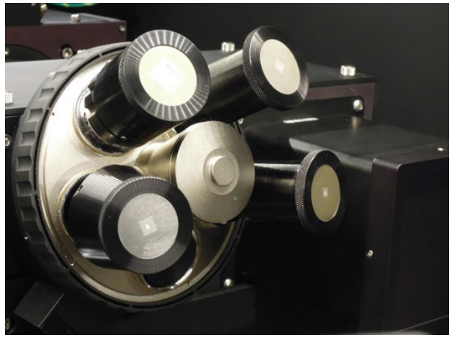

Electron tomography

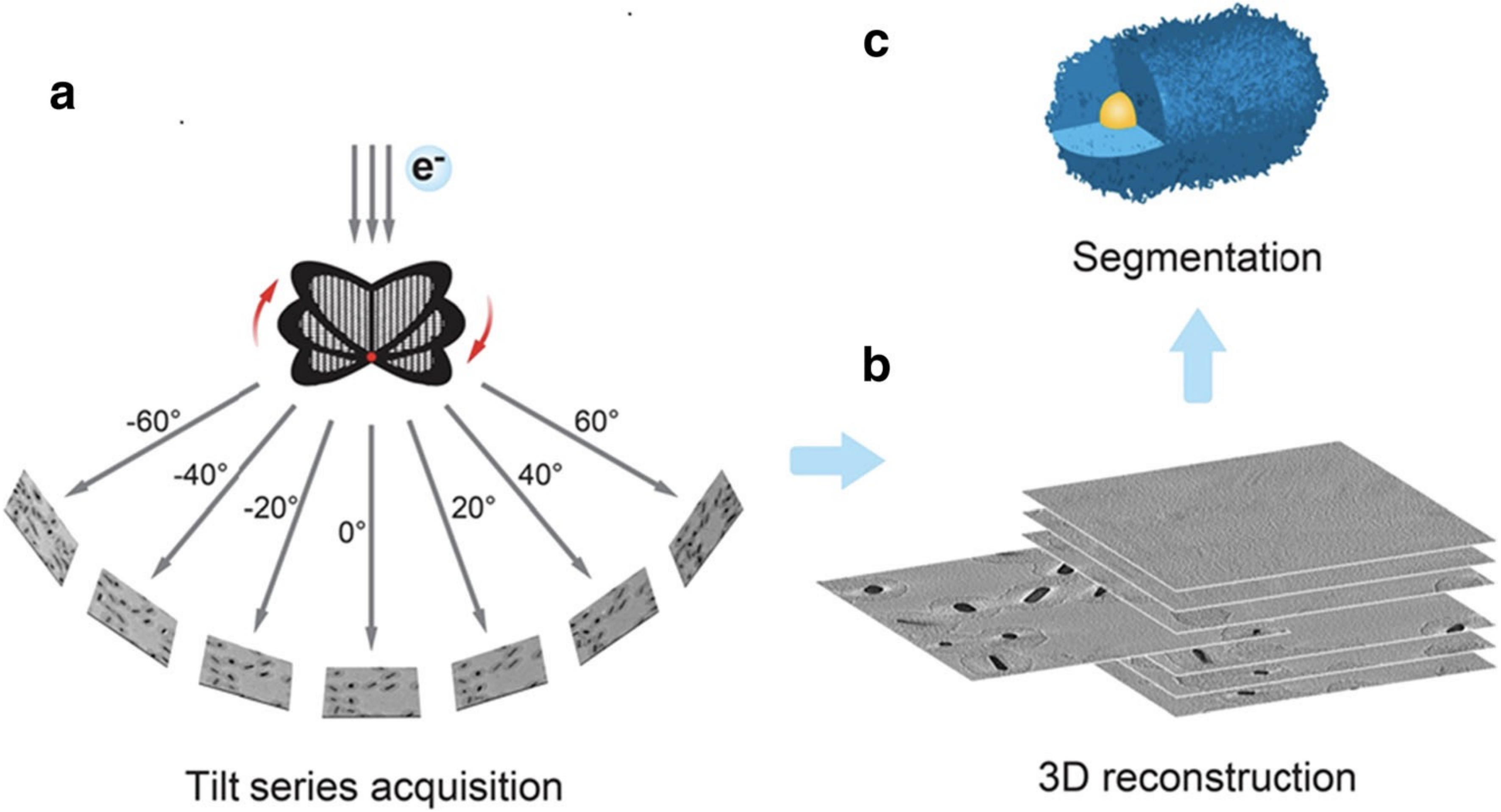

Figure from Colloid and Polymer Science (2020) 298:707–717, https://doi.org/10.1007/s00396-020-04657-w

Neutron tomography

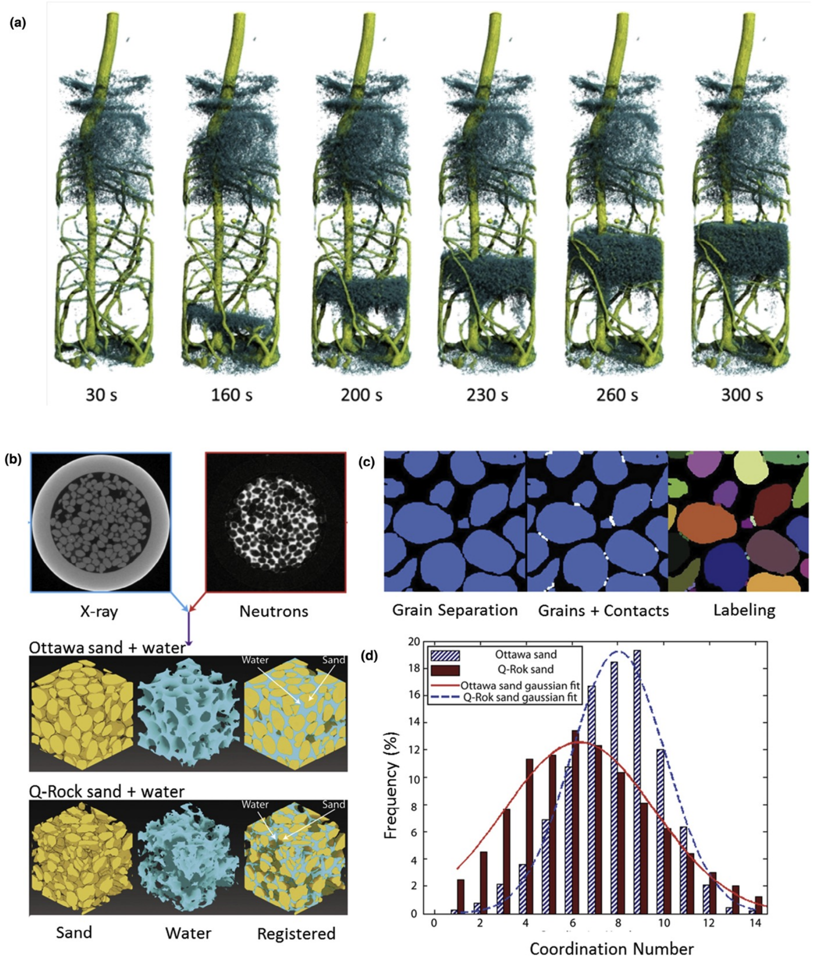

Water transport in roots of plants

Sand grains and voids

Figure from Materials today Volume 21, Issue 6, July–August 2018, Pages 652-672, https://doi.org/10.1016/j.mattod.2018.03.001

1571 radiograms recorded over a 360° rotation

Let use the x-rays for CT (computed tomography)

From the (many) 2D images we can construct a 3D "image"?

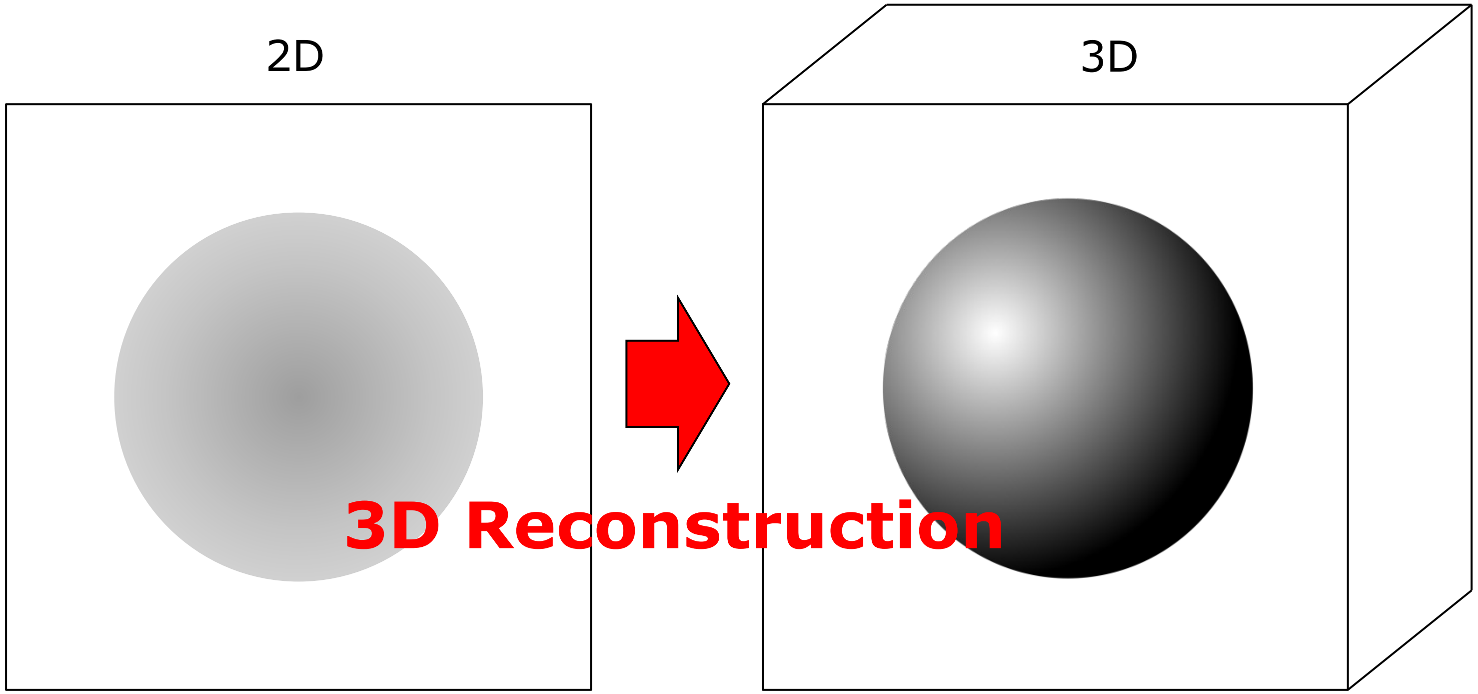

But how?

A voxel is a 3D version of a pixel

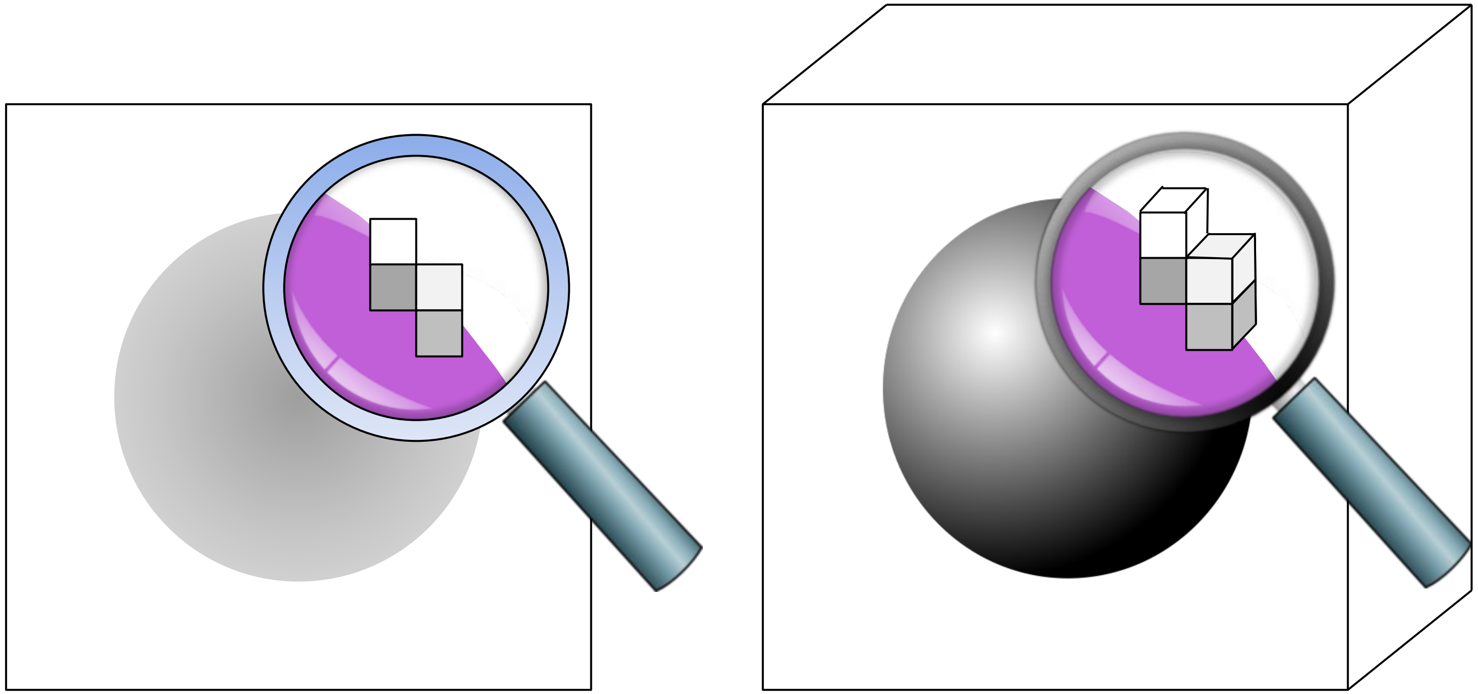

How to make the 3D reconstruction?

Example: a 2D x-ray image of a dense sphere

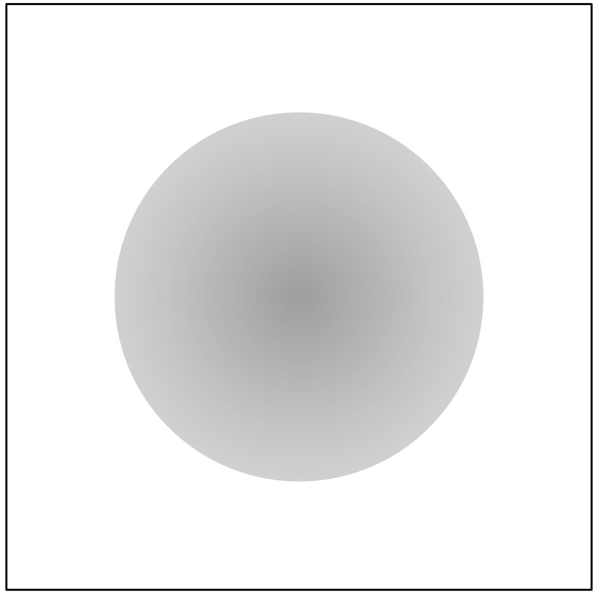

How to make the 3D reconstruction?

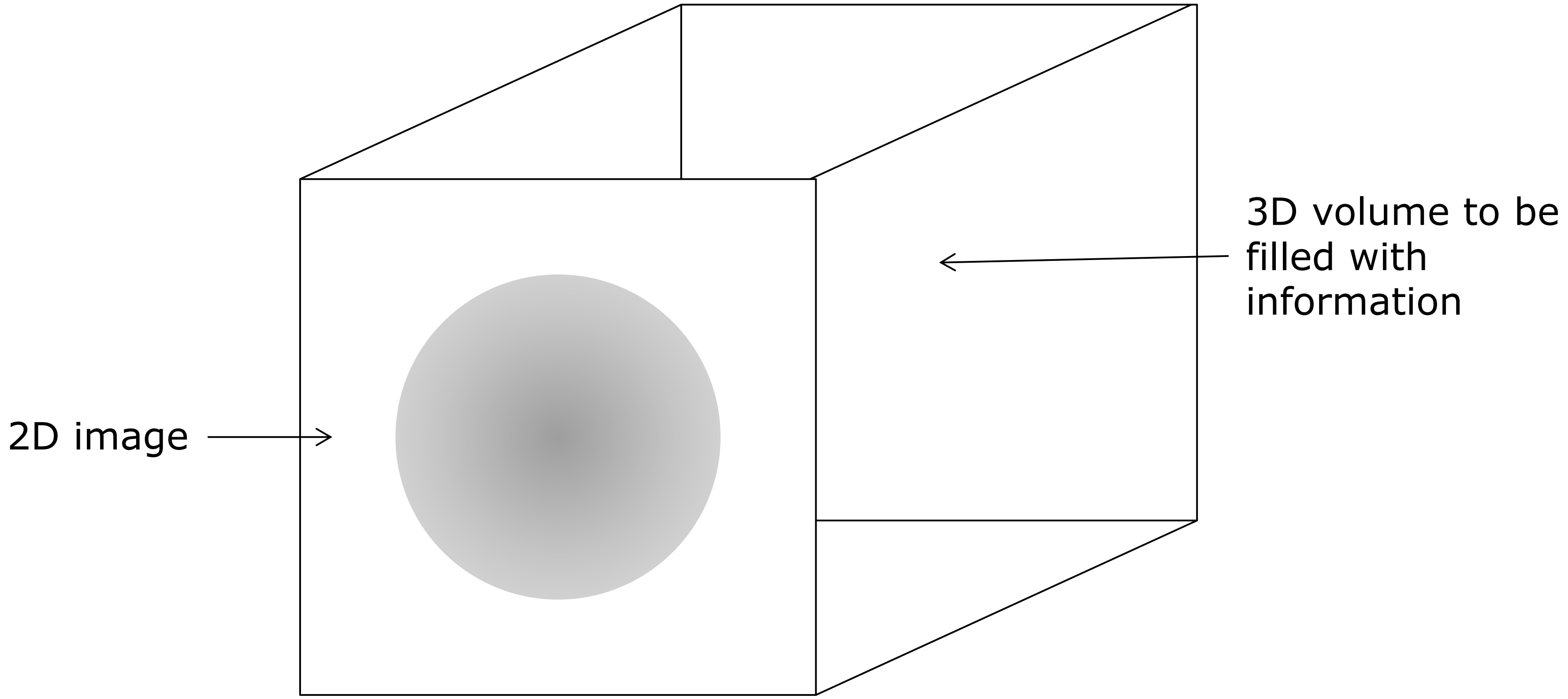

How to make the 3D reconstruction?

For simplicity, lest focus on one plane, and …

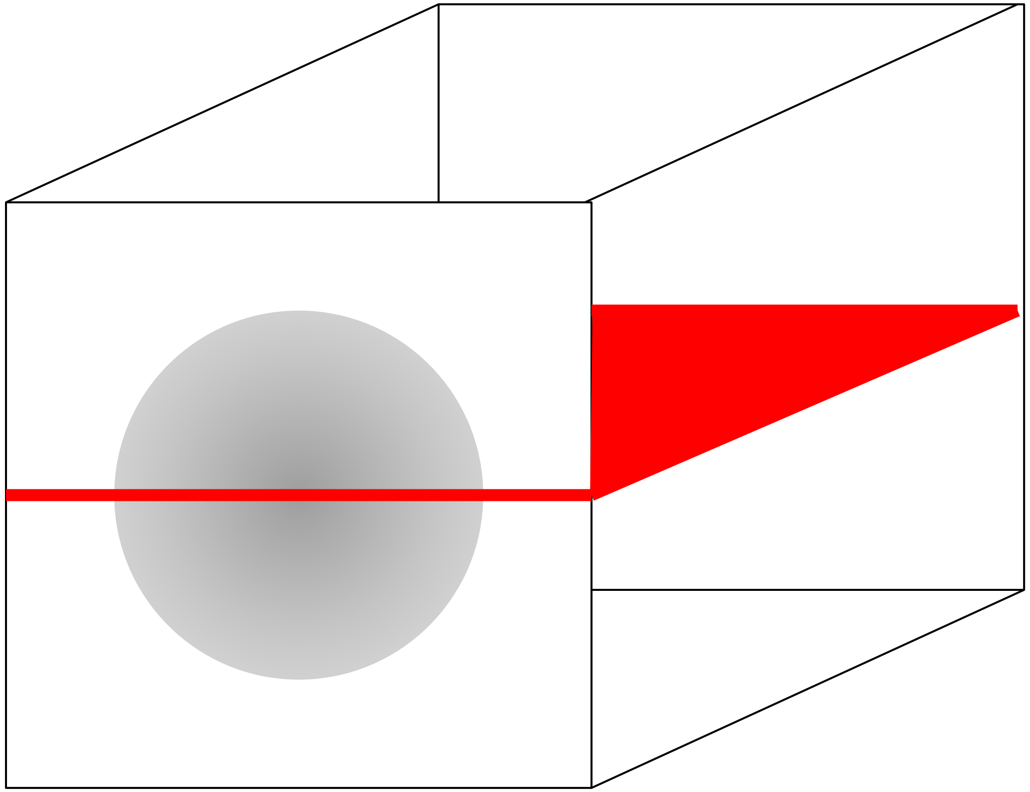

How to make the 3D reconstruction?

Imagine we look at this plane from above

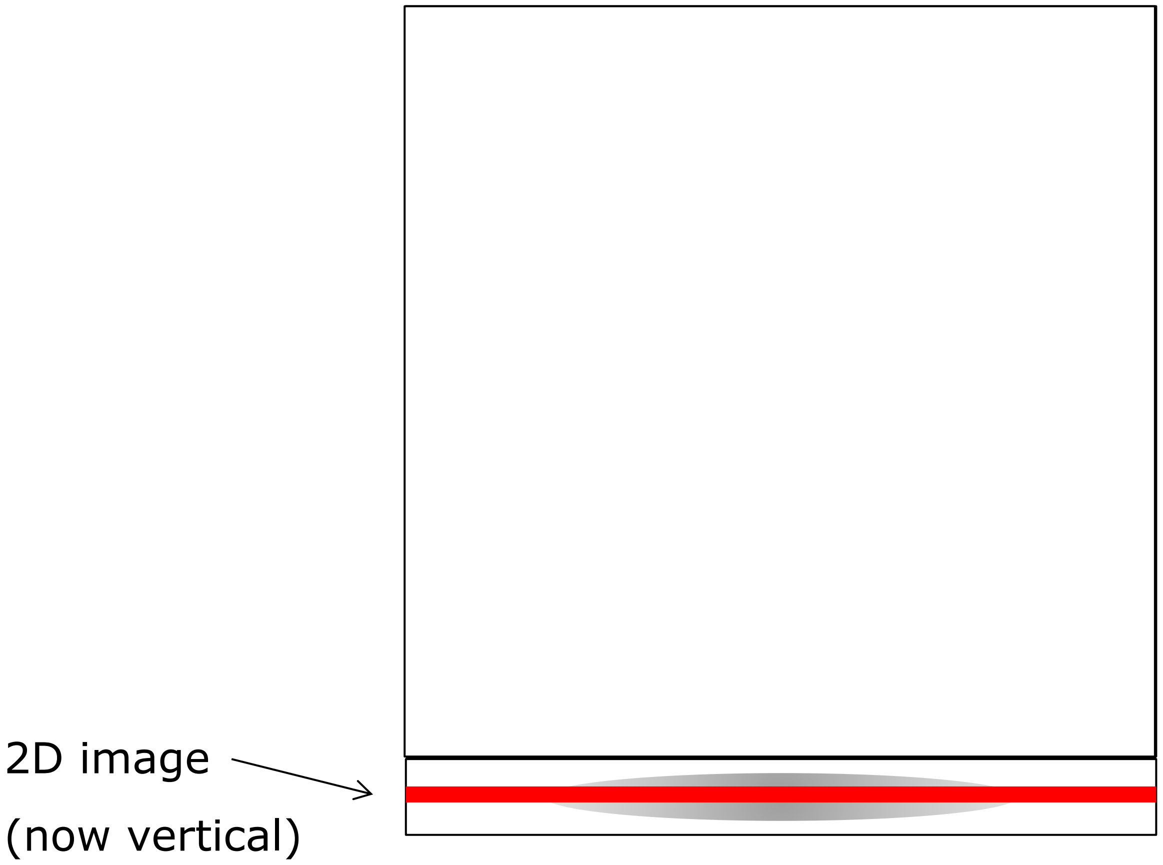

How to make the 3D reconstruction?

Backprojection: project the grey scale pixel values to all voxels in this plane at the direction normal to the 2D image

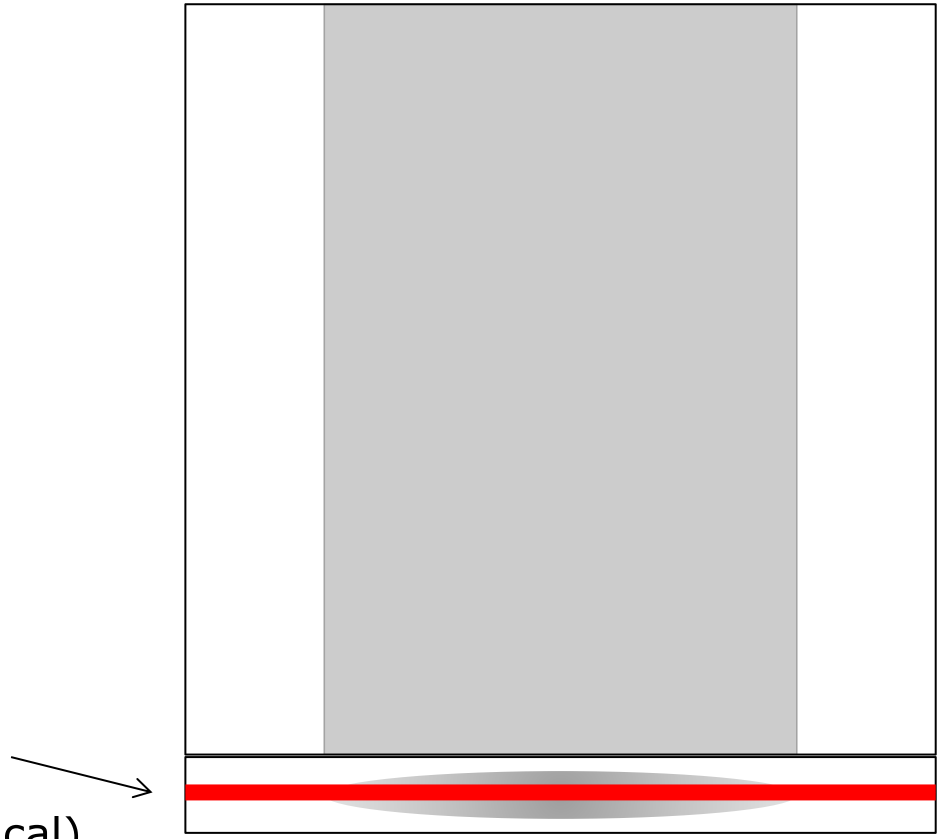

2D image

(now vertical)

How to make the 3D reconstruction?

Take a different 2D image recorded from a 90 degree angle relative to the first

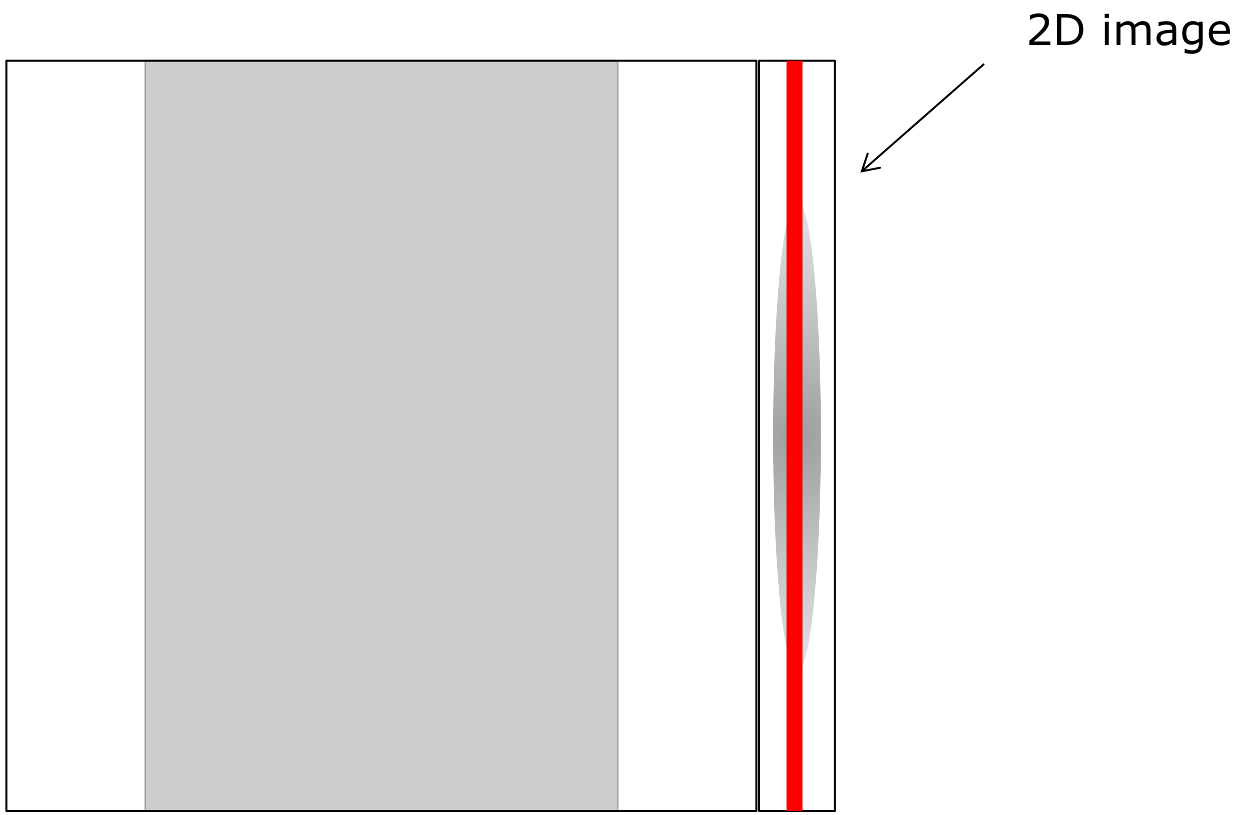

How to make the 3D reconstruction?

And backproject this

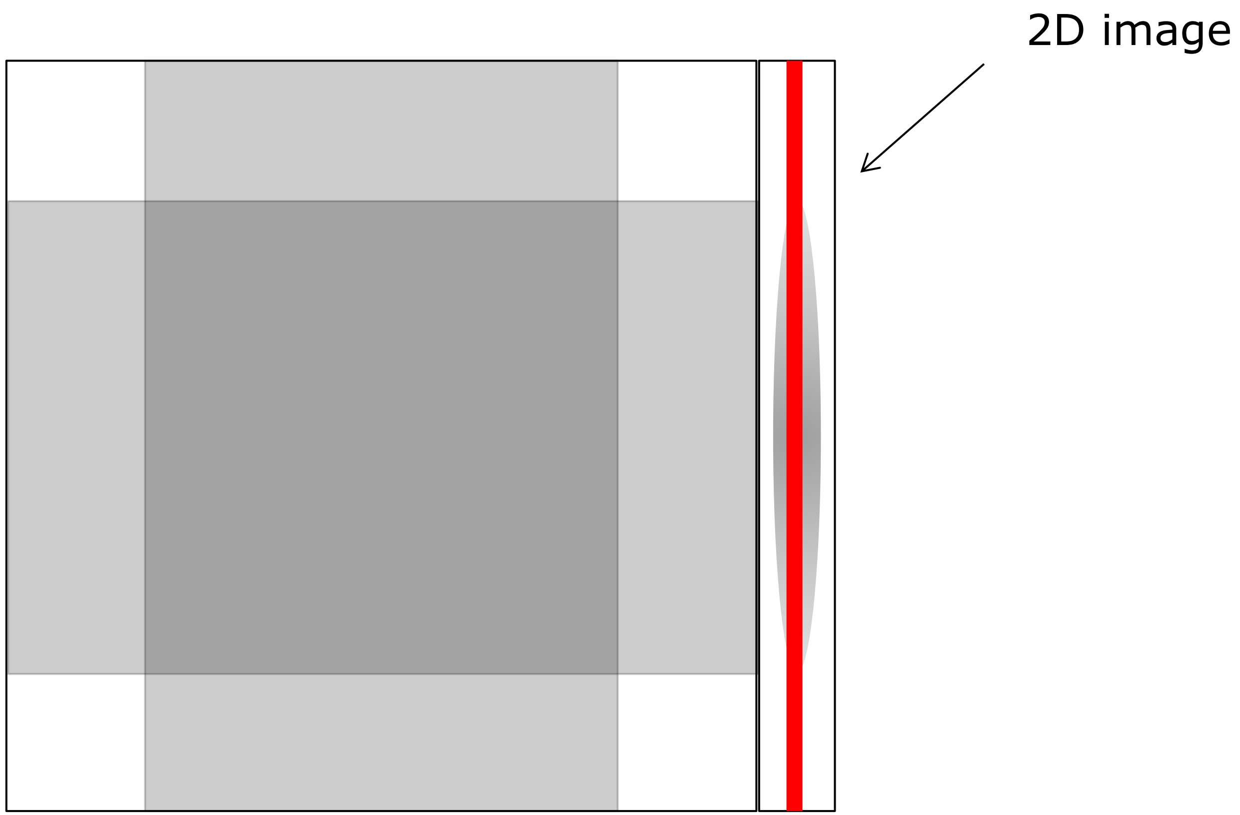

How to make the 3D reconstruction?

Add more backprojection from different angles

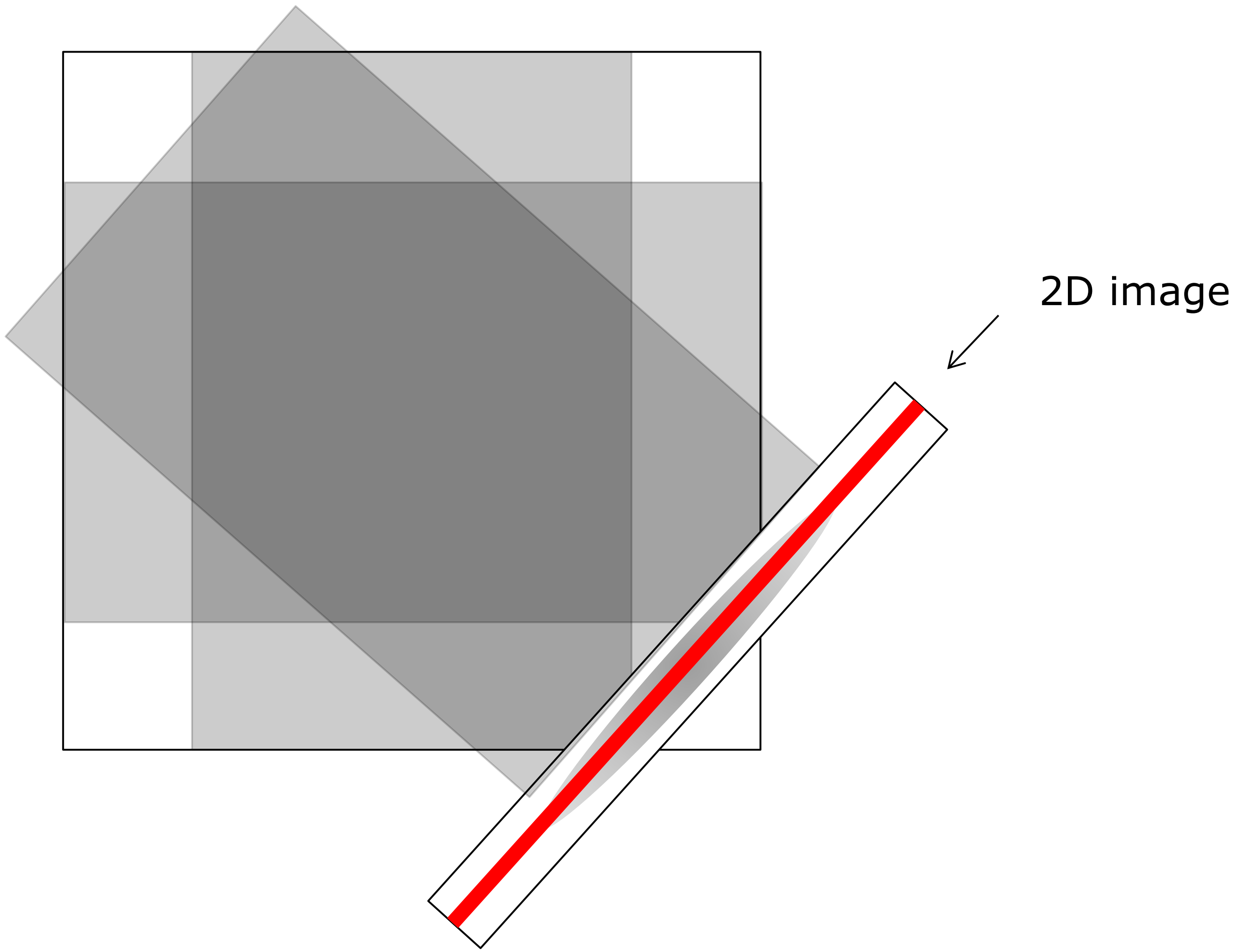

How to make the 3D reconstruction?

Add more backprojections from different angles

More 2D images

↓

Higher quality of the reconstruction

(For the shell 1571 images id u)

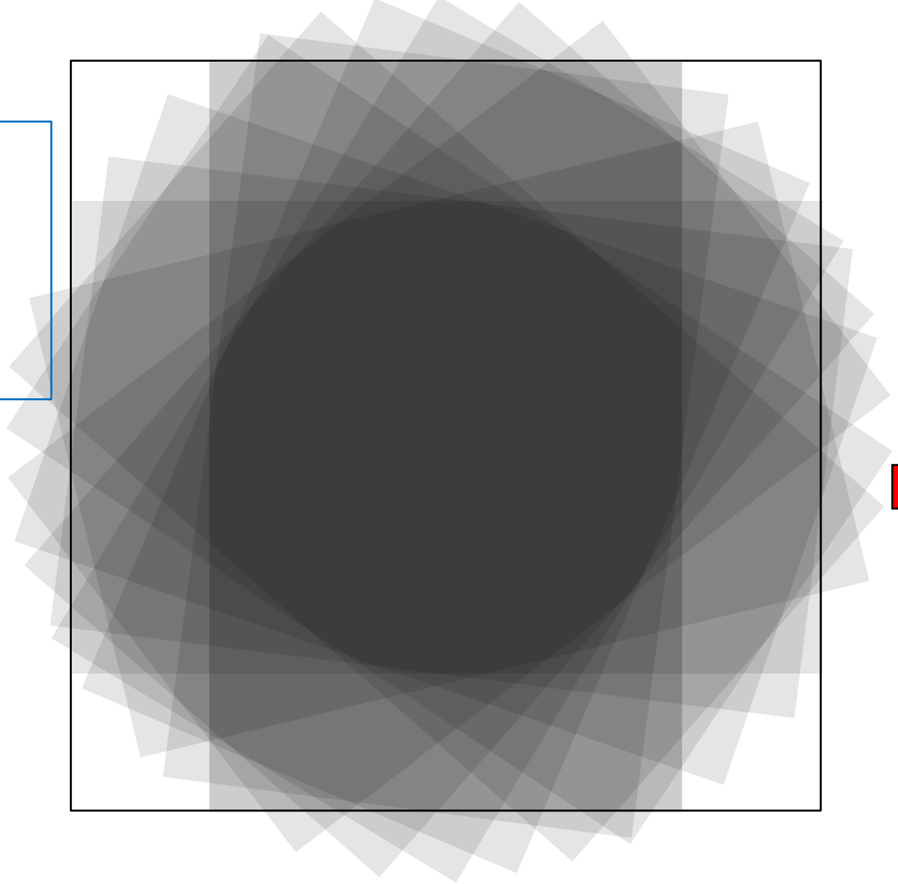

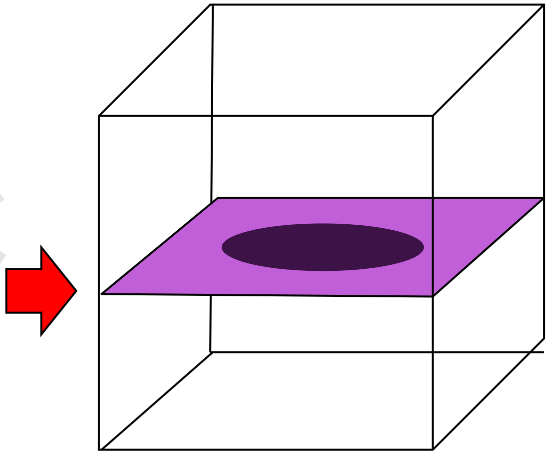

We have now reconstructed **one plane** in the 3D volume
(by using one row of pixels from ten 2D images)

How to make the 3D reconstruction?

All planes in the 3D volume is reconstructed in the same way

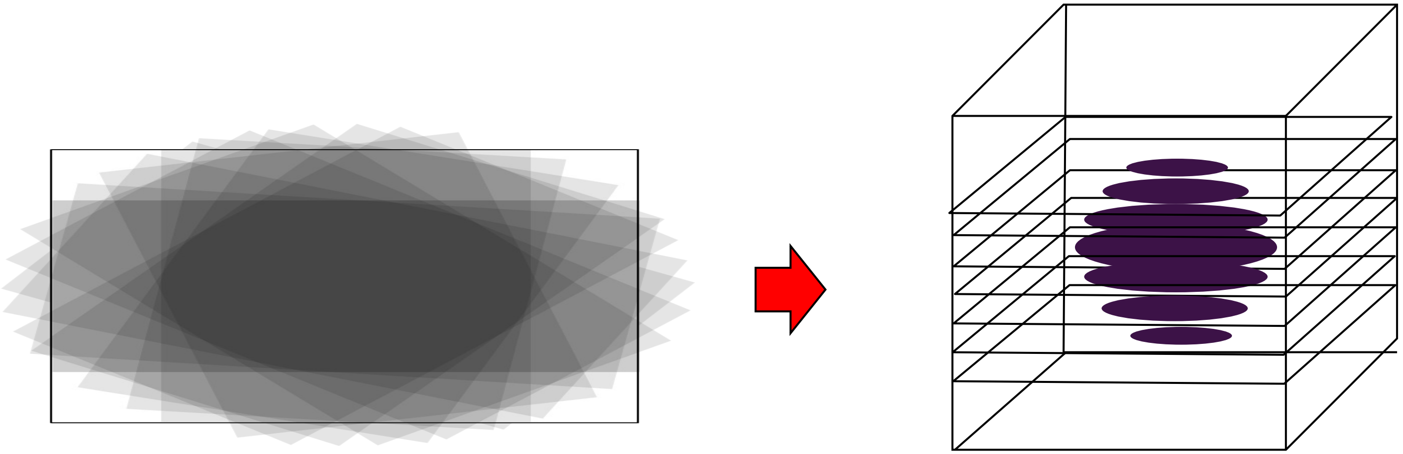

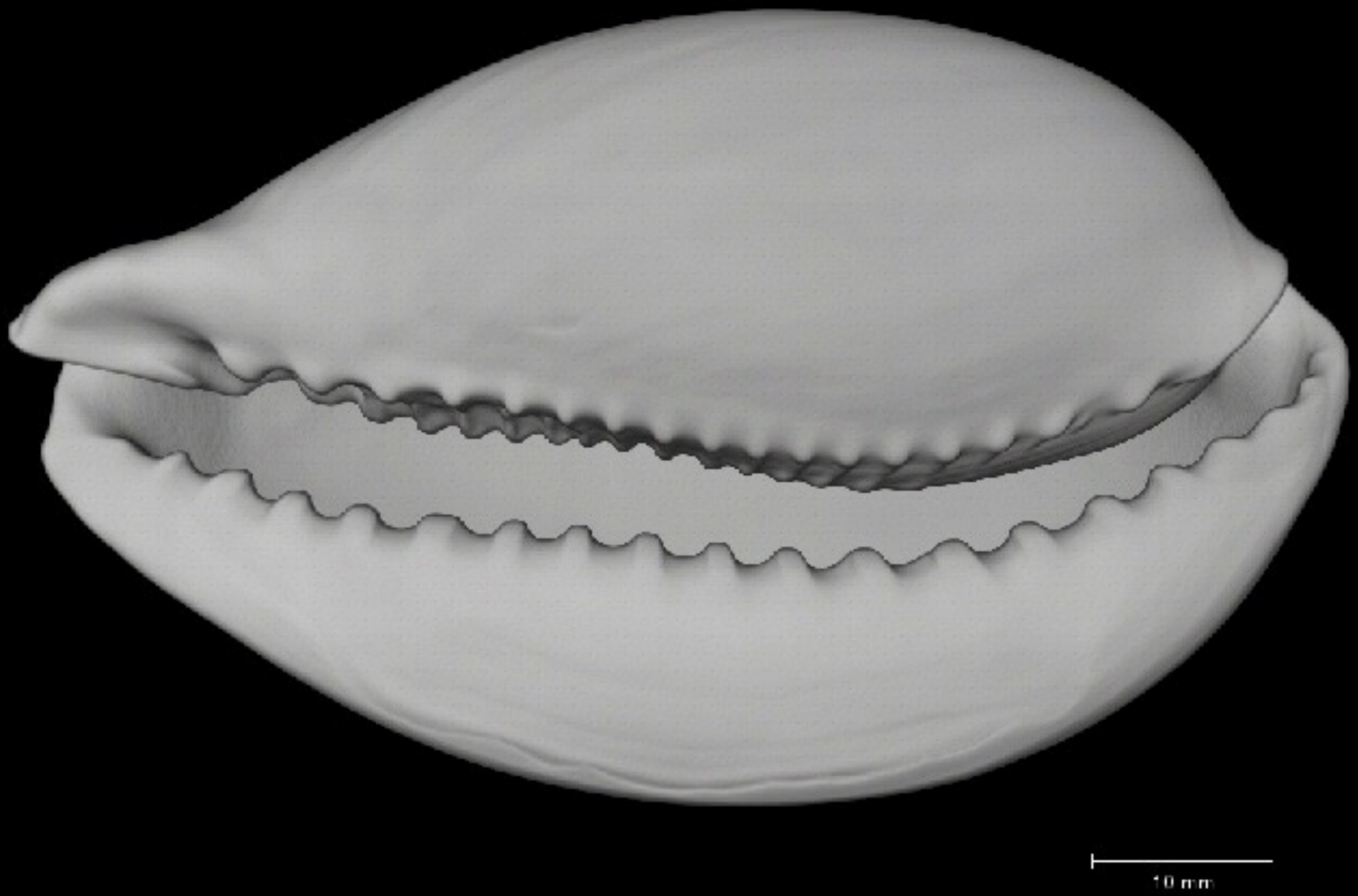
10 mm

2D x-ray image

3D reconstruction

One slice in the 3D reconstruction

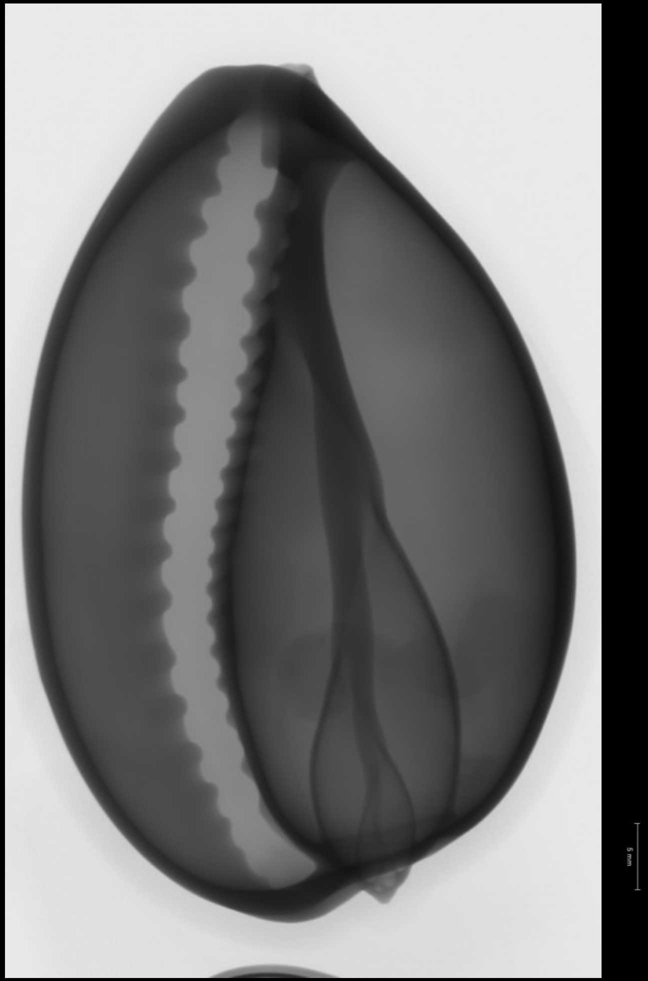

projection

surface

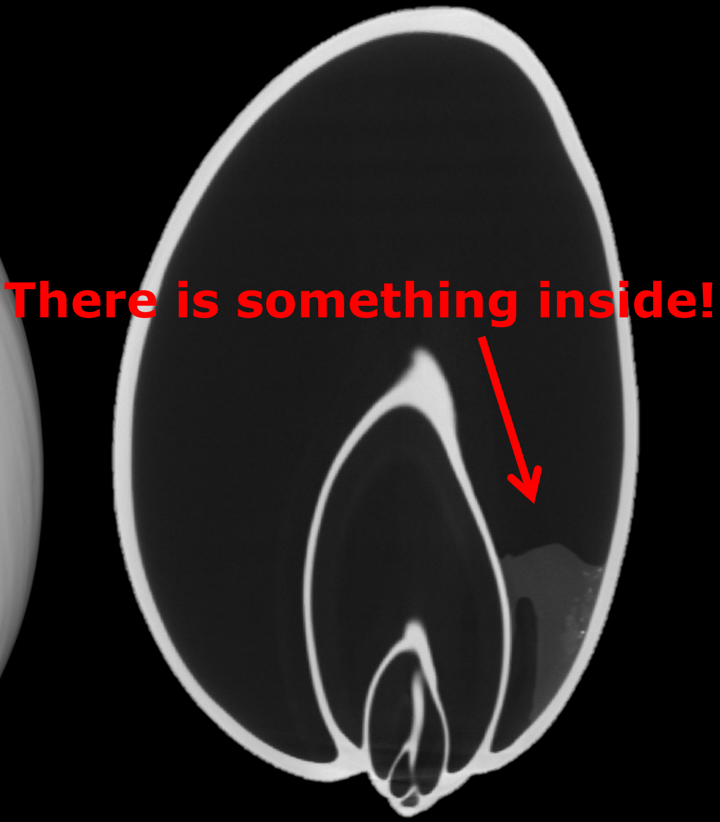

slice

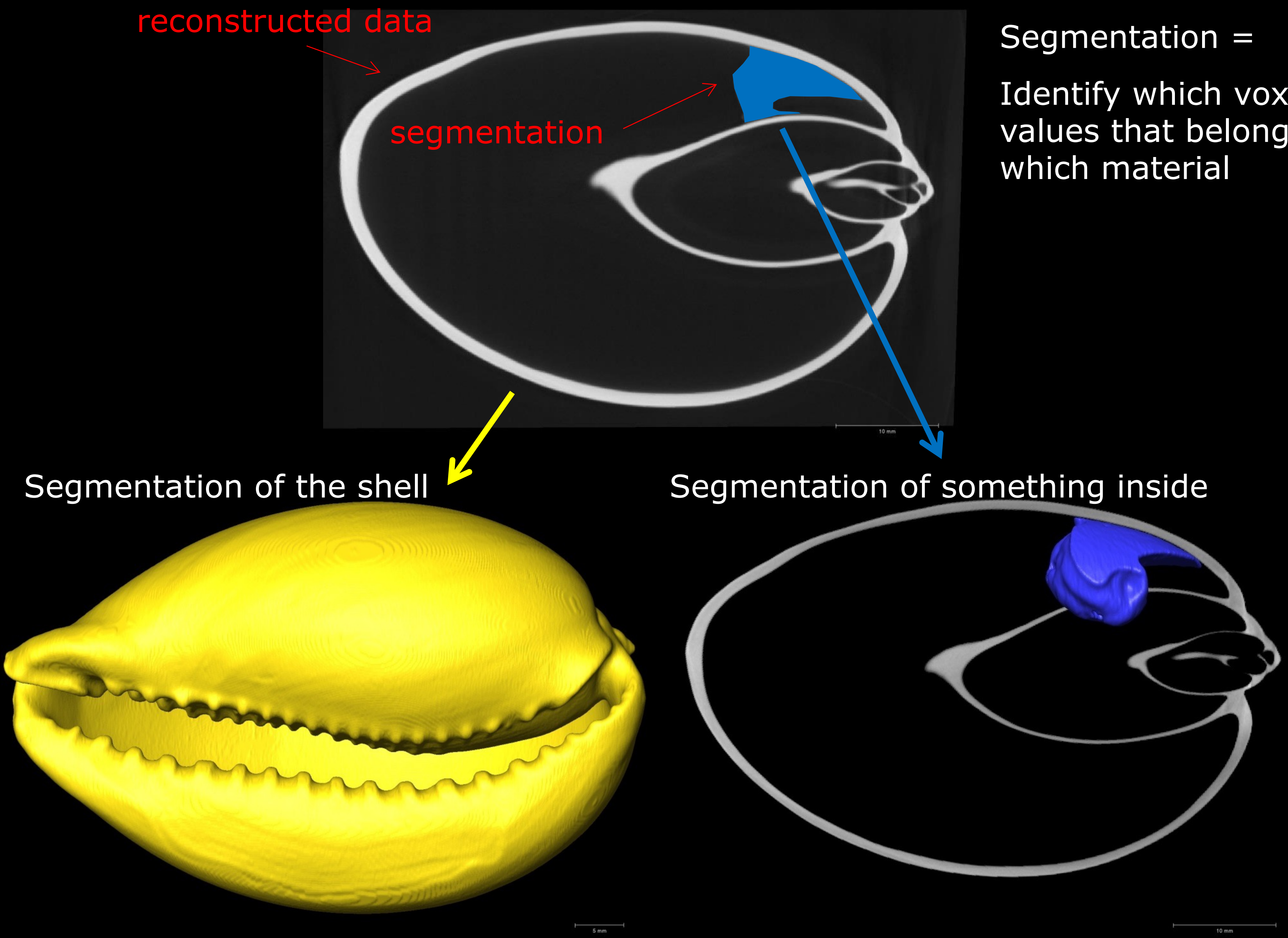

Segmentation =

Identify which voxel values that belong to which material

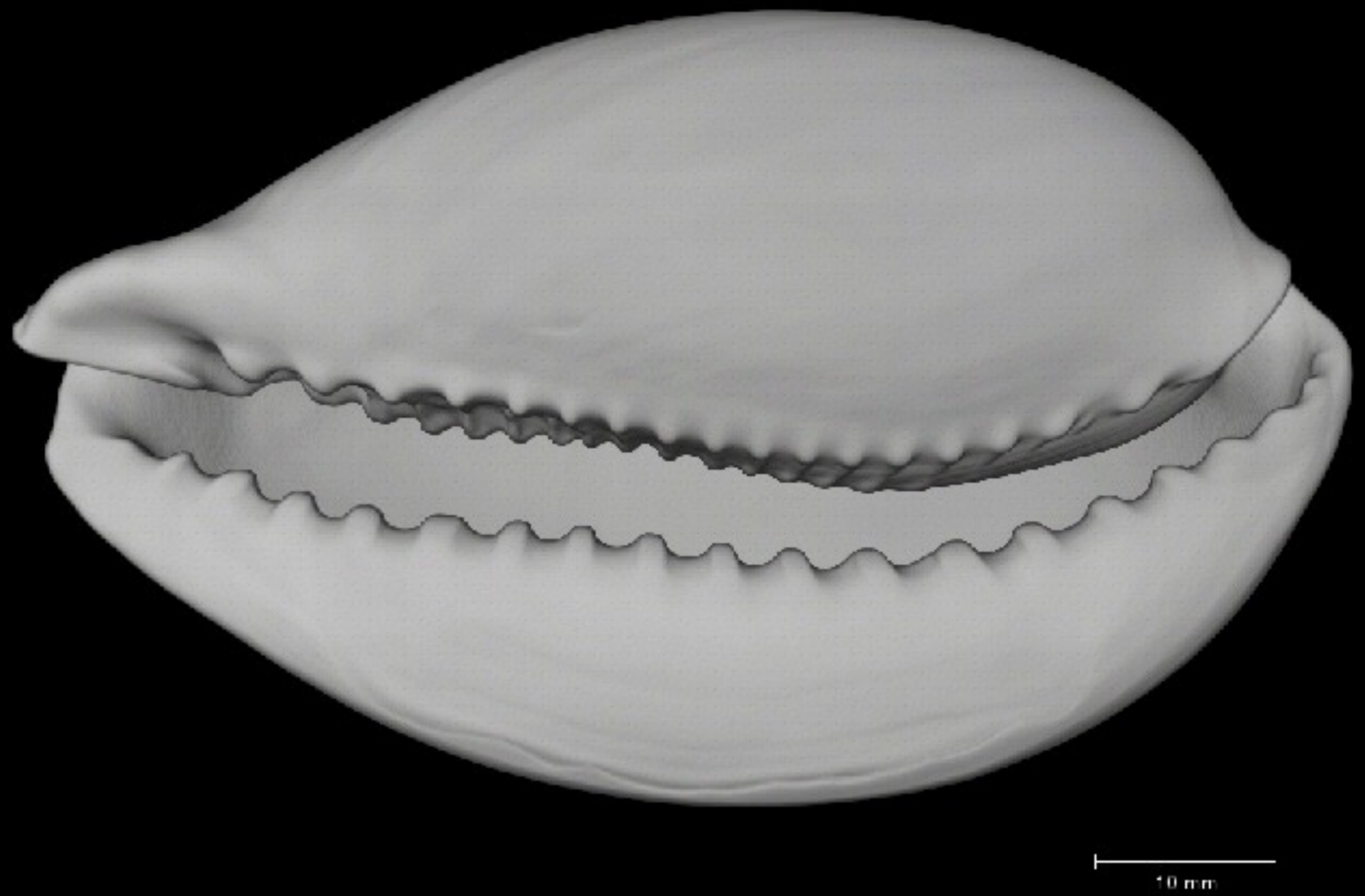
10 mm

Micro component injection moulding

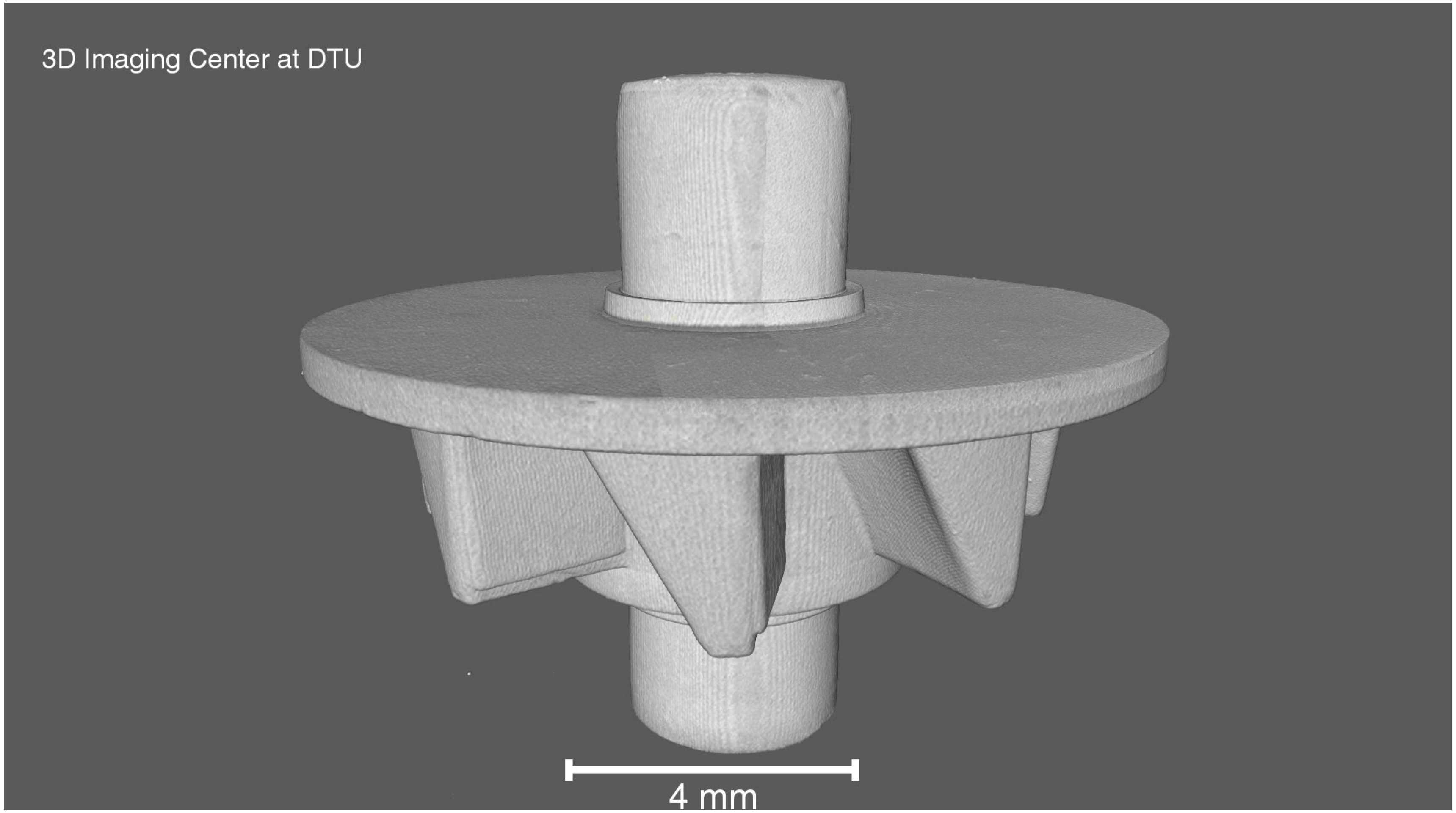

Micro component injection moulding

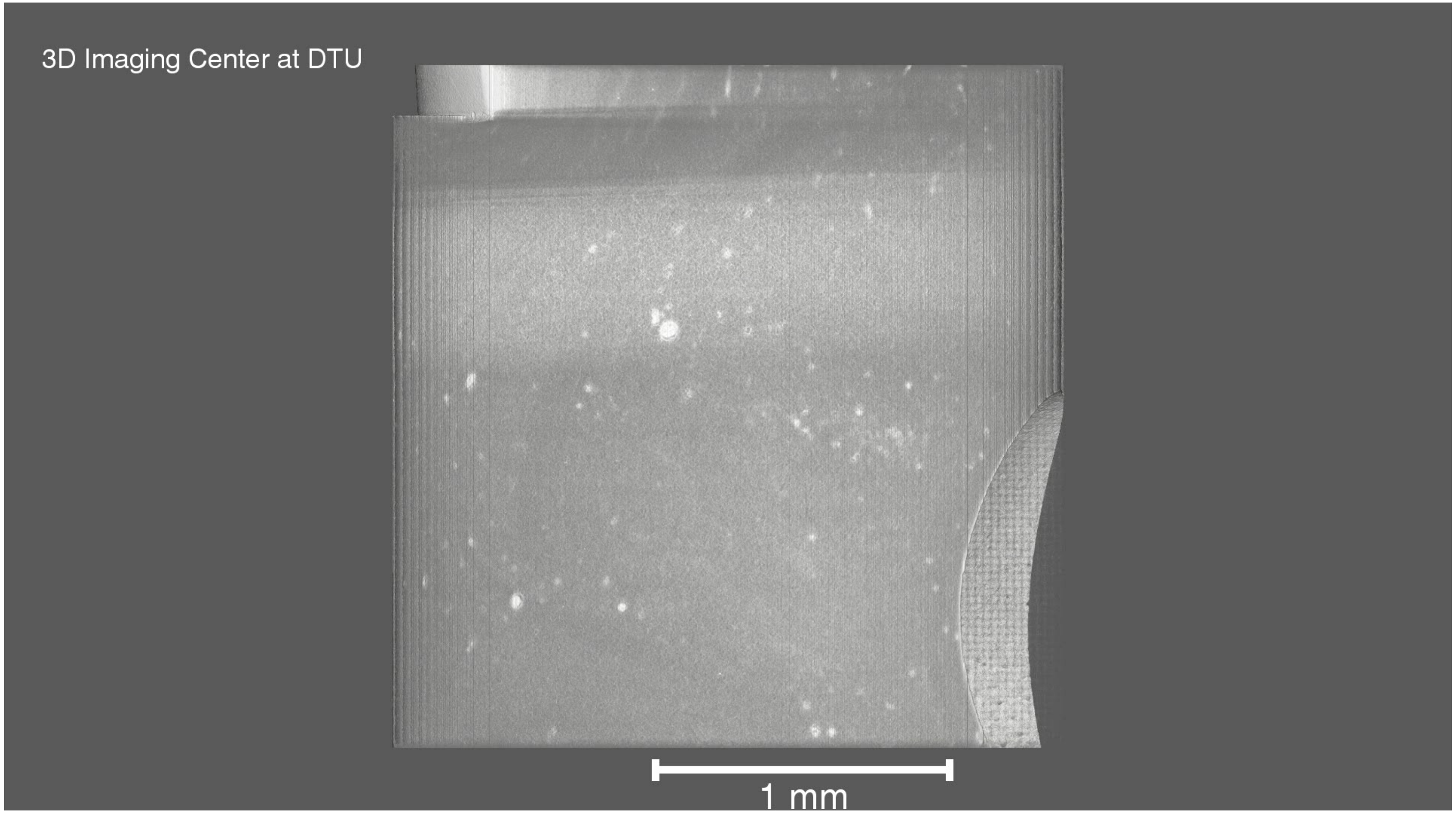

Magic of X-ray tomography

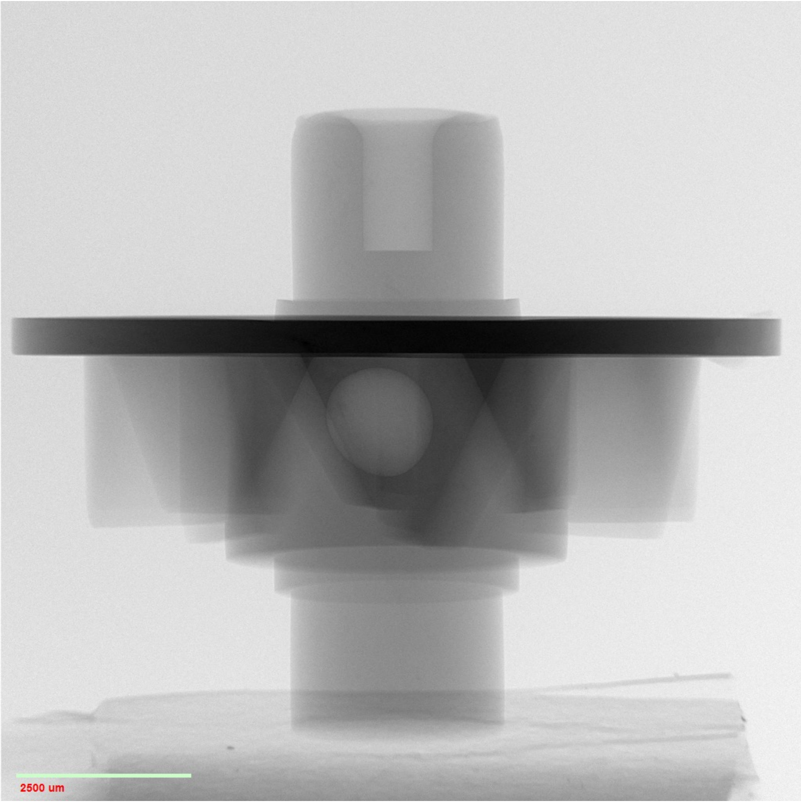

Micro component of Wolfram

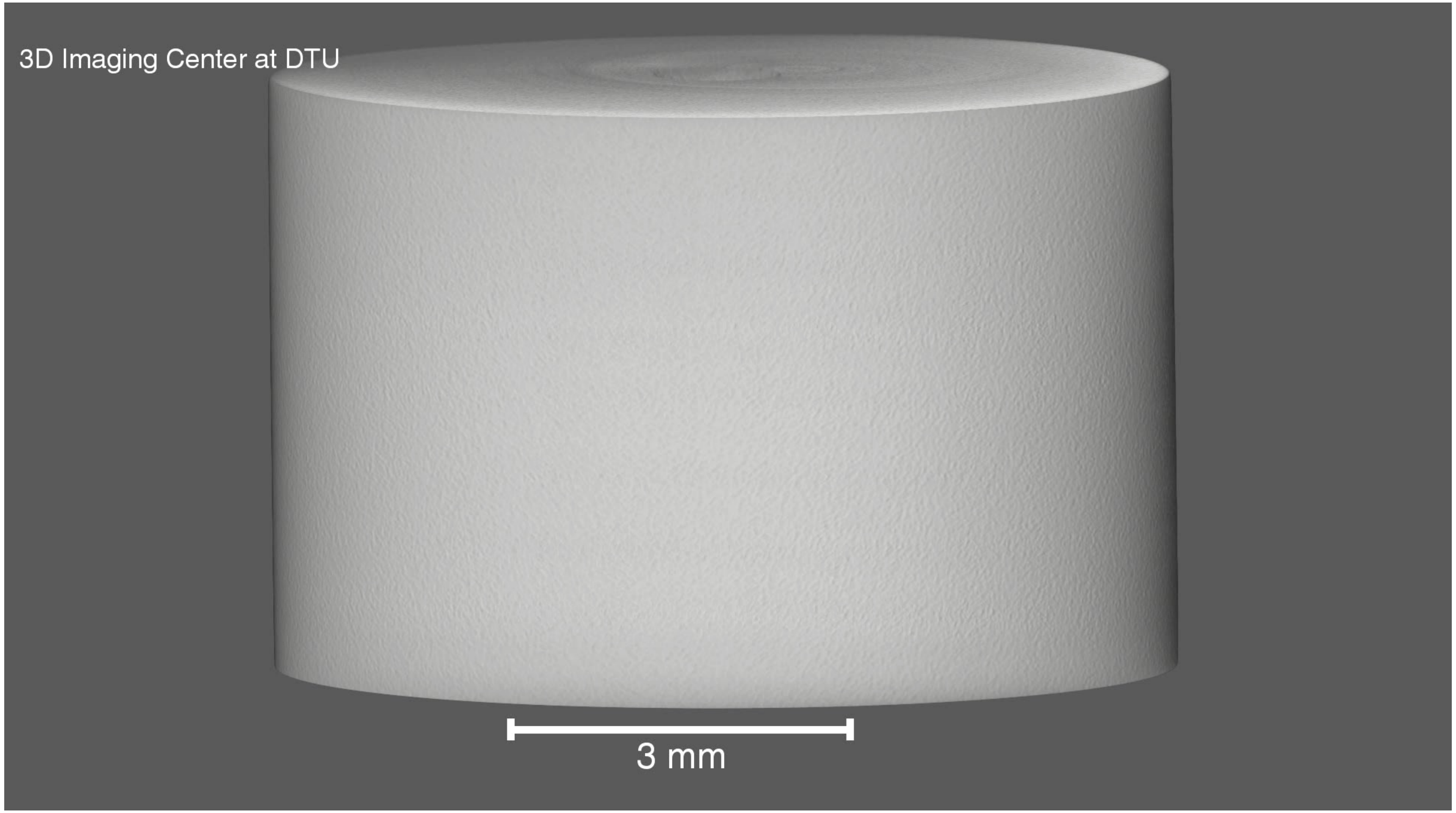

We are not done with this lecture, but let's take a break

3D imaging Center at DTU

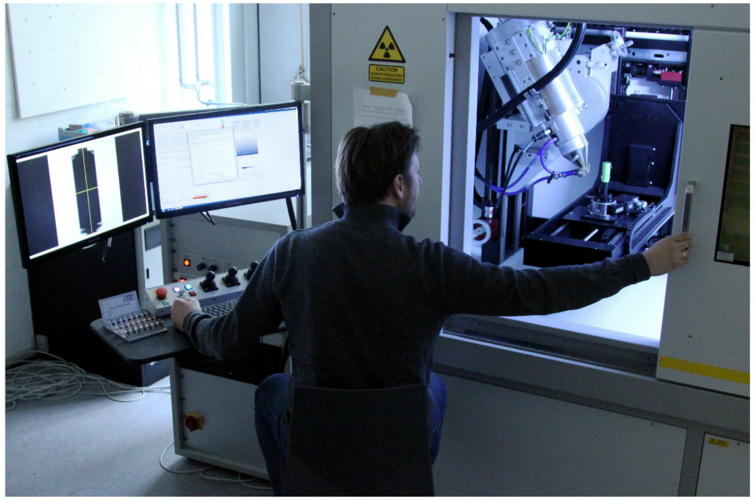

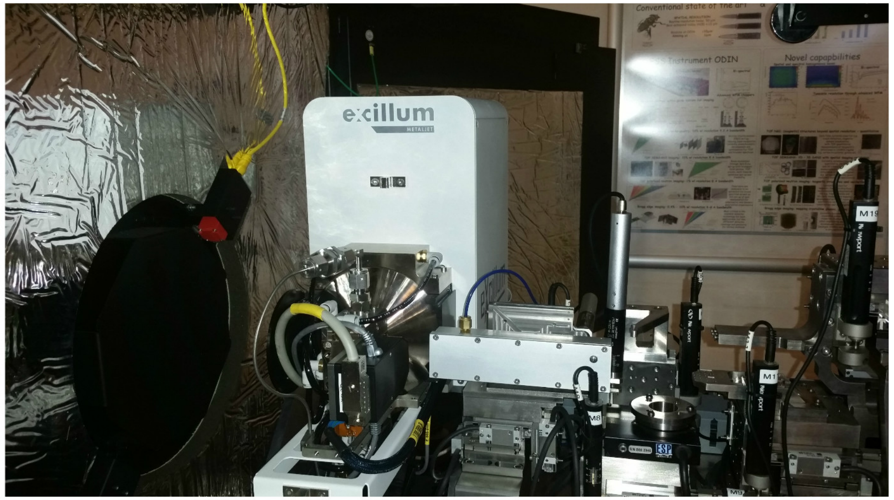

The 3D Imaging Center is a collaborations between different departments with different strengths.

- DTU Physics – Development within X-ray methods and focus on hard materials
- DTU COMPUTE – Development of tomography reconstructions and image segmentation
- DTU Energy – X-ray science and energy materials
- DTU Mechanical Engineering – Mechanical properties of materials and metrology
- DTU Wind Energy – Extensive use of X-ray imaging for materials

3D imaging Center at DTU

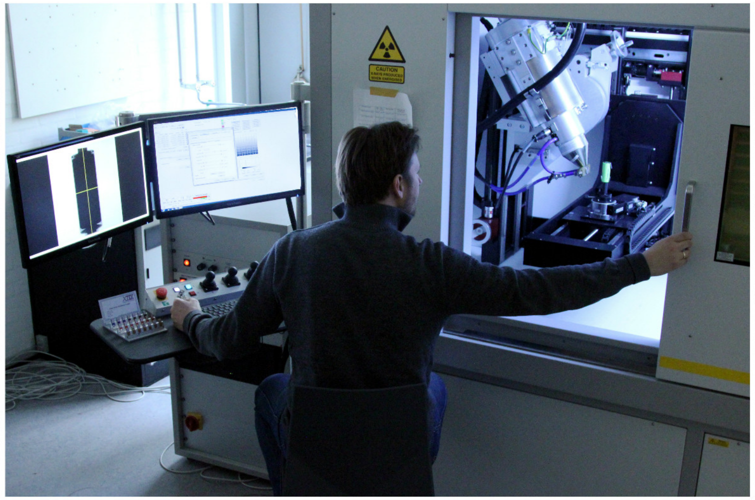

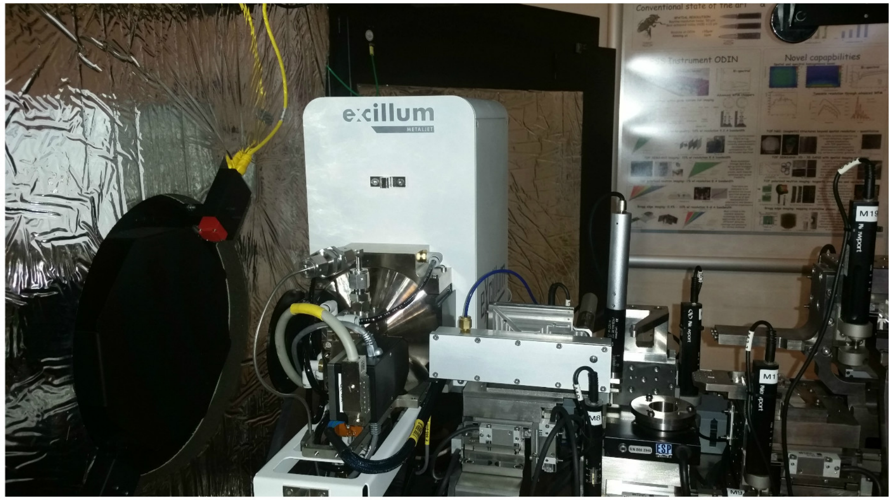

- A national infrastructure for x-ray imaging: DANFIX
- A regional facility for data analyses: QIM
- An ESS lighthouse: SOLID
- An industry portal
- A science hub for materials and bioimaging

QIM: The Center for Quantification of Imaging Data
DTU, KU, LU, MAX IV & The 3D Imaging Centre

Imaging

Structural quantification is the most time-consuming part of imaging

Users are often not analysis experts
- difficulty in handling data
- difficulty in finding method that match problem

Can lead to that data is not utilized to its full potential!

Purpose

Support users at MAX IV & lab facilities with image analysis

- Case-specific collaboration
- Competence development
- Development of tools and analysis pipelines

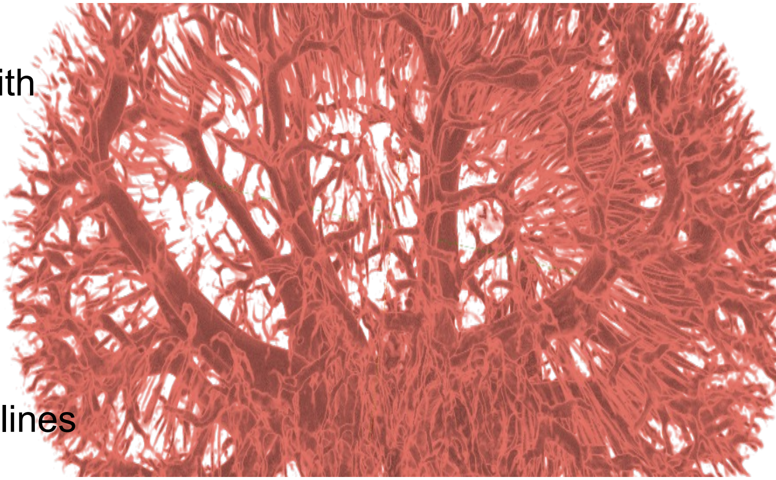

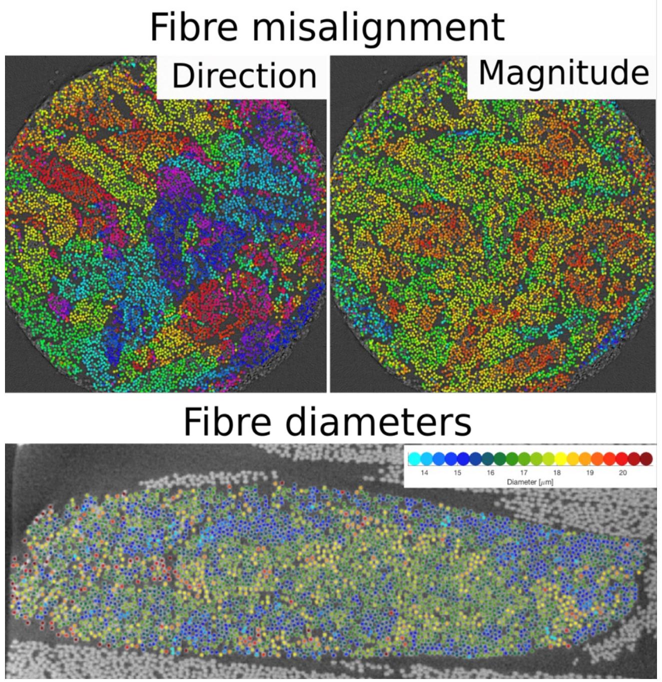

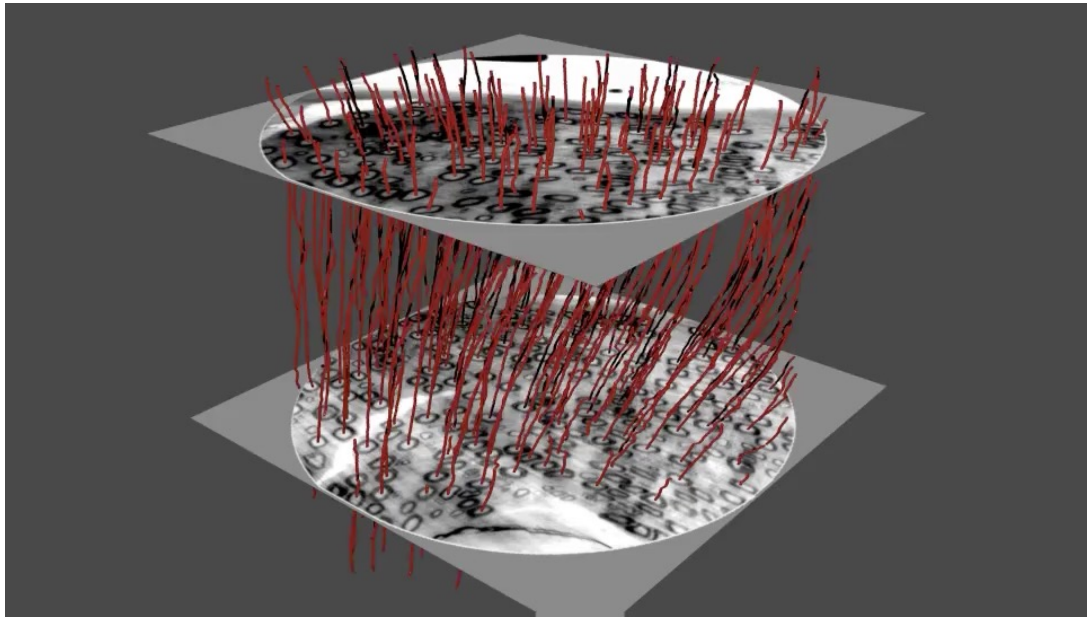

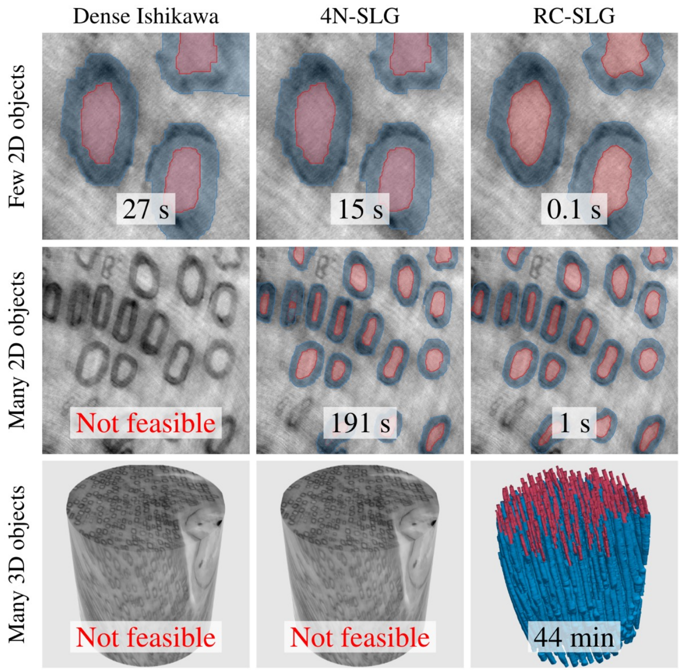

Characterization of subcutaneous insulin injections

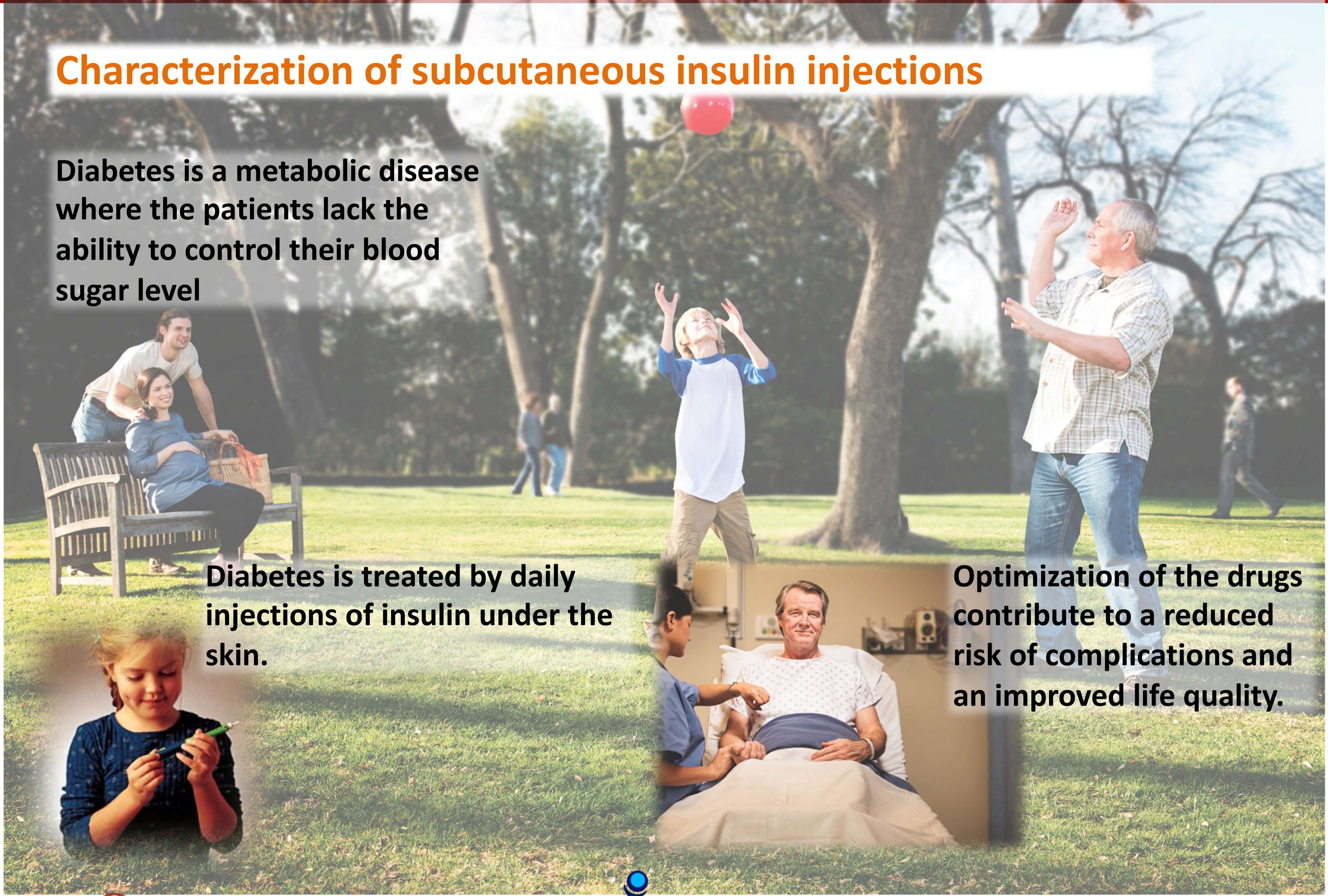

Diabetes is a metabolic disease where the patients lack the ability to control their blood sugar level

Diabetes is treated by daily injections of insulin under the skin.

Optimization of the drugs contribute to a reduced risk of complications and an improved life quality.

FACULTY OF SCIENCE
UNIVERSITY OF COPENHAGEN

novo nordisk®

DTU Technical University of Denmark

Characterization of subcutaneous insulin injections

Pigs are commonly used as an animal model for optimization of new drug formulations.

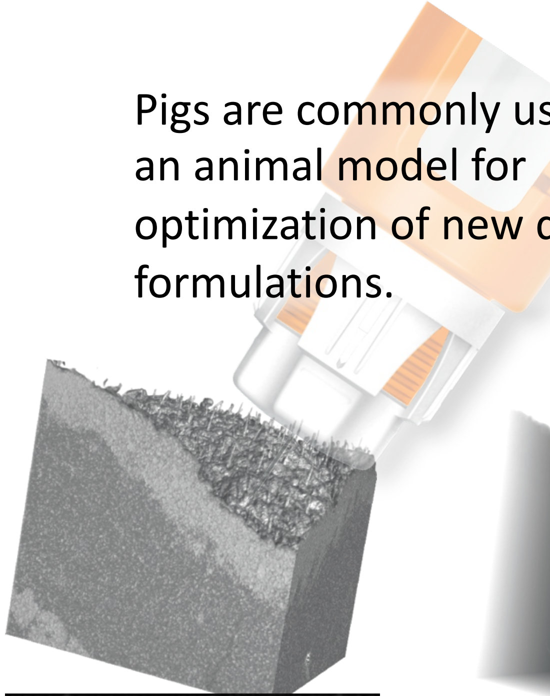

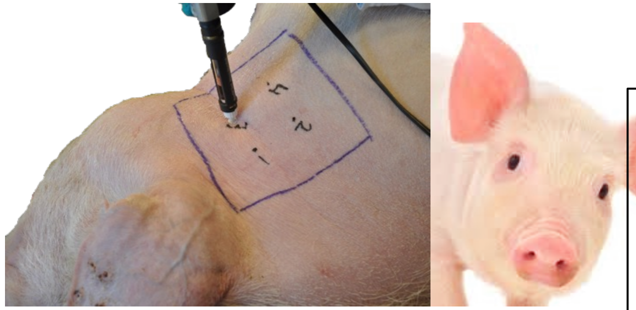

- LFOV
- 40 kV
- 5 sec
- LE2
- 401 projections

Insulin drugs mixed with an iodine based contrast agent has been injected under the skin of research pigs.

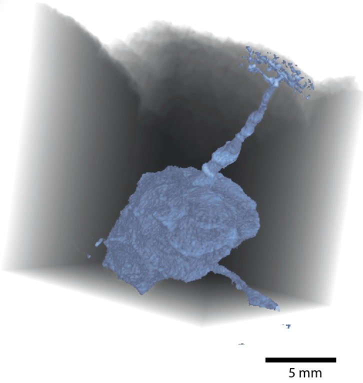

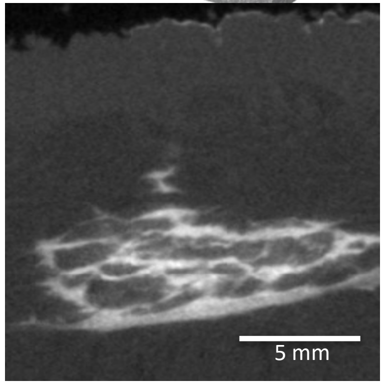

The drug distribution has been visualized with high spatial resolution using the Xradia Versa VRM-410 at DTU.

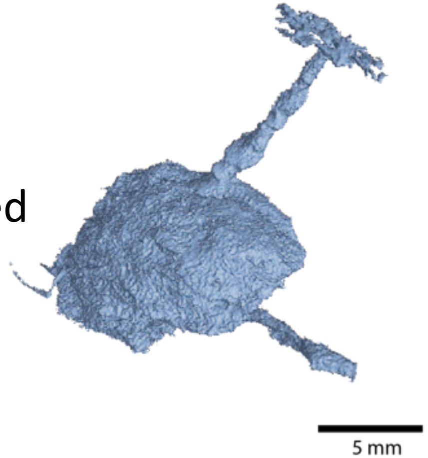

FACULTY OF SCIENCE
UNIVERSITY OF COPENHAGEN

novo nordisk®

DTU Technical University of Denmark

Injection depth and drug dissolution

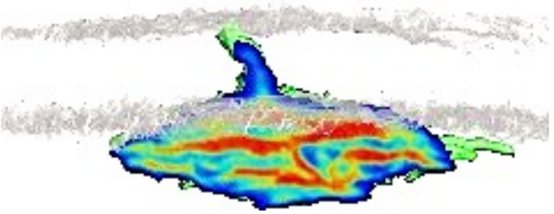

The different skin layers can be separated and the dissolution of insulin can be evaluated for the CT-scan.

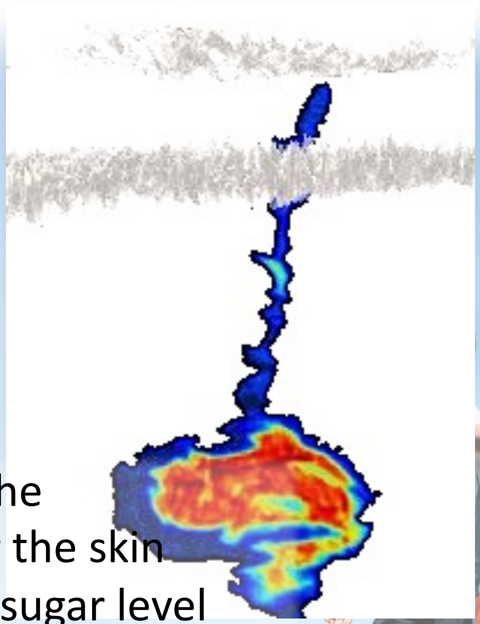

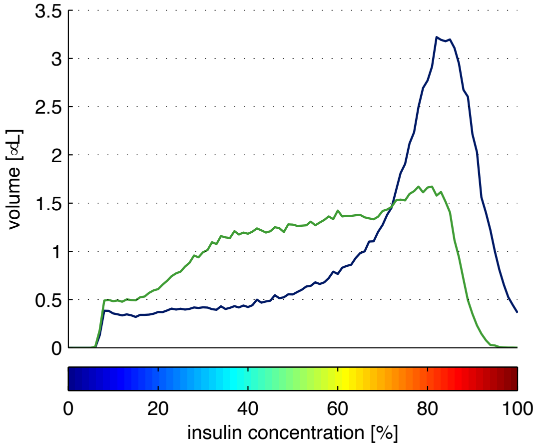

The position of the drug and the concentration of insulin under the skin influences how fast the blood sugar level decreases after the drug has been injected.

Visualization of the injection process is an important step on the way to understanding the drug device interaction and to potentially improve both drugs and devices in the future.

FACULTY OF SCIENCE
UNIVERSITY OF COPENHAGEN

novo nordisk®

DTU Technical University of Denmark

Micro containers for drug delivery

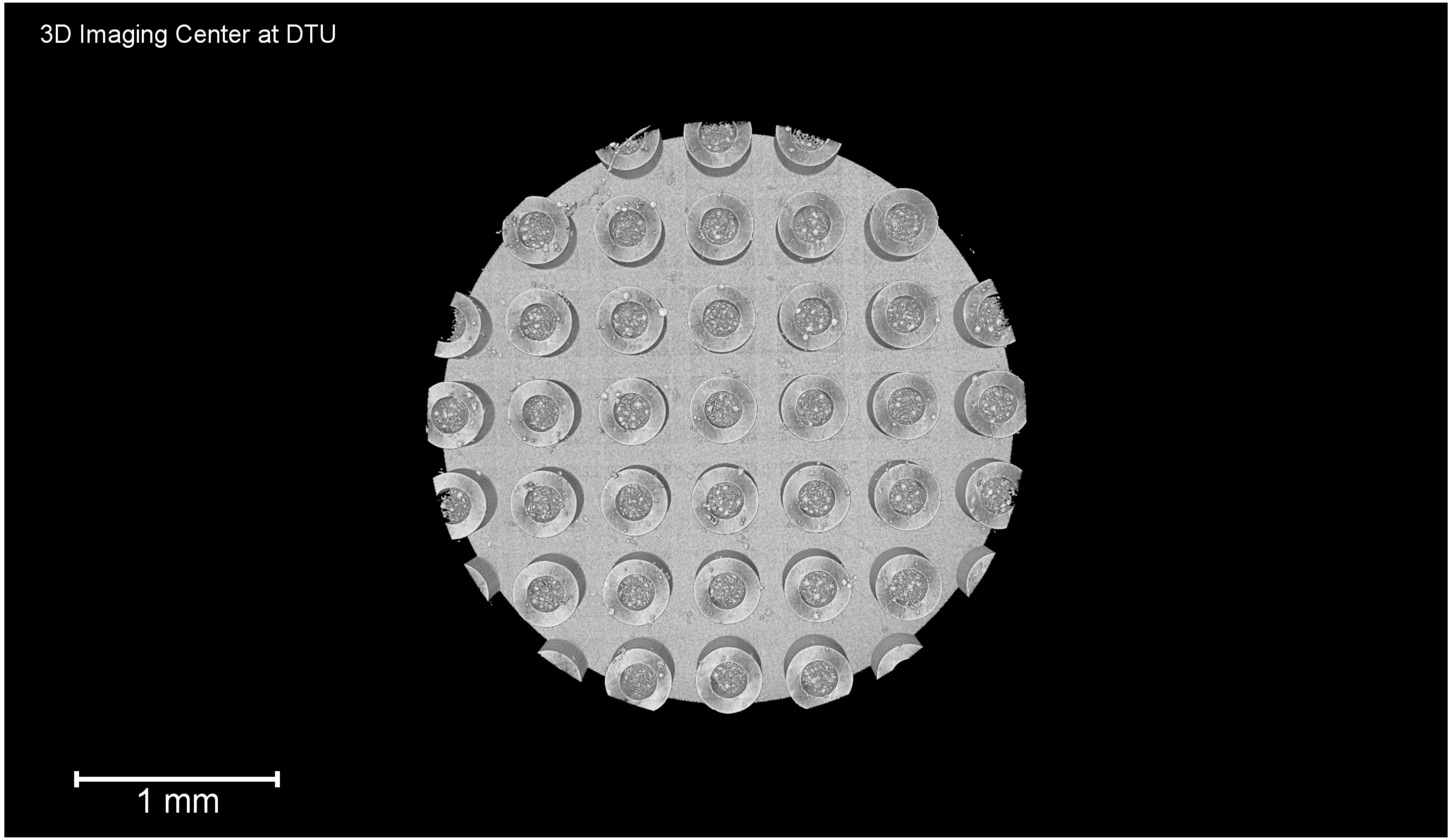

Collaboration with IDUN

Micro containers for drug delivery

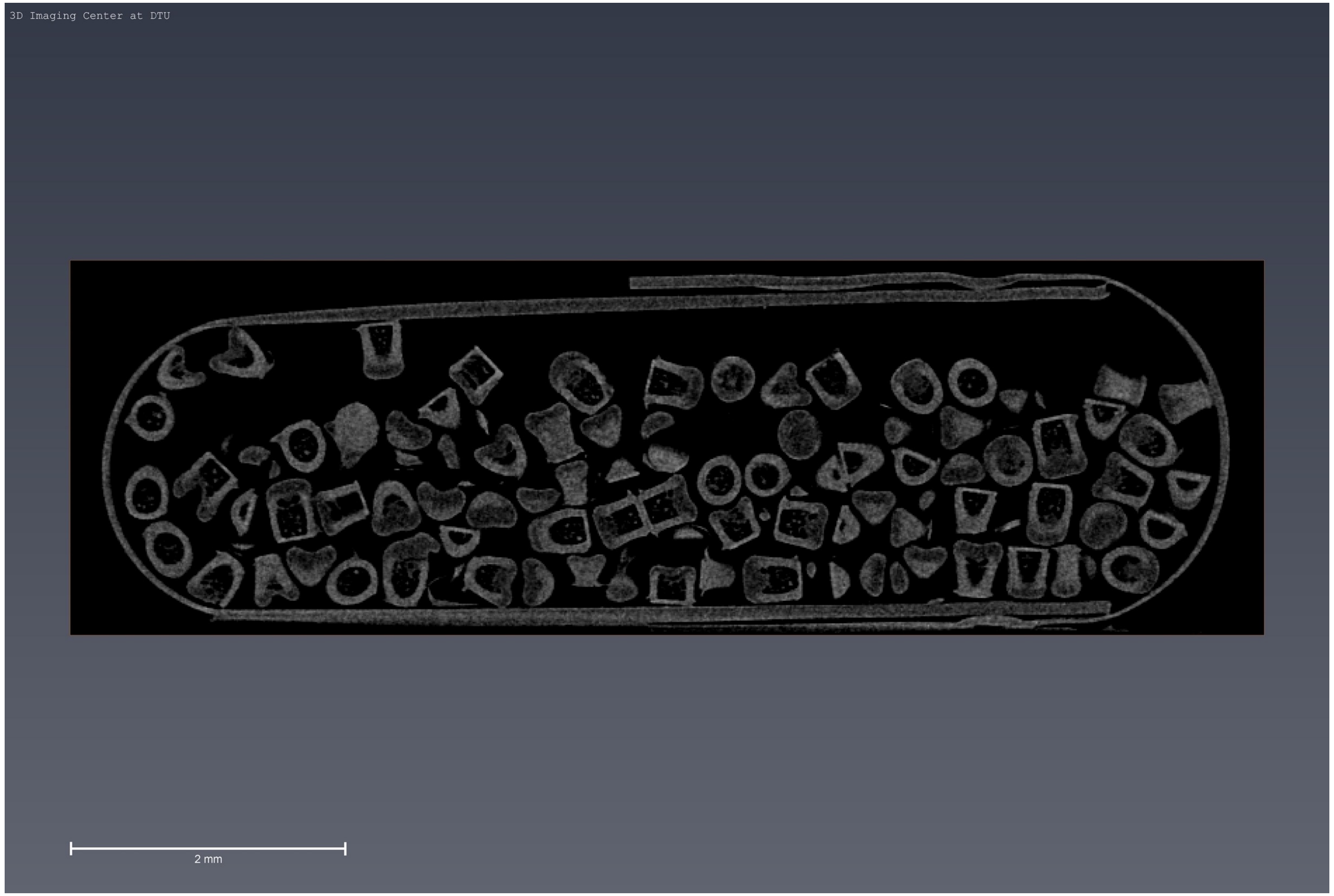

Collaboration with IDUN

Micro containers for drug delivery

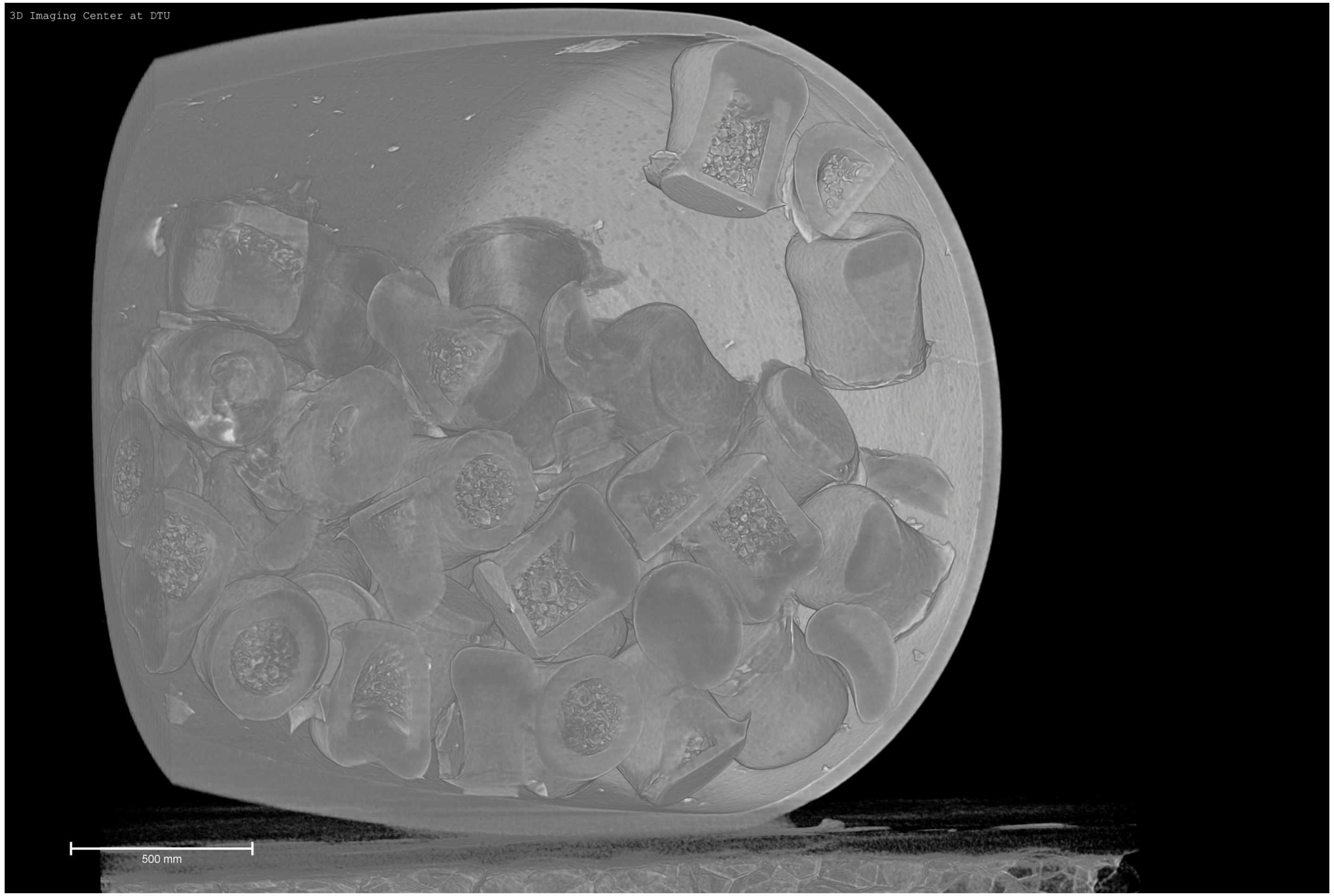

Collaboration with IDUN

Micro container in rat

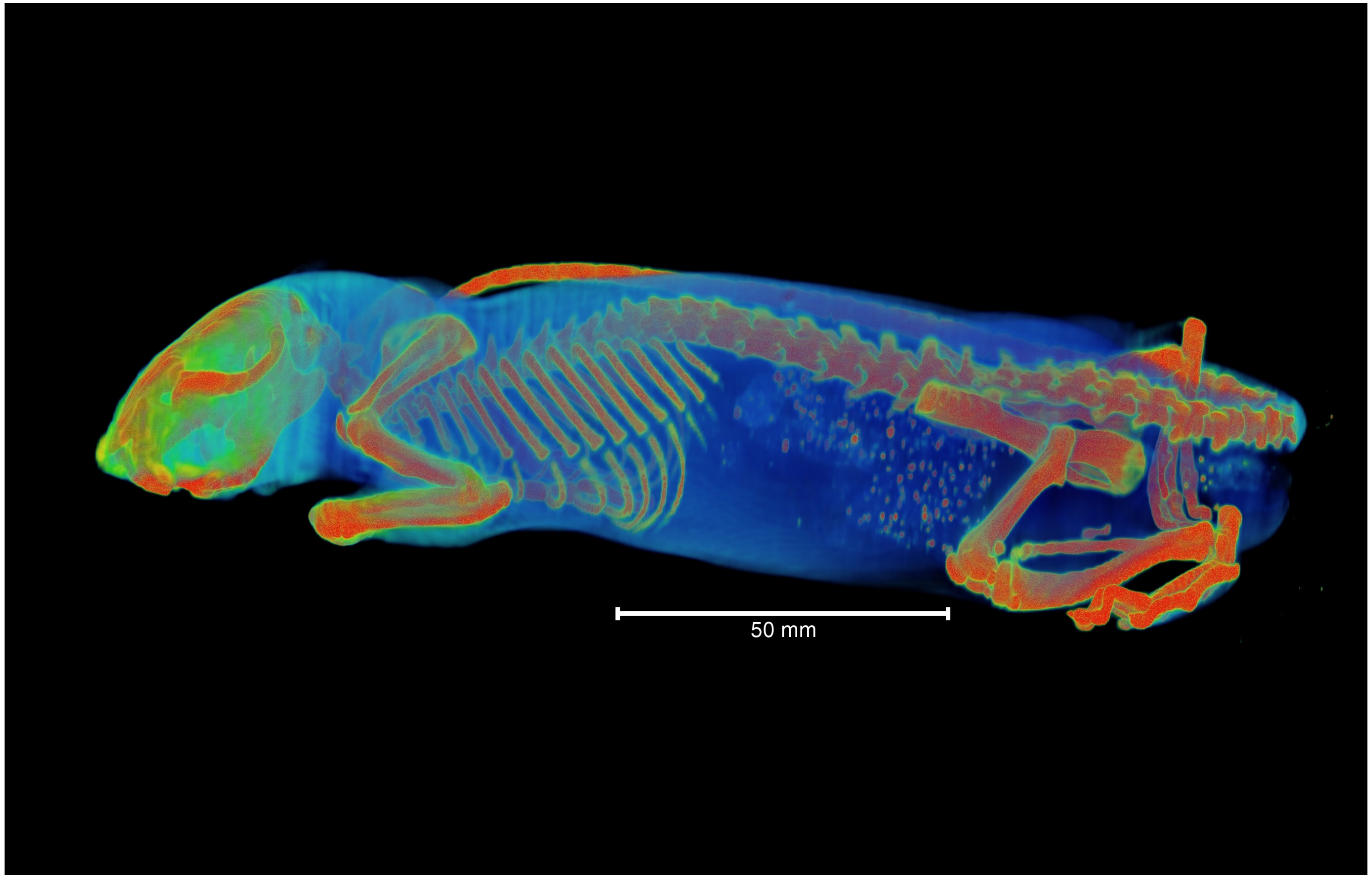

Rat Kidney

Collaboration with groups of Jørgen Ahrent Jensen and Charlotte Mehlin Sørensen

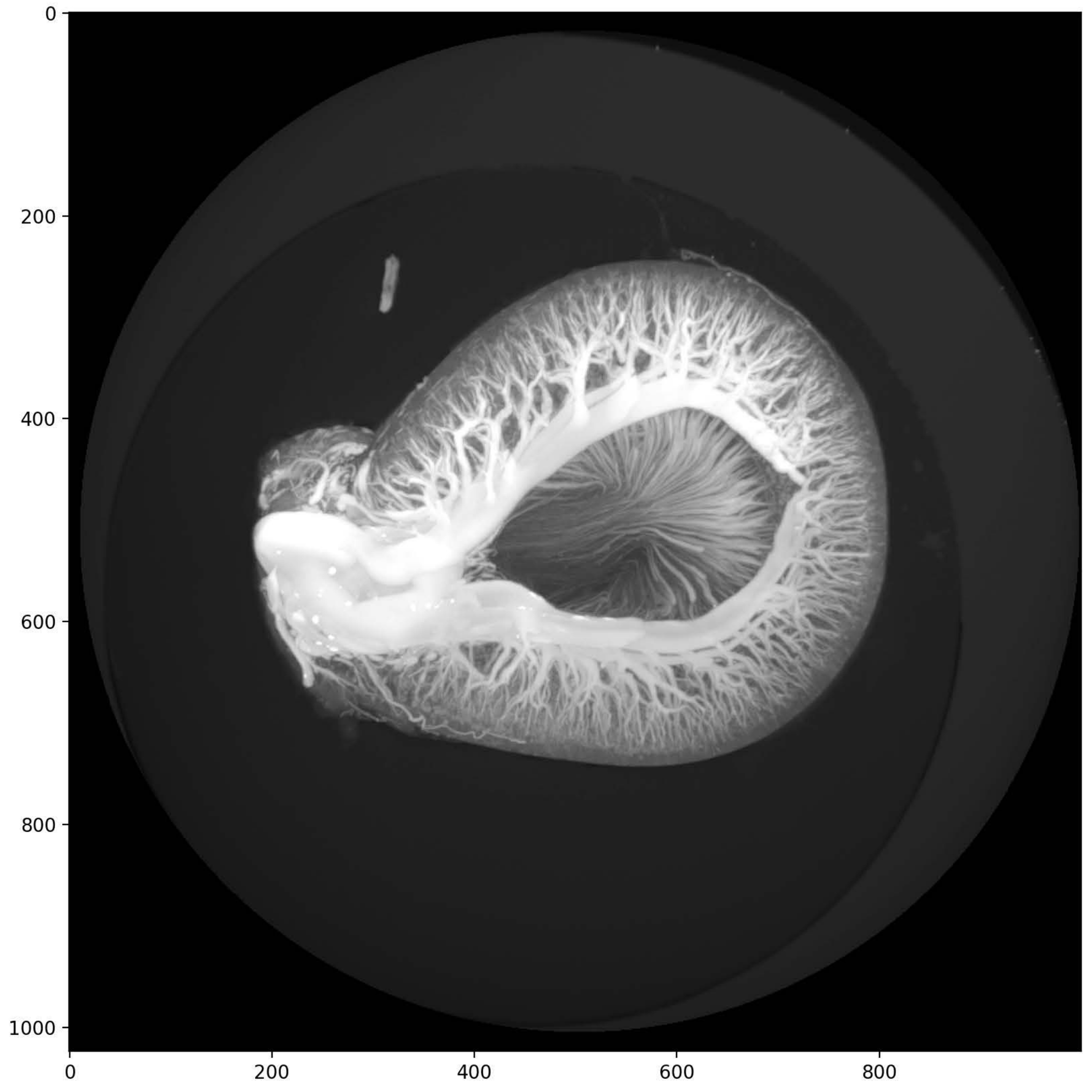

Collaboration with groups of Jørgen Ahrent Jensen and Charlotte Mehlin Sørensen

Project 3: Full kidney in ‘high res’

- Synchrotron experiment
  - Effective volume size: ~ [5500 x 6300 x 9000]

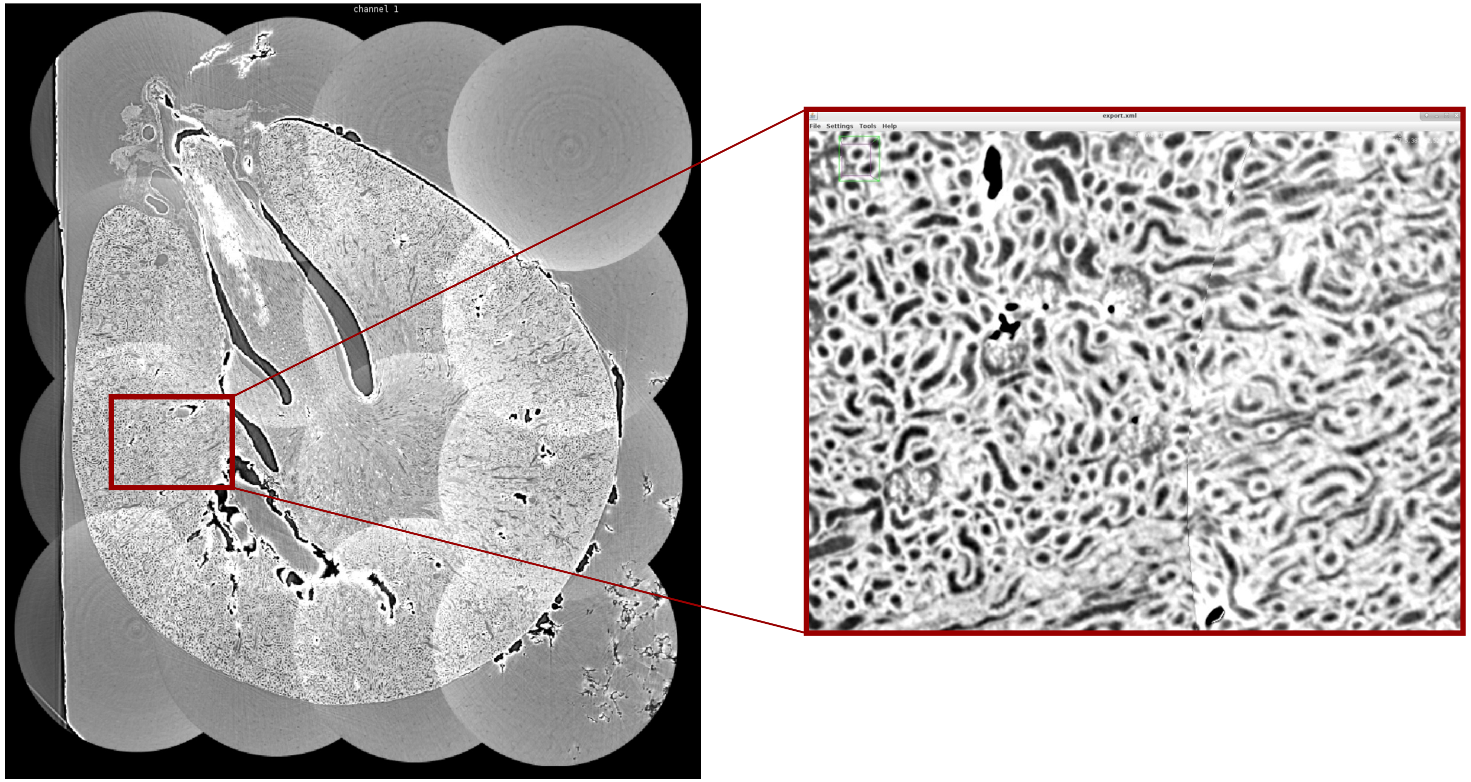

BiotoBank: optical nerve

Acquired with Zeiss Versa 520

Pixel size= 3.4 µm

Field of view= 3.5 mm

Scan time = 3 h

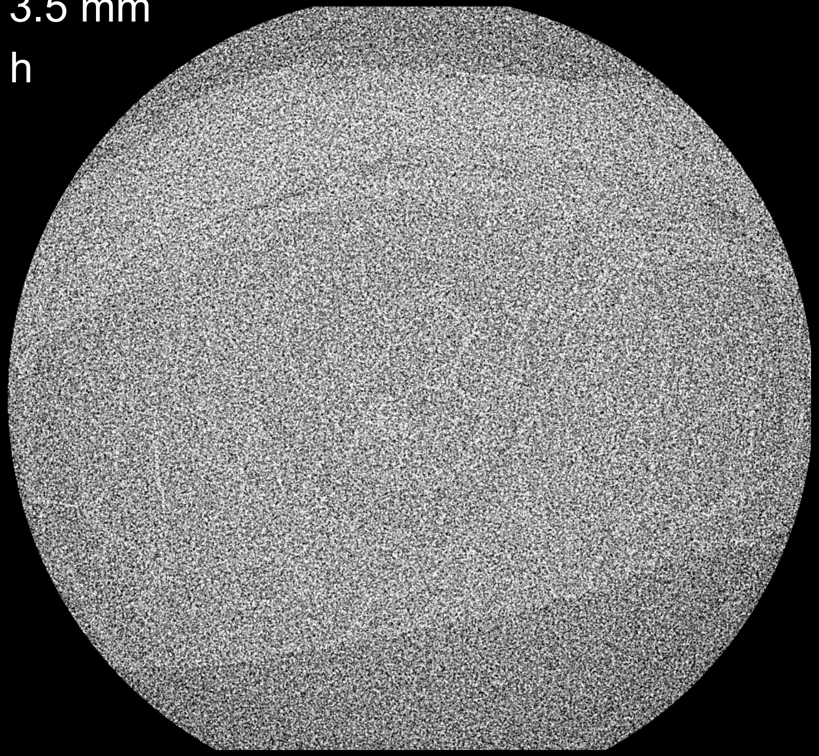

Acquired with exciscope

Pixel size= 3 µm

Field of view= 12 mm

Scan time = 1 h

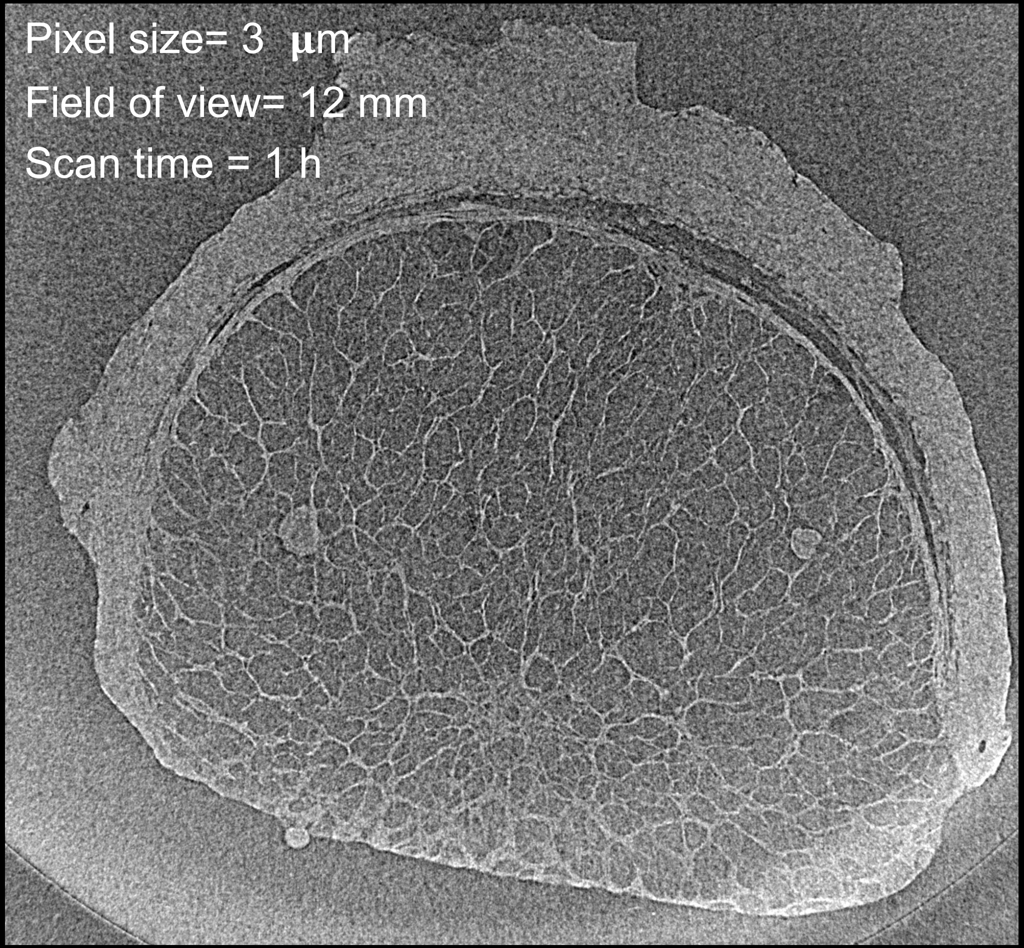

reference

3D X-ray imaging of grass

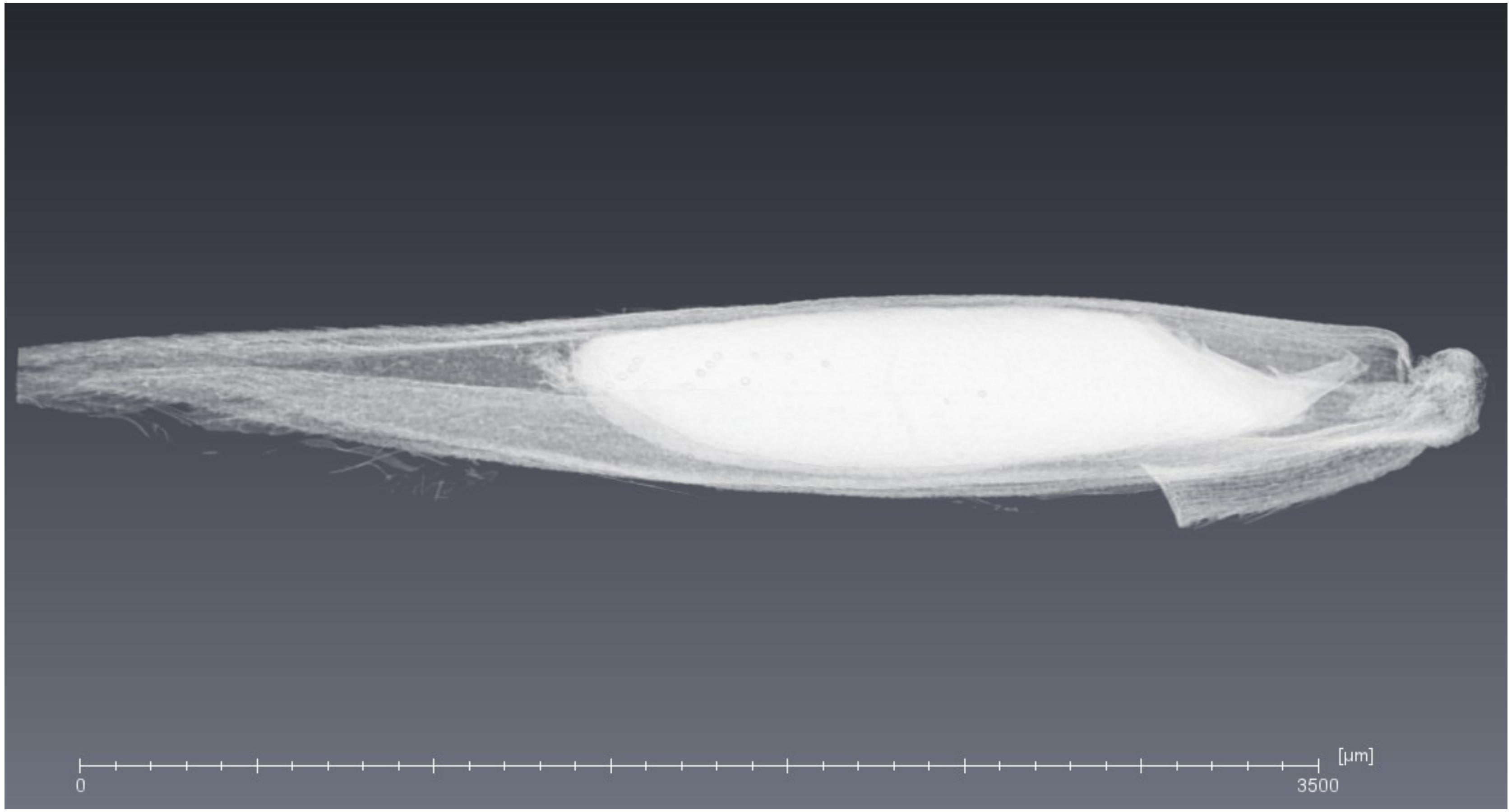

13/4-2015

3D X-ray imaging of grass

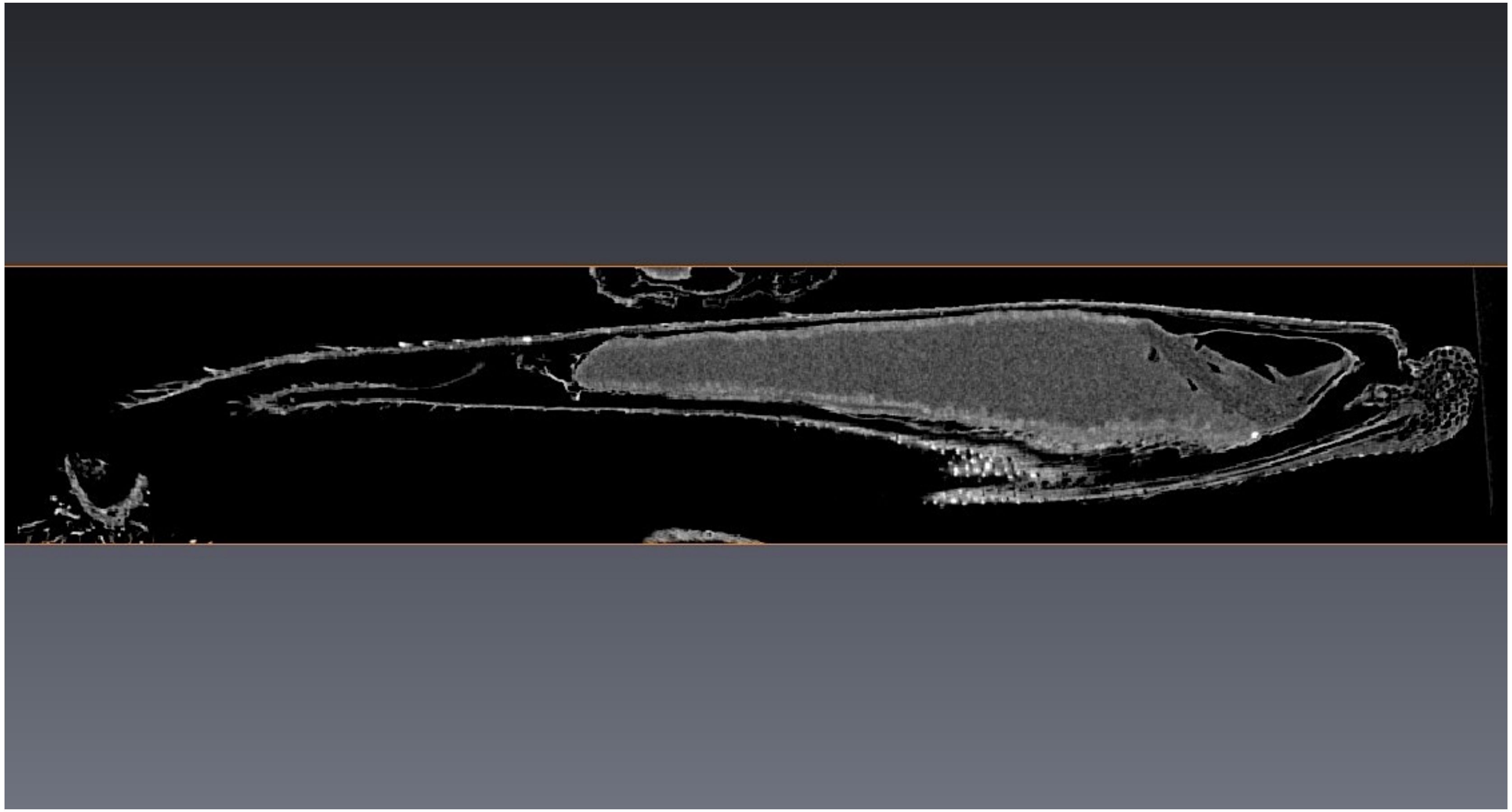

13/4-2015

3D X-ray imaging of grass

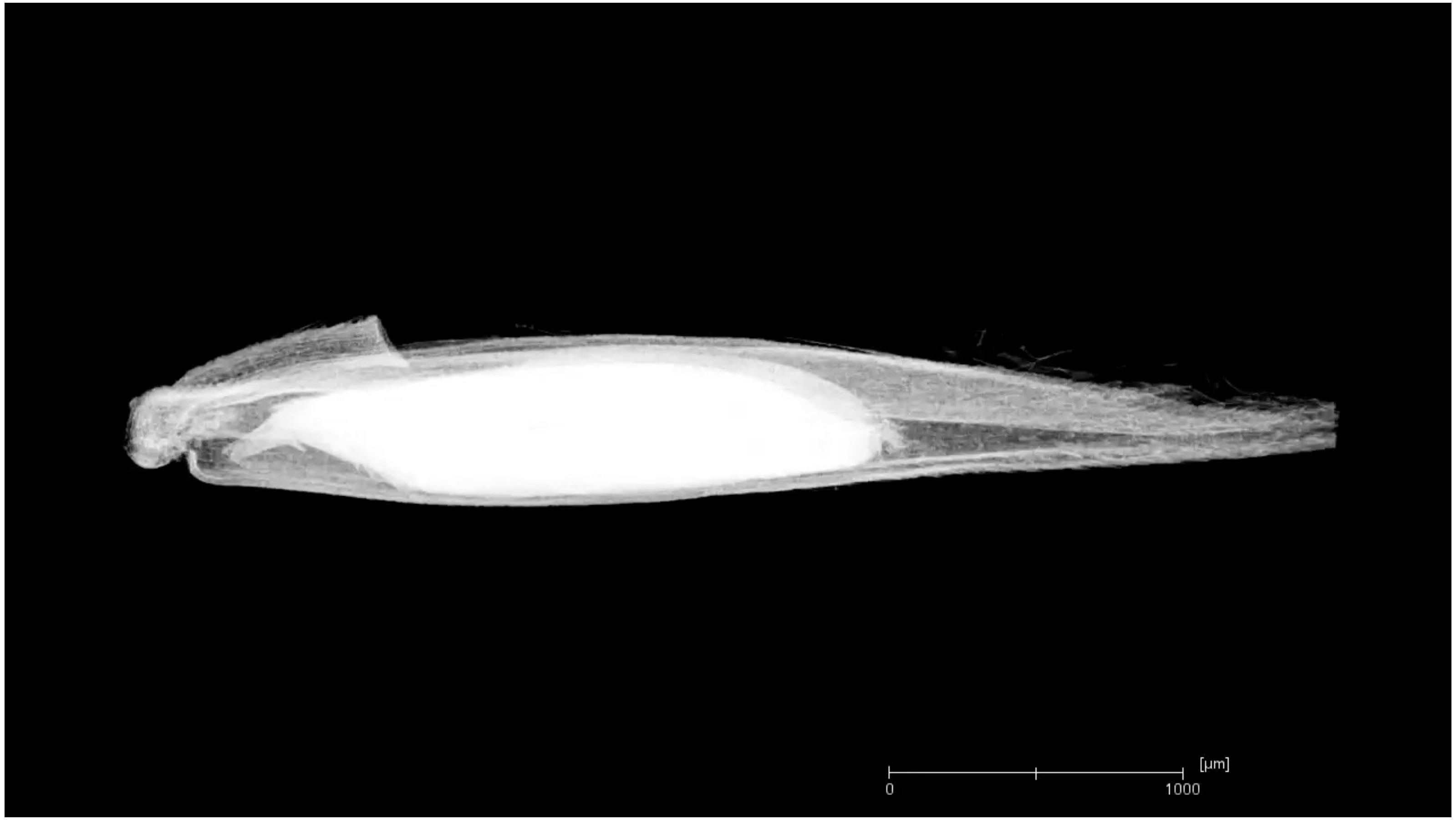

Micro-CT study of Barley micro-malting

In this study we investigate the malting process of barley utilising micro-CT tomography, image analysis and biochemical analysis, connecting visual clues with enzyme activity kinetics. Using micro-CT, the 3D void network structure of the barley kernel is visualized. The proximal void located close to the crease and the whole void structure was filled with water from the third day into the malting process. The 3D void network may play an important role in water and nutrient translocation during germination, especially within the first 24 hours of malting. During malting, we did not observe a major difference in starch structure in both micro-CT images and the biochemical analysis. This is in agreement with previous knowledge of limited starch changes during malting. Furthermore, we found that cell wall structural components: arabinoxylan, xyloglucan, arabinogalactan proteins and pectin components show limited changes in amount and recalcitrance, whereas the amount of starchy endosperm localised beta-glucan and (gluco)mannans are reduced during malting, as expected. This is in contrast with our 3D micro-CT images of the aleurone layer, which shows a clear decrease in density, starting from the side of the grease and the scutellum. This we interpret as remobilisation of nutrients from the endosperm towards the germ without the breakdown of the cell walls of the aleurone layer. Note that both the central void and the starting point of aleurone layer disappearance locate near the grease. It is possible that the void system assists the transportation of nutrients distribution from the aleurone layer to the starchy endosperm

Image segmentation

Layer detection

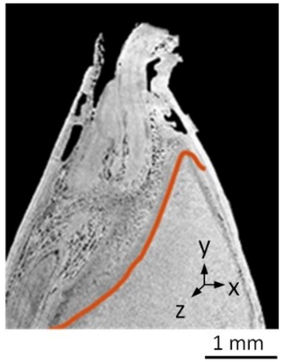

Random forest

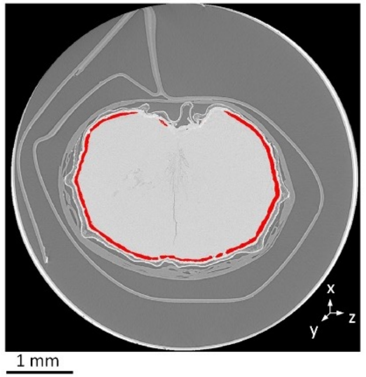

Segmented kernel

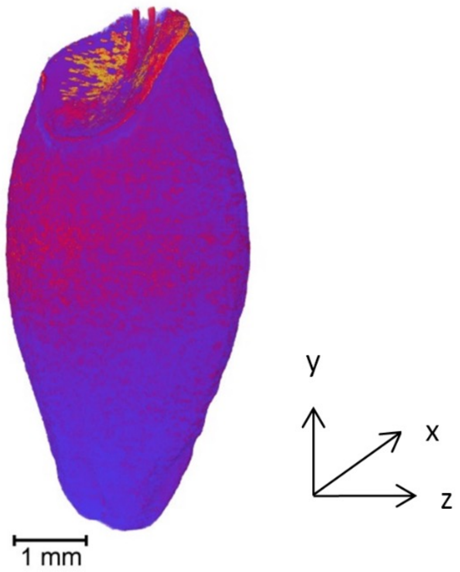

Crack in the kernel

Due to the similar image intensity in the CT images, it is impossible to segment the structure of Barley based on thresholding based segmentation method. Therefore, we apply the layer detection to separate the embryo and the kernel, and use random forest segmentation method to extract the aleurone layer.

the kernel changes and emzyme analysis

CT slices

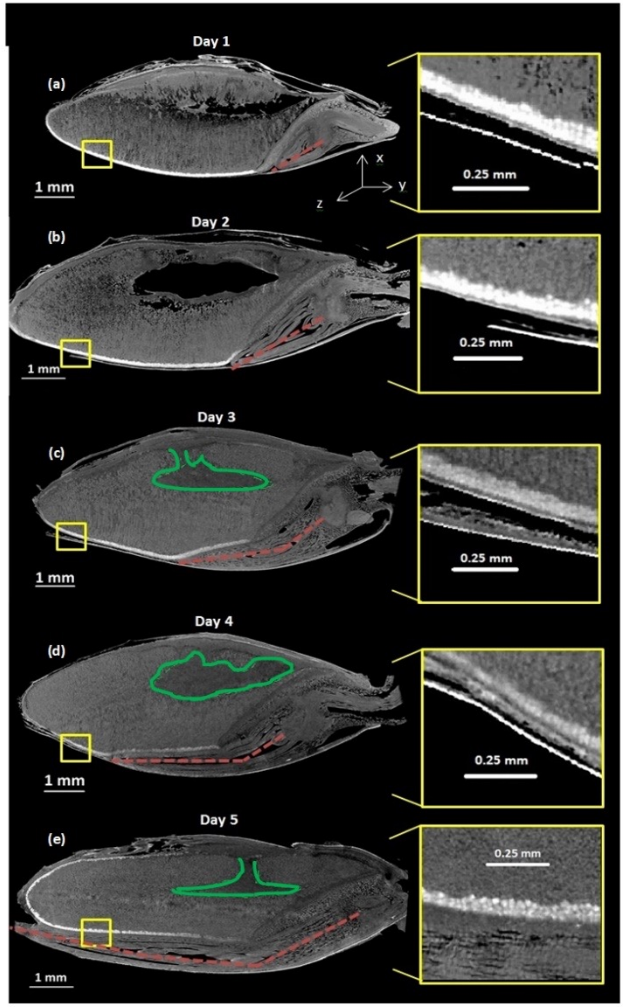

Emzyme activities

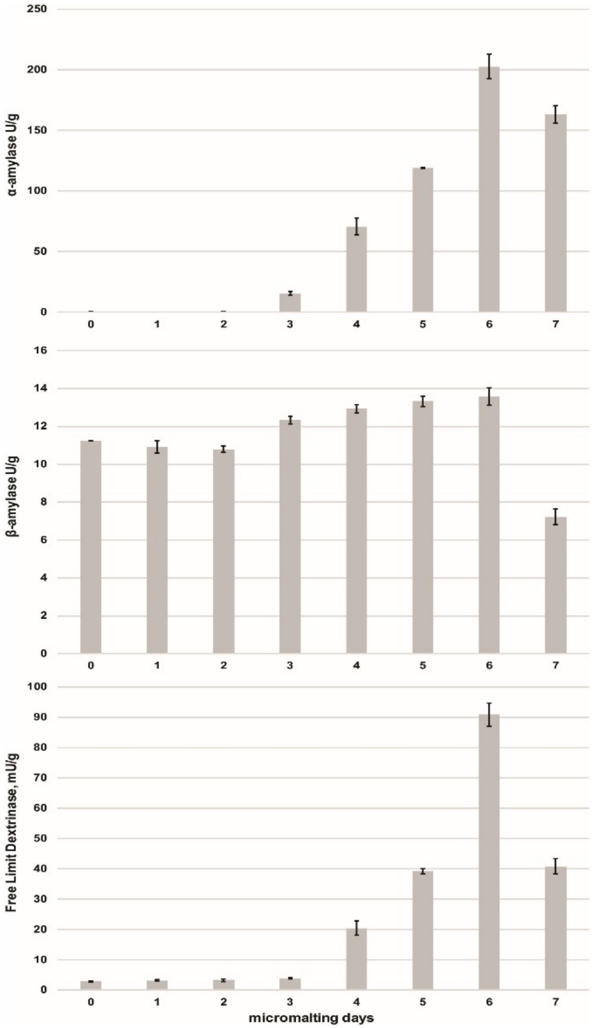

Conclusions

We did not see the degrading of the kernel in the first 5 days of the micromalting process, which matches literature reporting that in this stage, the kernel degradation is no more than 10%. The enzyme analysis also showed low enzyme activities in the first 5 days, which match the micro-CT observation.

the aleurone layer and cell wall analysis

Aleurone layer in 3D

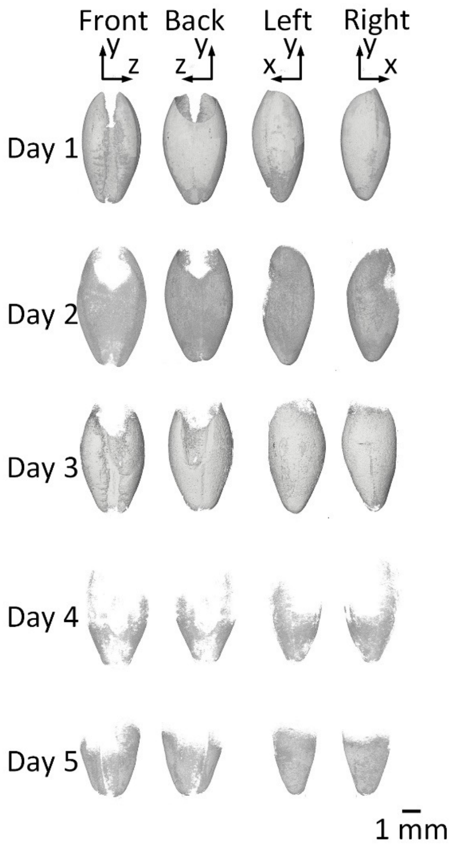

Cell wall analysis

Extraction	Sample	(1→4)-β-D-galactan (mAb LM5)	(1→5)-α-L-arabinan (mAb LM6)	Linearised (1→5)-α-L-arabinan (mAb LM13)	Feruloylate on any polymer (mAb LM12)	(1→4)-β-D-(galacto)mannan (mAb BS-400-4)	(1→4)-β-D-(galacto)(gluco)mannan (mAb LM21)	(1→4)-β-D-(gluco)mannan (mAb LM22)	(1→3)(1→4)-β-D-glucan (mAb BS-400-3)	Xyloglucan (XXXG motif) (mAb LM15)	Xyloglucan / unsibstituted β-D-glucan (mAb LM25)	(1→4)-β-D-xylan (mAb LM10)	(1→4)-β-D-xylan/arabinoxylan (mAb LM11)	Anti-grass xylan preparations (mAb LM27)	Xylan (mAb LM28)	Extensin (mAb JIM20)	AGP (mAb JIM13)
CDTA	Carl Day 0	0	20	0	19	99	69	0	0	0	10	0	26	0	8	0	8
CDTA	Carl Day 1	0	17	0	20	100	67	0	0	0	18	0	23	0	0	0	9
CDTA	Carl Day 2	0	16	0	16	100	67	0	0	0	13	0	22	0	4	0	8
CDTA	Carl Day 3	0	15	0	17	96	66	0	0	0	8	0	23	0	0	0	7
CDTA	Carl Day 4	0	16	0	13	79	48	0	0	0	7	0	20	0	3	0	7
CDTA	Carl Day 5	3	21	0	11	65	35	0	0	0	7	0	16	0	3	0	6
CDTA	Carl Day 6	0	19	0	12	42	19	0	0	0	7	0	11	0	6	0	6
CDTA	Carl Day 7	0	22	0	13	43	19	0	0	0	9	0	12	0	4	0	7
NaOH	Carl Day 0	19	23	11	0	32	16	0	63	10	14	0	65	0	44	0	0
NaOH	Carl Day 1	17	23	9	0	25	11	0	62	8	13	0	68	0	43	0	0
NaOH	Carl Day 2	19	23	11	0	34	13	0	78	10	18	0	69	6	43	0	0
NaOH	Carl Day 3	20	23	10	0	34	13	0	67	10	18	0	69	6	41	0	0
NaOH	Carl Day 4	21	20	9	0	27	9	0	45	11	16	0	65	7	39	0	0
NaOH	Carl Day 5	22	23	9	0	23	8	0	42	12	19	0	67	8	49	0	0
NaOH	Carl Day 6	22	21	8	0	20	6	0	38	13	19	0	62	9	43	0	0
NaOH	Carl Day 7	25	25	9	0	22	7	0	40	15	24	0	69	13	61	0	0

Conclusions

The cell wall analysis shows that the cell wall is structurally intact, meaning the disappearing of the aleurone layer in the CT images is not due to the broke down of the cell wall, but more likely due to heavy materials, such as minerals and protein transportation crossing the cell wall.

Vascular flow

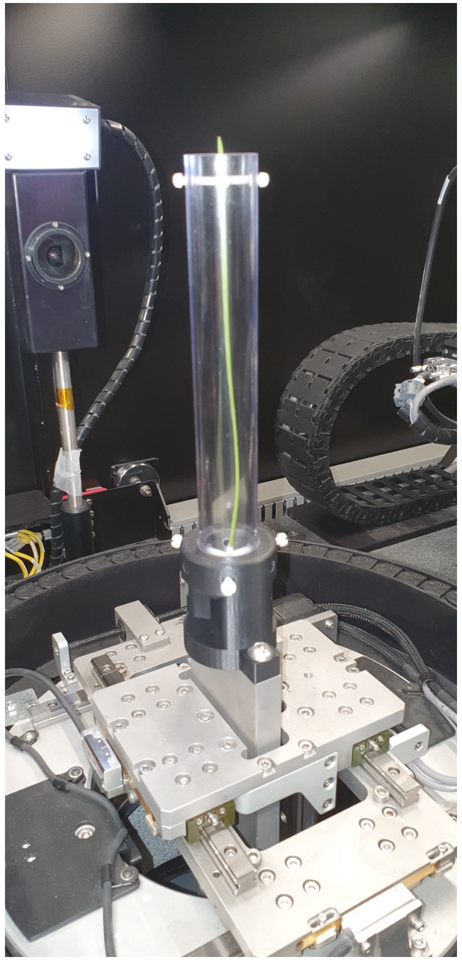

4X objective with 3.4 µm pixels
40kV and no filter
1601 projections
2 seconds exposure
1 hour 35 minutes

Vascular flow

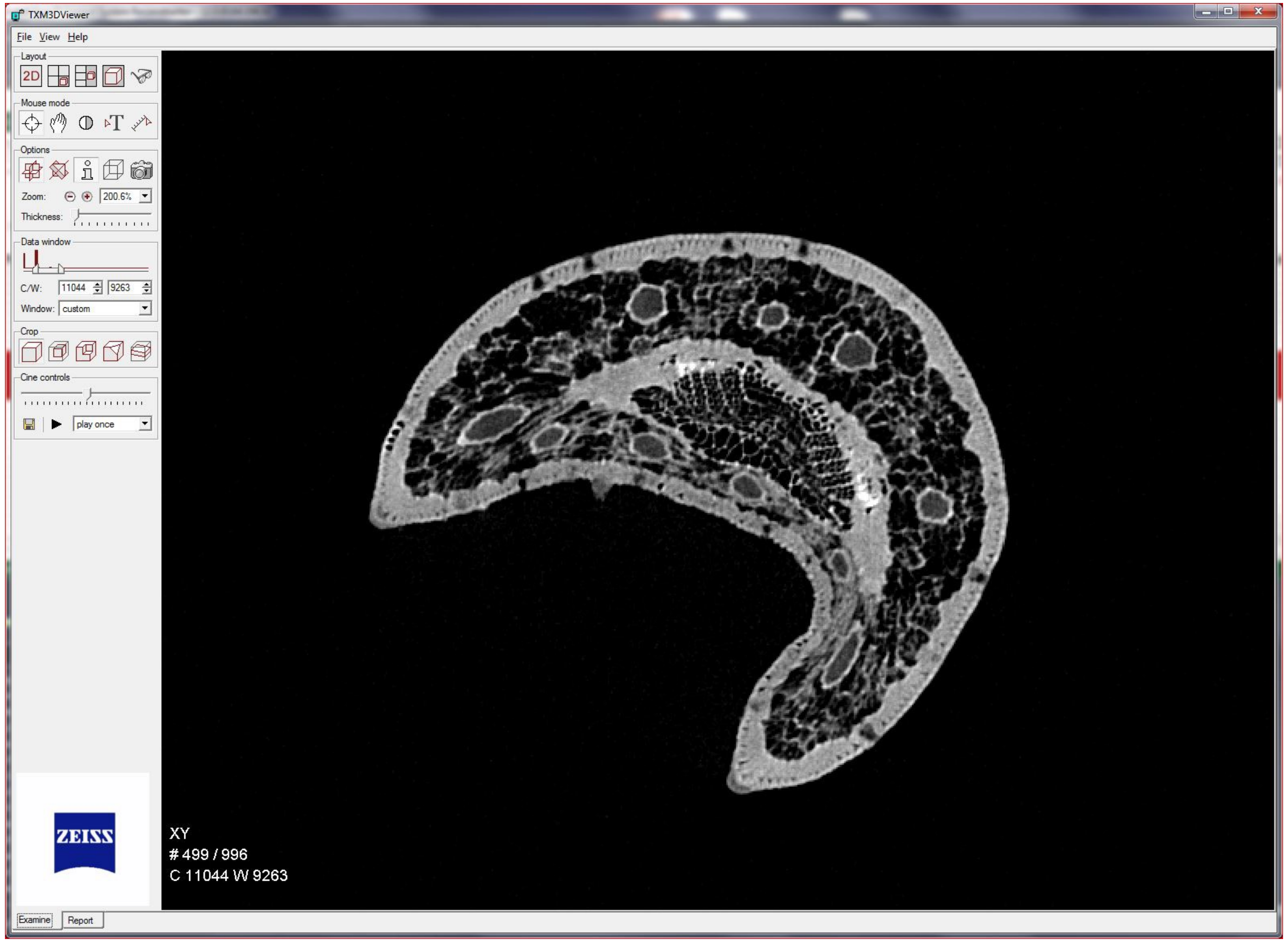

4X objective with 3.4 µm pixels

40kV and no filter

1601 projections

2 seconds exposure

1 hour 35 minutes

Vascular flow

10X objective with 1.7 µm pixels
40kV and no filter
1601 projections
5 seconds exposure
2 hour 59 minutes


2 / 983
366 W 16804

Vascular flow

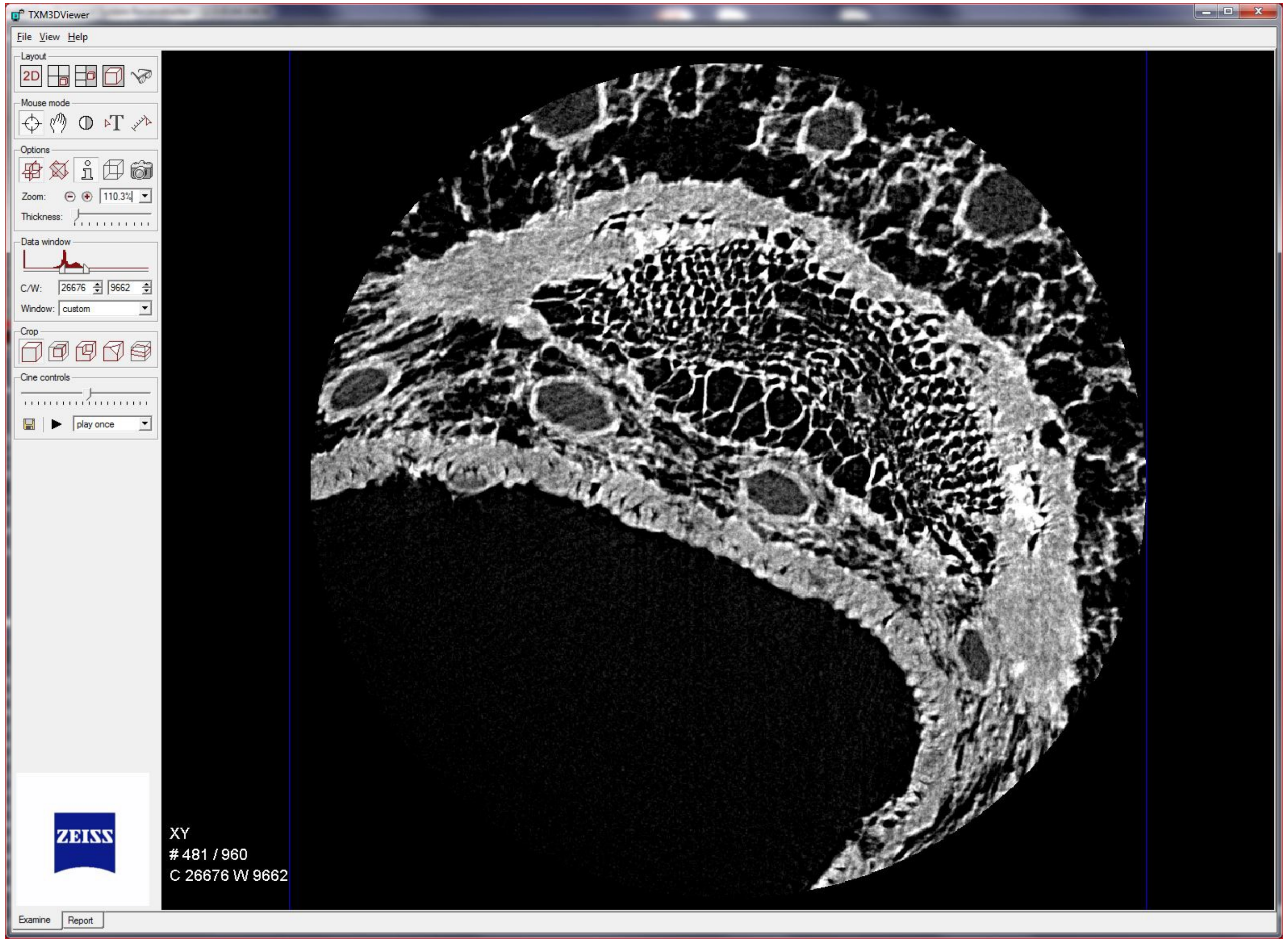

20X objective with 0.9 µm pixels

40kV and no filter

3201 projections

20 seconds exposure

19 hour 20 minutes

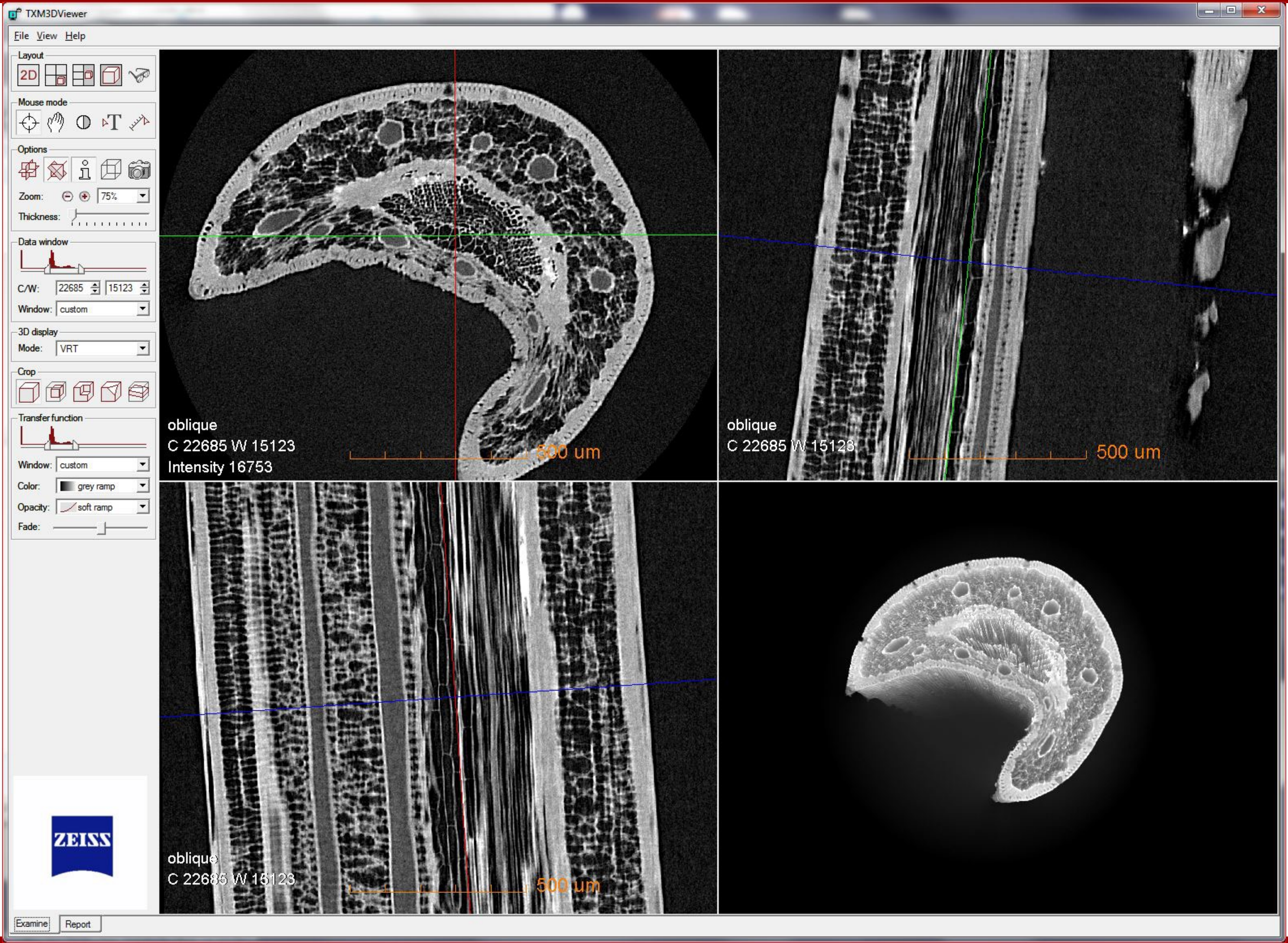
TXM3DViewer
File View Help
Layout
Mouse mode
Options
Zoom: 75%
Thickness:
Data window
C/W: 22685 15123
Window: custom
3D display
Mode: VRT
Crop
Transfer function
Window: custom
Color: grey ramp
Opacity: soft ramp
Fade:
oblique
C 22685 W 15123
Intensity 16753
500 um
oblique
C 22685 W 15123
500 um
oblique
C 22685 W 15123
500 um
ZEISS
Examine
Report

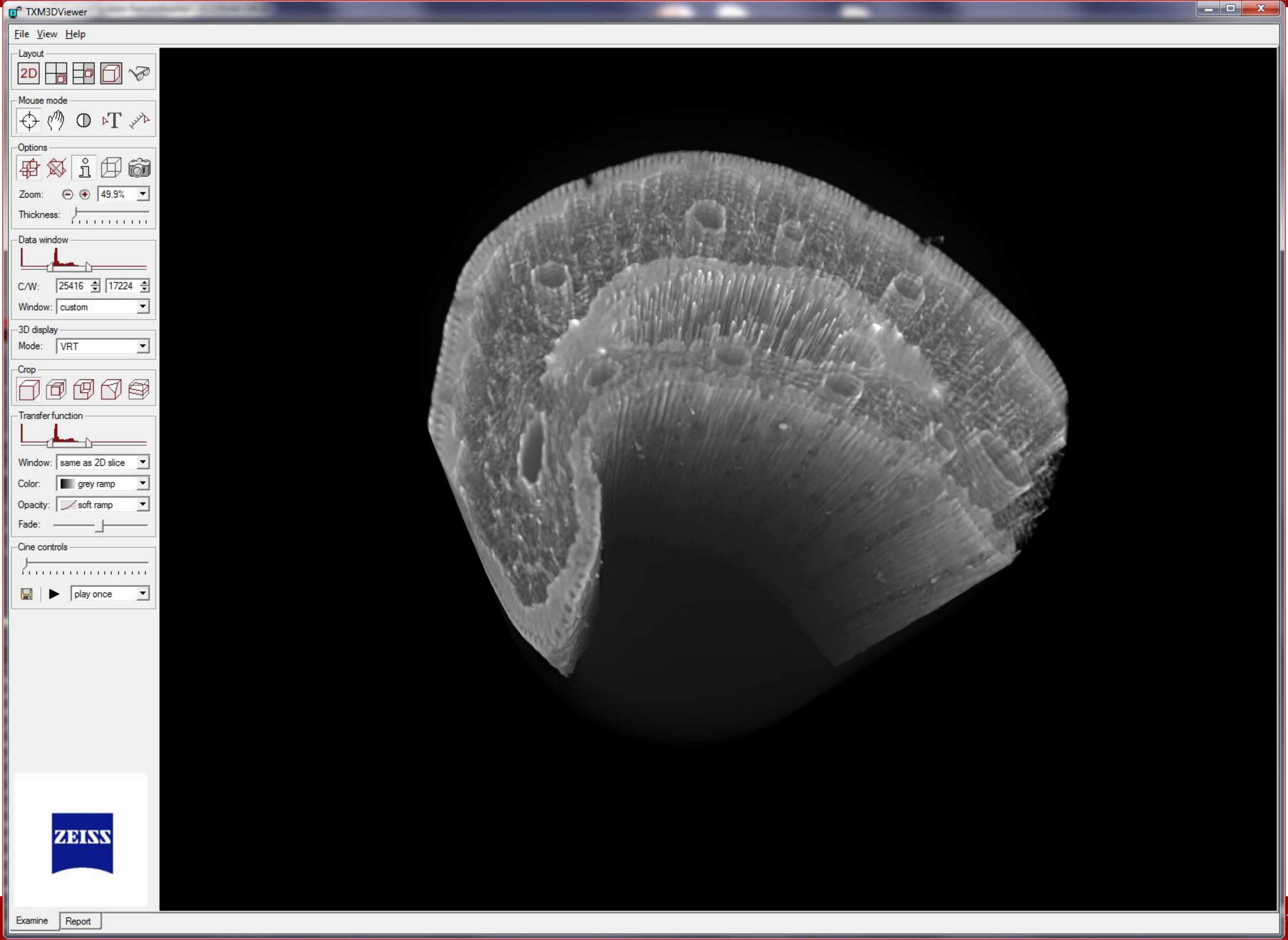
TXM3DViewer
File View Help
Layout
2D
Mouse mode
Options
Zoom:
49.9%
Thickness:
Data window
C/W:
25416
17224
Window:
custom
3D display
Mode:
VRT
Crop
Transfer function
Window:
same as 2D slice
Color:
grey ramp
Opacity:
soft ramp
Fade:
Cine controls
play once
ZEISS
Examine
Report

Vascular flow - segmentation

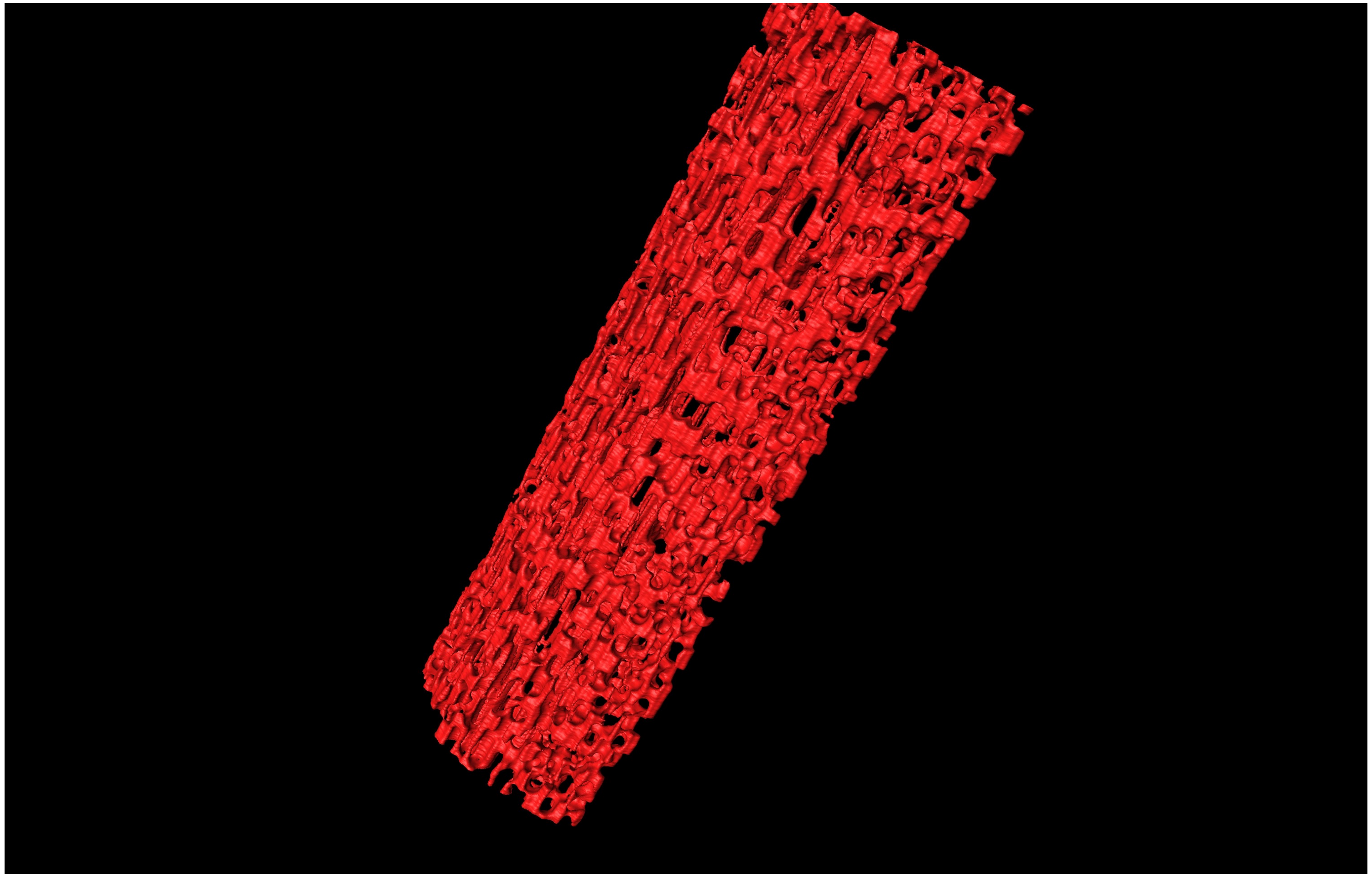

Insects

Mastigusa


mastigusa_F_Lugol_ethanol_4X-40kV-LE1-10s-5.6micro
DTU 3D Imaging Center

Hunt for ants

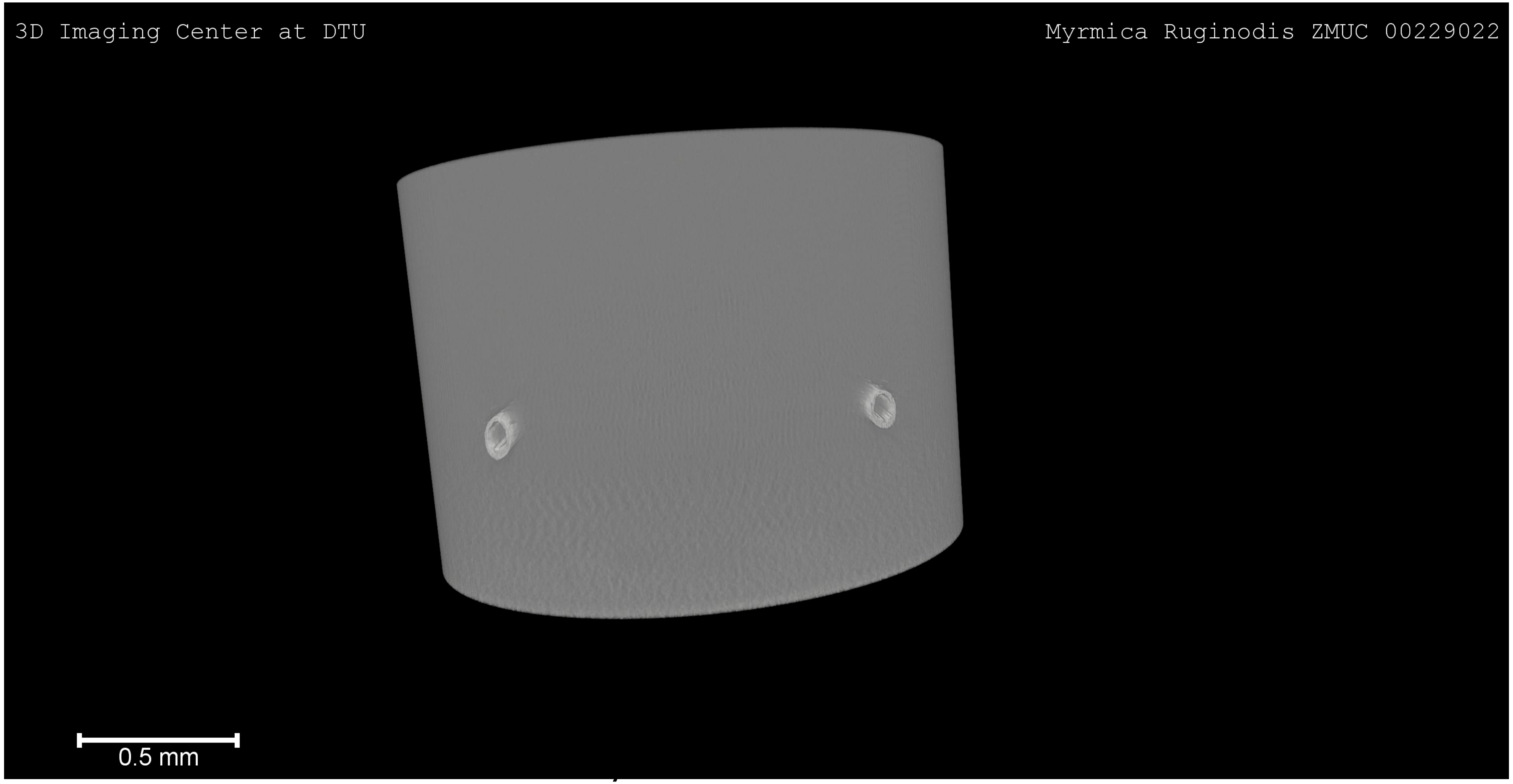

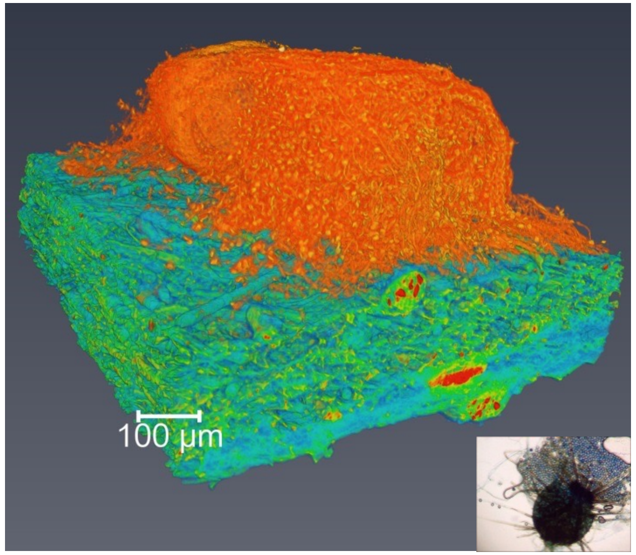

Chaetomium *globosum* in wall paper

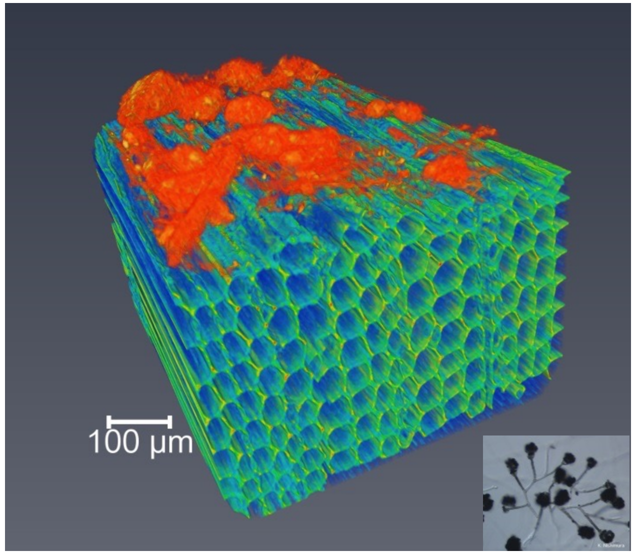

Stachybotrys *chartaum* in plywood

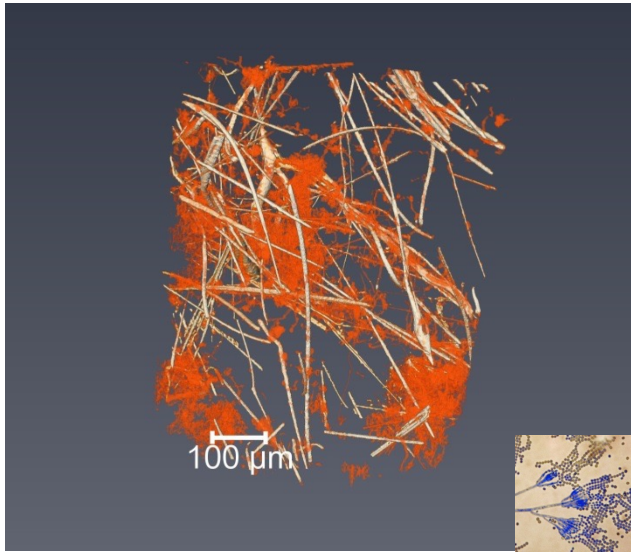

Penicillium *chrysogenum* in stone wool

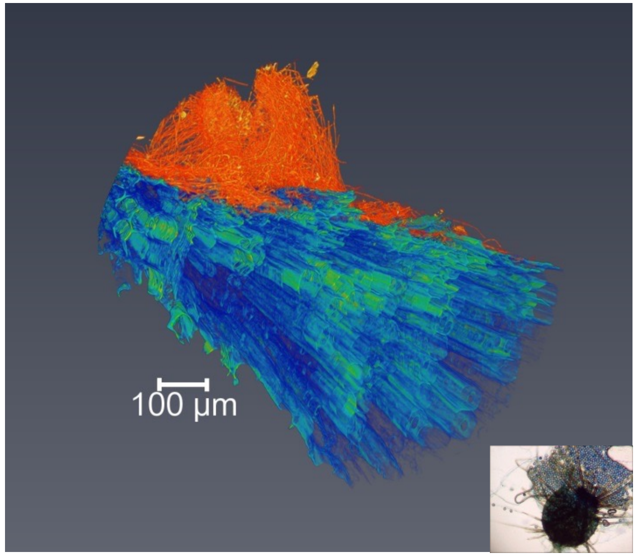

Chaetomium *globosum* in plywood

Skulls

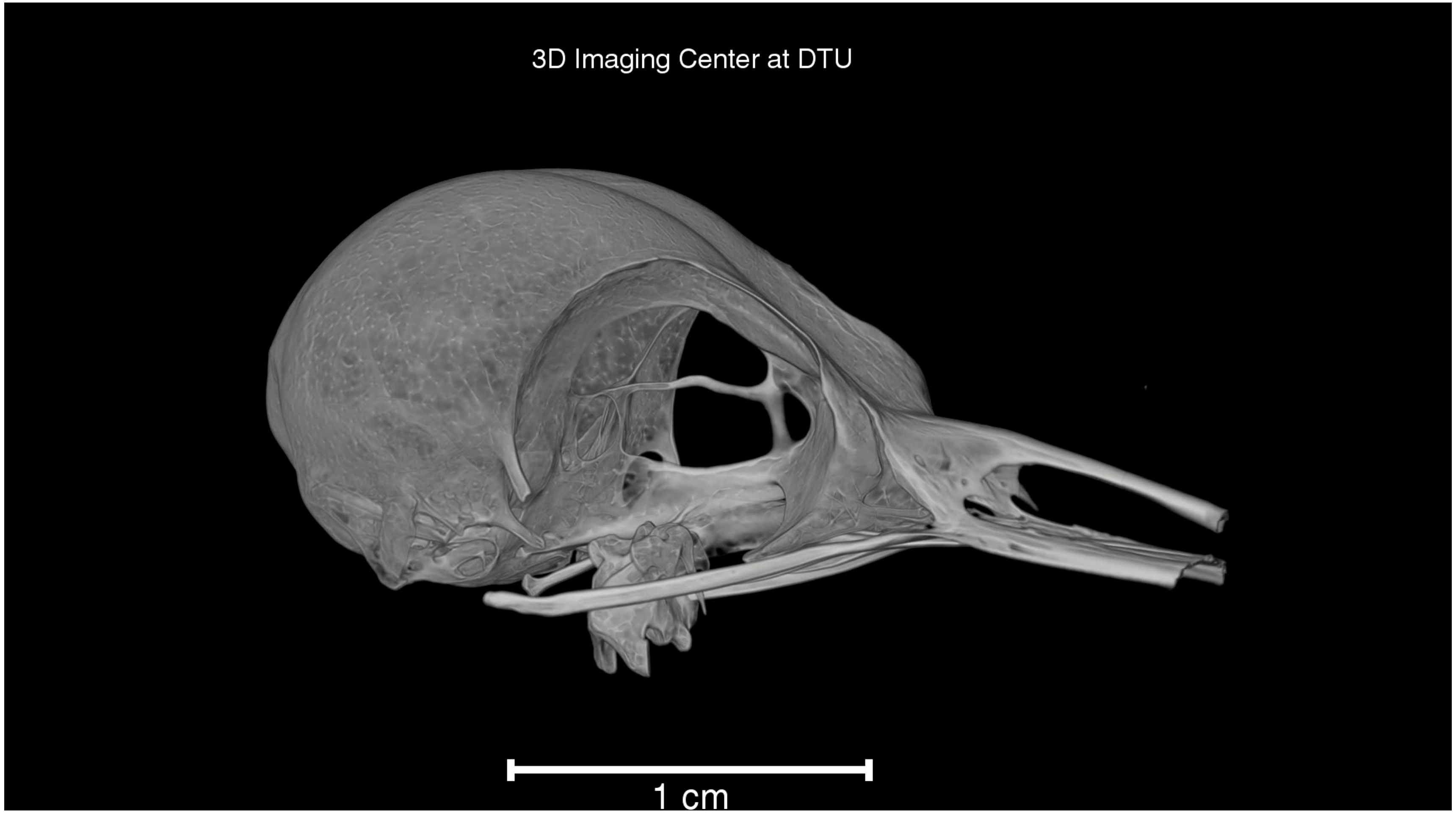

Skulls

?

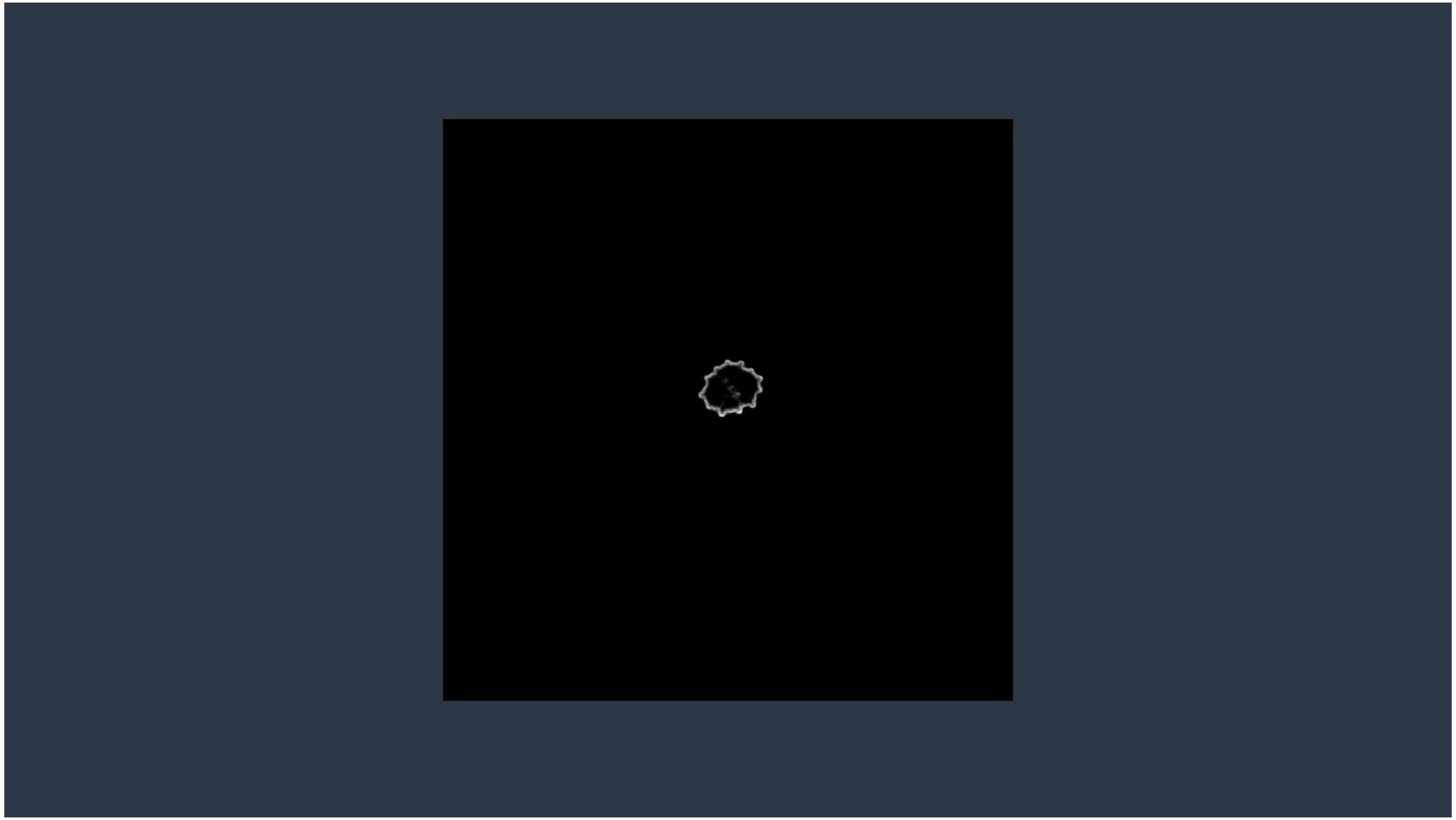

?

Food

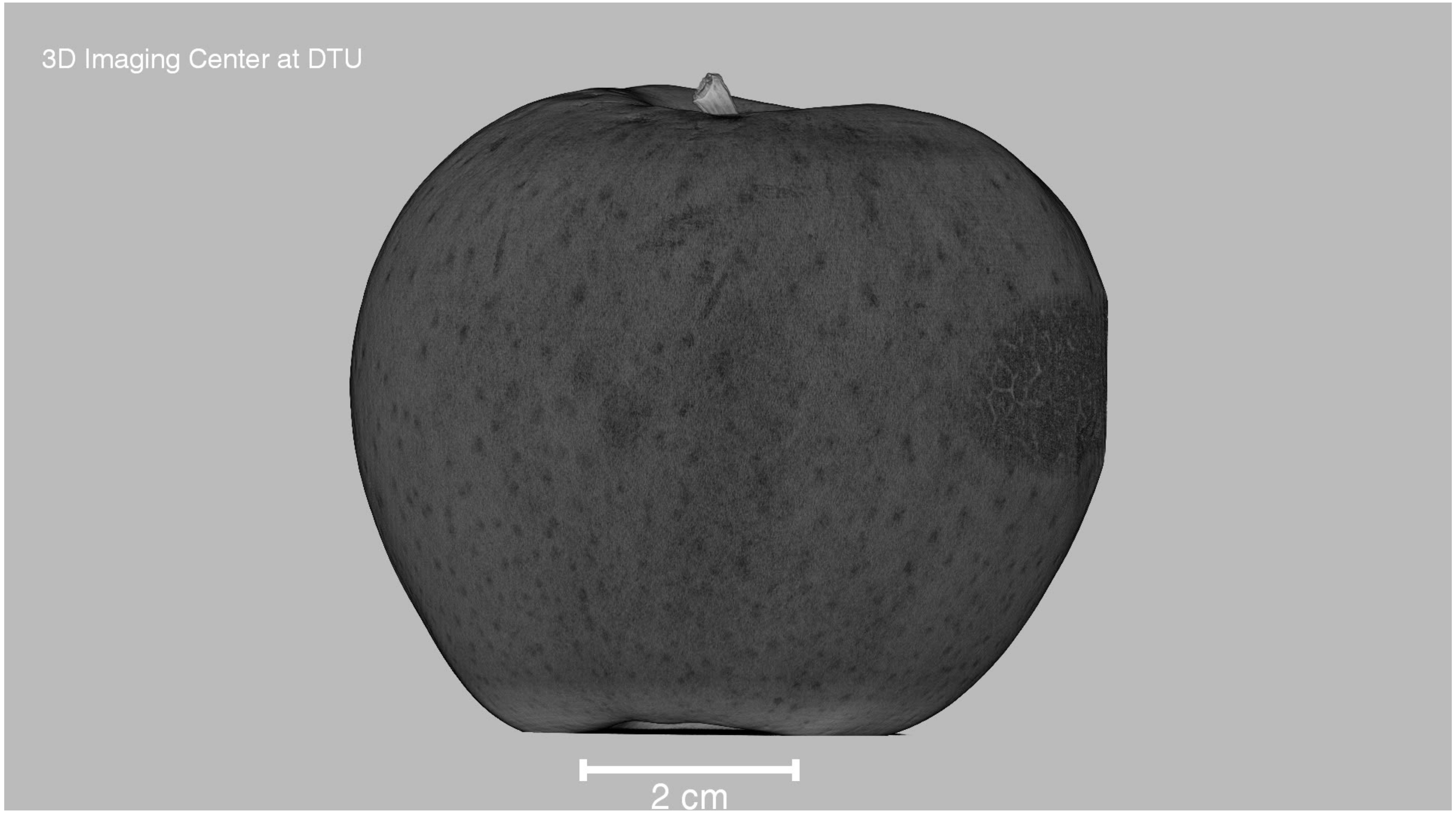

Corrosion studied by X-ray imaging

Example of corrosion on steel

- X-ray image of a large part of a steel pipe is shown.
- White areas are the steel.

- Weakly seen is also a surface layer of the pipe.

- Sediments from the corrosion are seen inside of the pipe.

- Possibility to look at a local scale

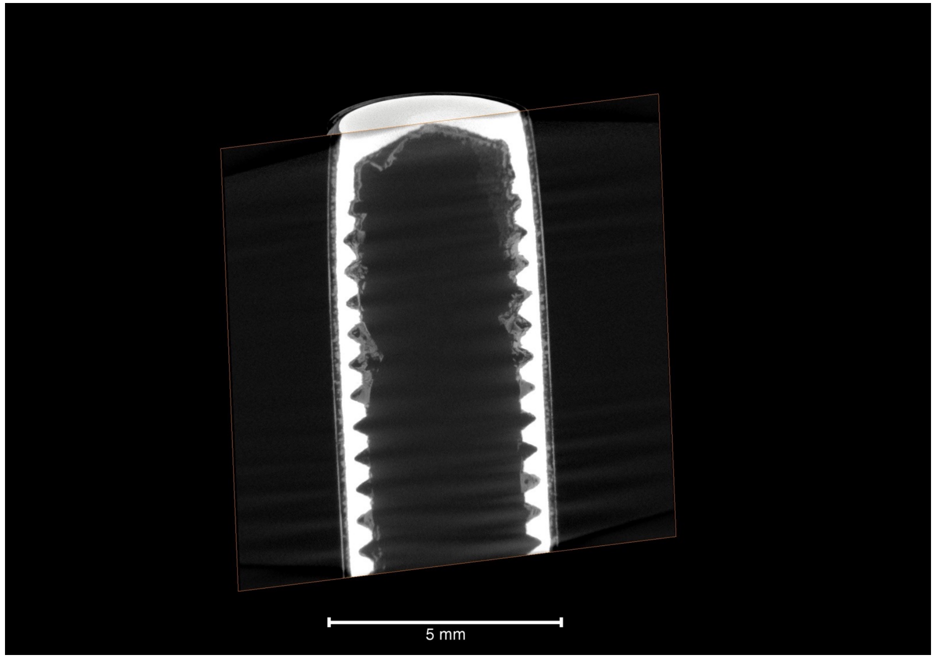

Corrosion studied by X-ray imaging

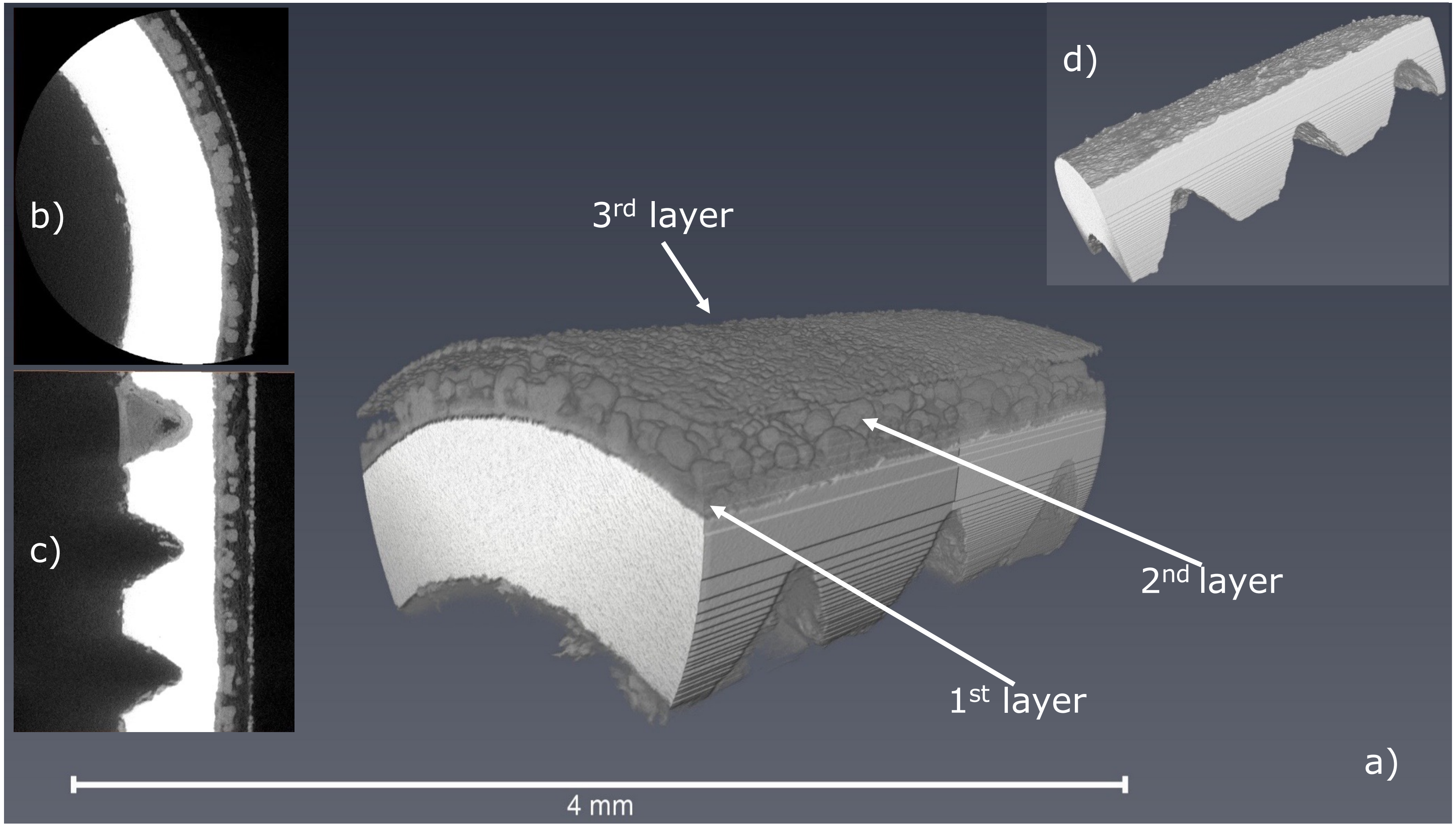

Corrosion studied by X-ray imaging

Visual inspection

- From the 3D images it is possible to separate the different layers in the wall.
- Top layer in red

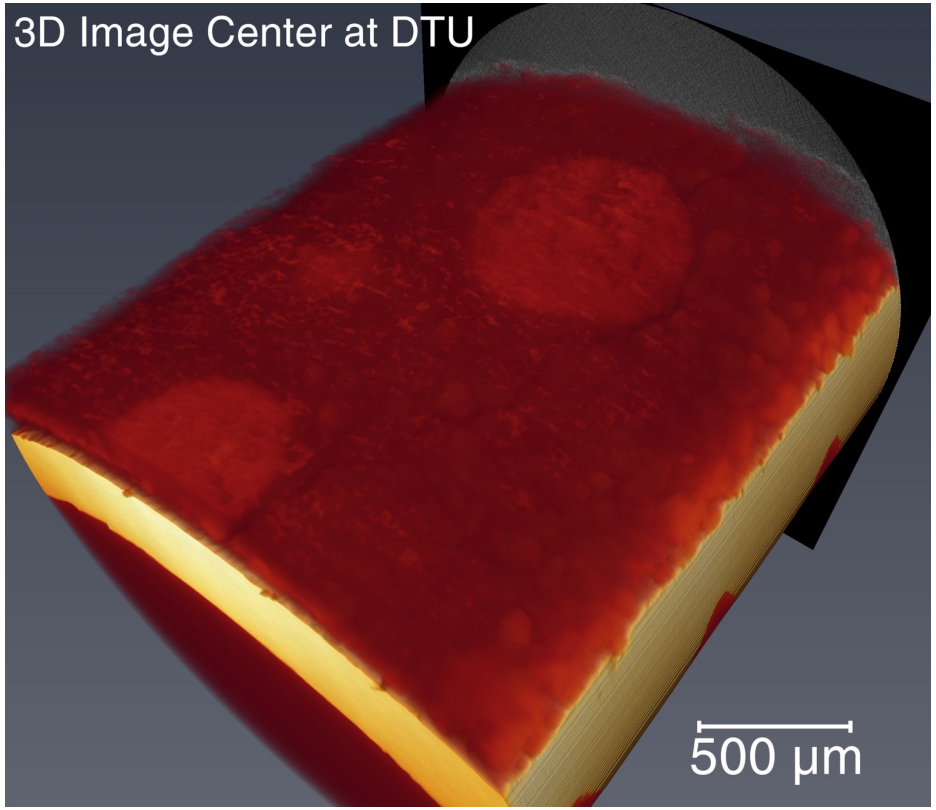

Corrosion studied by X-ray imaging

Visual inspection

- From the 3D images it is possible to separate the different layers in the wall.
- Top layer in red

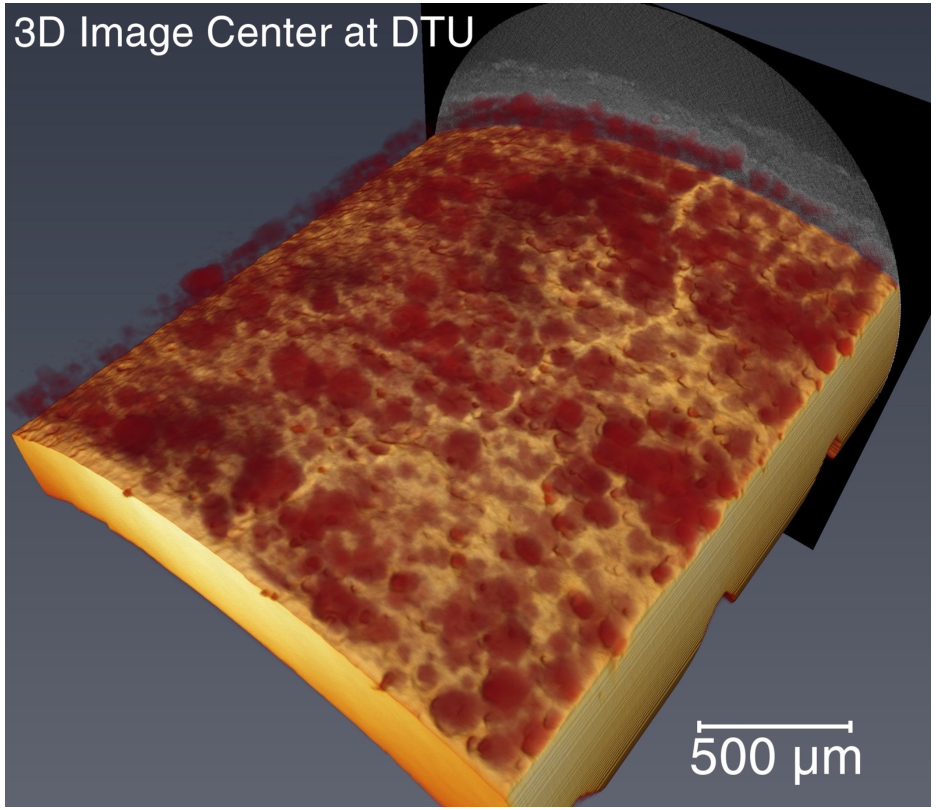

Corrosion studied by X-ray imaging

Visual inspection

- From the 3D images it is possible to separate the different layers in the wall.
- Surface layer in red
- Effected sub-surface layer.

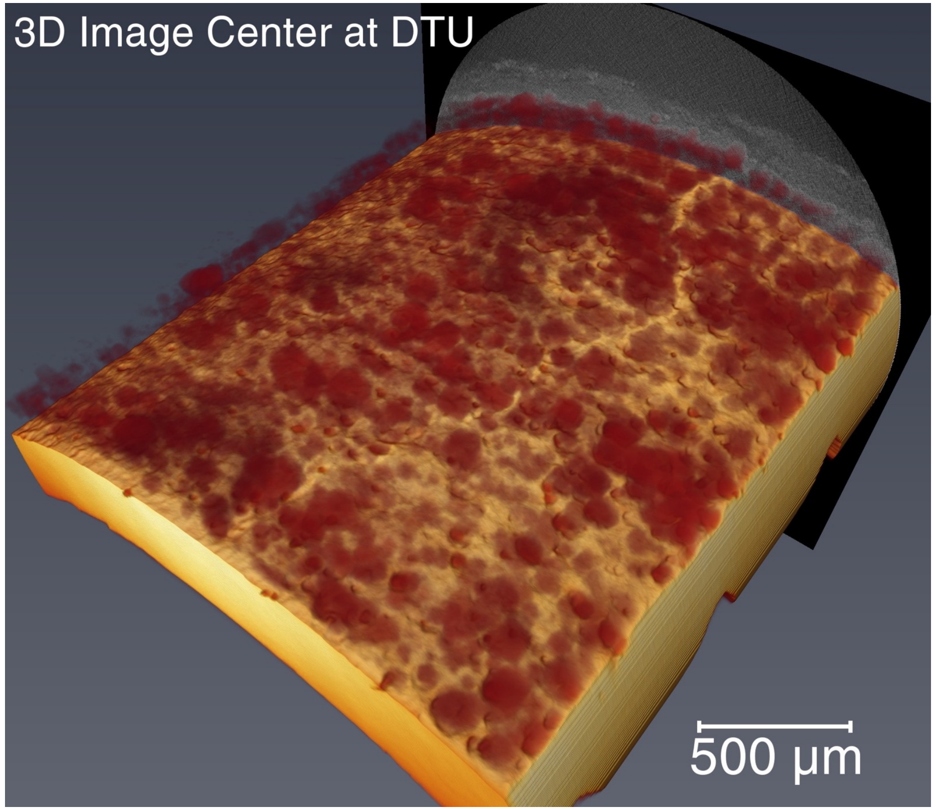

Corrosion studied by X-ray imaging

Visual inspection

- From the 3D images it is possible to separate the different layers in the wall.
- Surface layer in red
- Effected sub-surface layer
- Un-effected wall layer

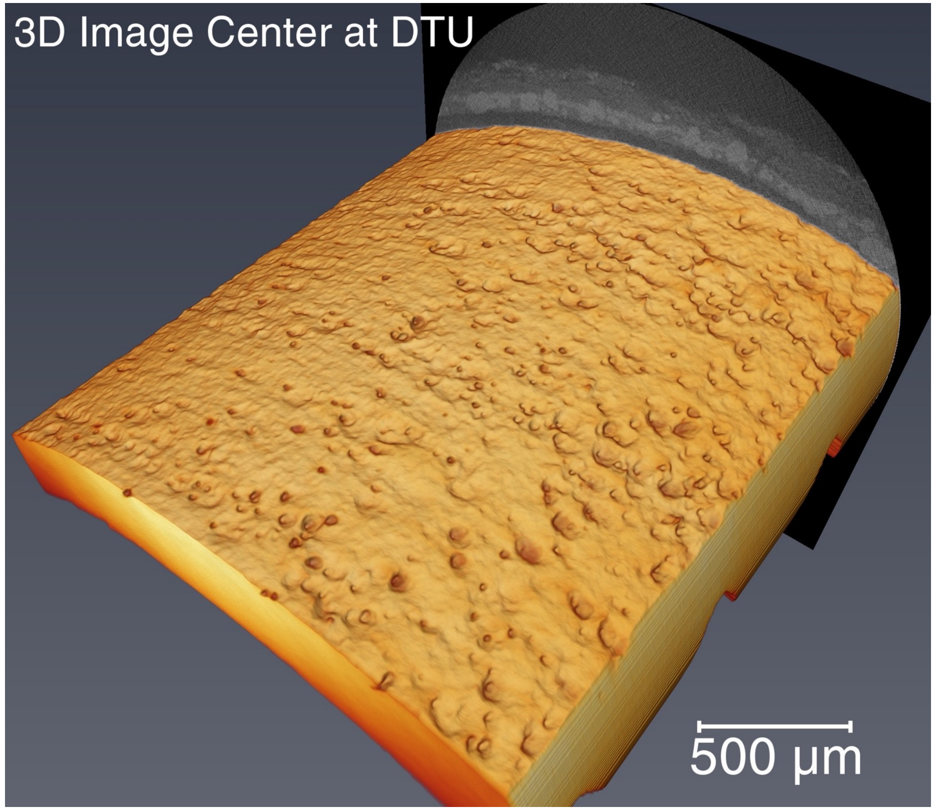

Casper
-
a young T. rex

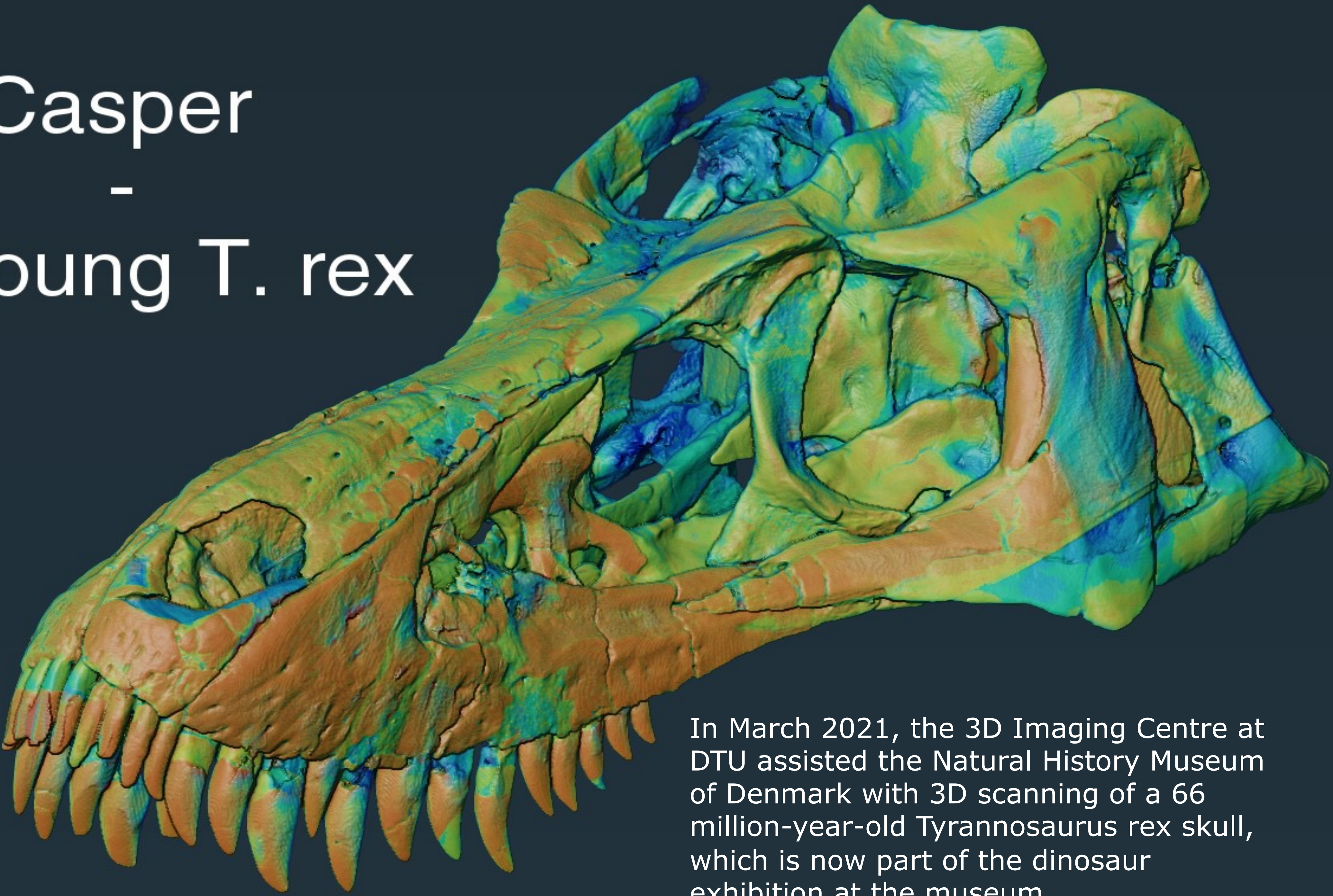

In March 2021, the 3D Imaging Centre at DTU assisted the Natural History Museum of Denmark with 3D scanning of a 66 million-year-old Tyrannosaurus rex skull, which is now part of the dinosaur exhibition at the museum.

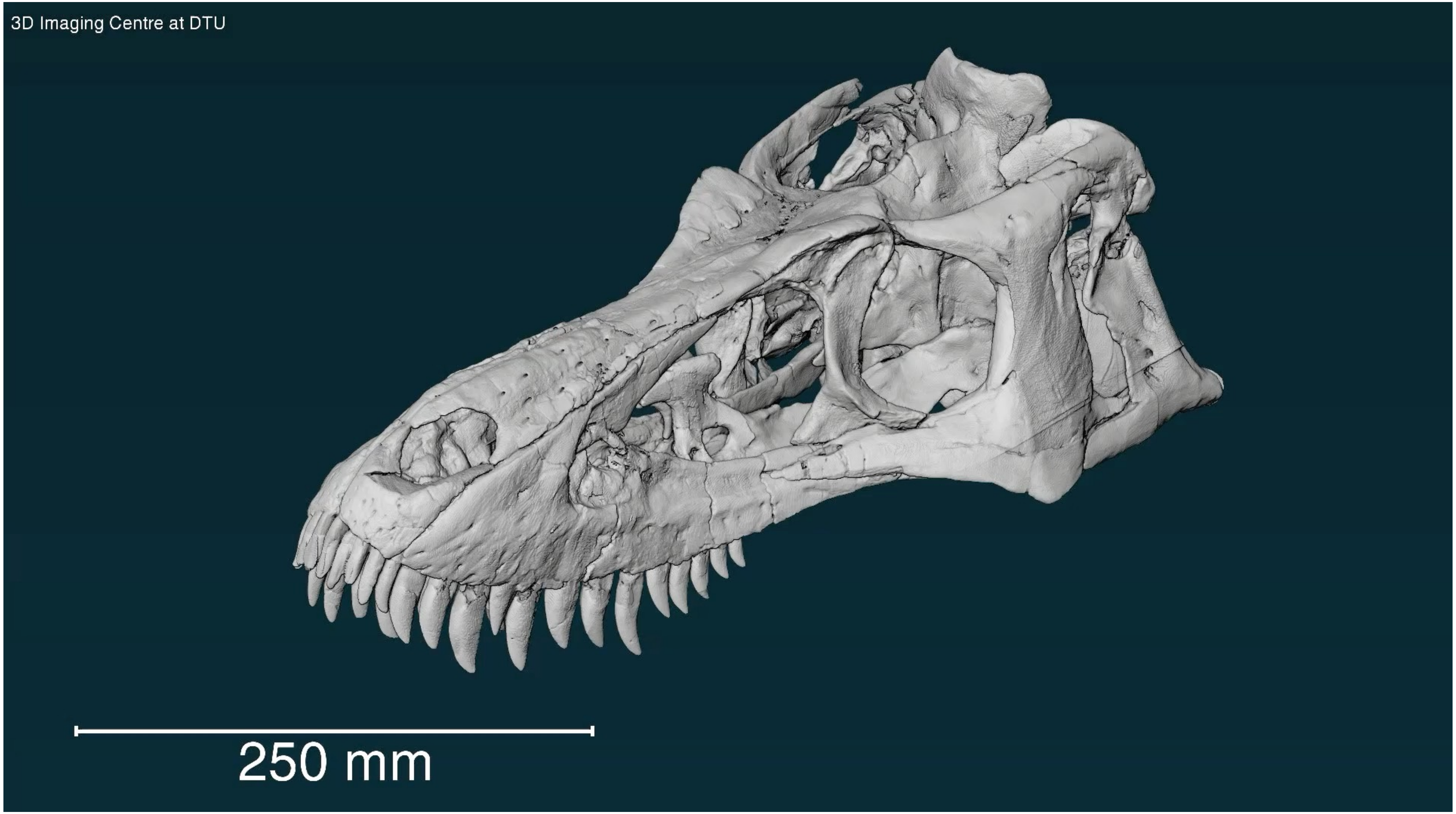
3D Imaging Centre at DTU
250 mm

Questions?